VOLUME I

SUMMARY

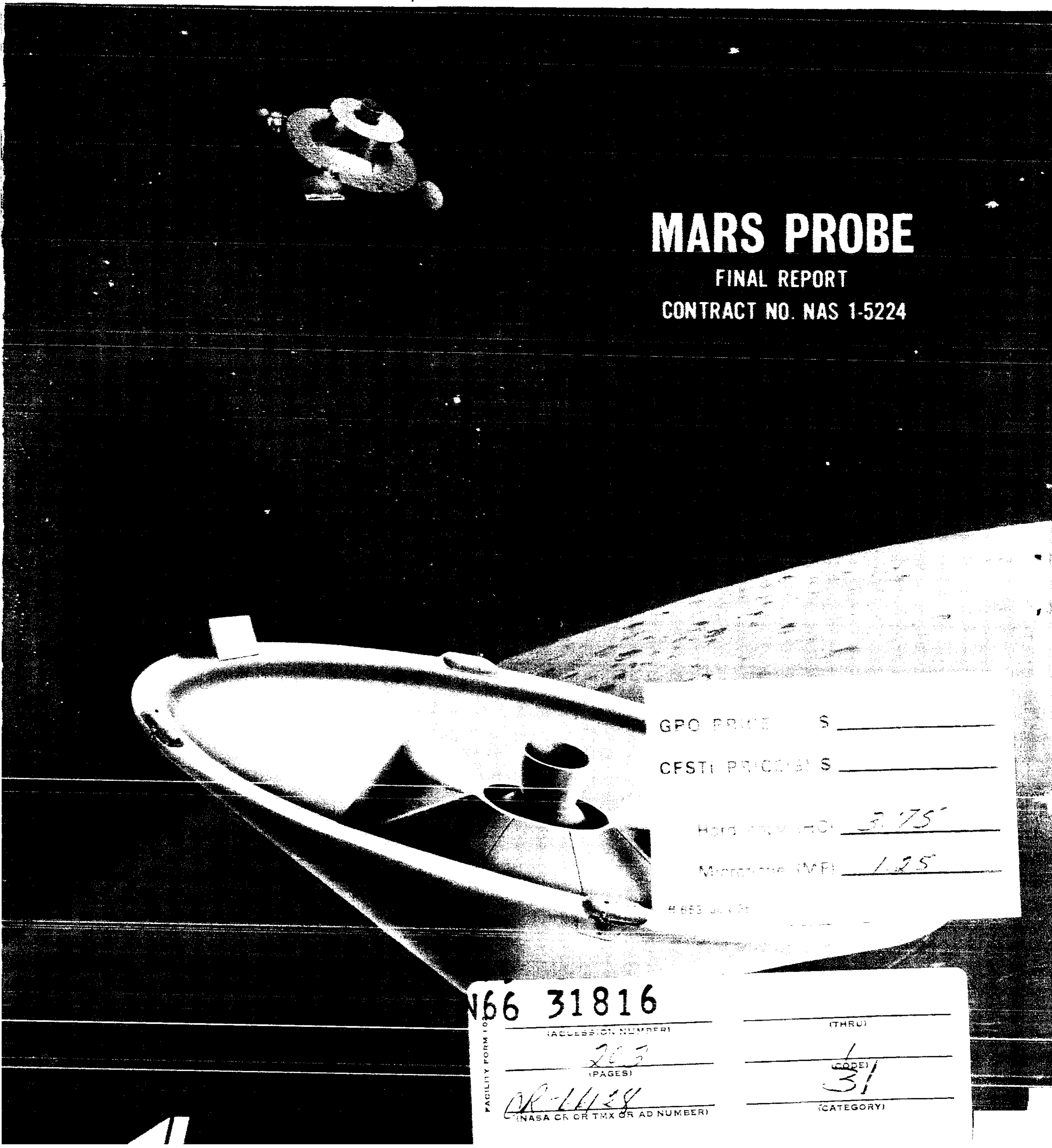

MARS PROBE

FINAL REPORT

CONTRACT NO. NAS 1-5224

BOOK INDEX

NASA CR-66128

COMPARATIVE STUDIES OF CONCEPTUAL DESIGN AND QUALIFICATION PROCEDURES FOR A MARS PROBE/LANDER

FINAL REPORT

VOLUME I - SUMMARY

Prepared by

SPACE SYSTEMS DIVISION
AVCO CORPORATION
Lowell, Massachusetts

AVSSD-0006-66-RR
Contract NAS 1-5224

11 May 1966

Prepared for

NATIONAL AERONAUTICS AND SPACE ADMINISTRATION
LANGLEY RESEARCH CENTER
LANGLEY STATION
Hampton, Virginia 23365

PREFACE

The results of Mars Probe/Lander studies, conducted over a 10-month period for Langley Research Center, NASA, are presented in detail in this report. Under the original contract work statement, studies were directed toward a direct entry mission concept, consistent with the use of the Saturn IB-Centaur launch vehicle, wherein the landing capsule is separated from the spacecraft on the interplanetary approach trajectory, some 10 to 12 days before planet encounter. The primary objectives of this mission were atmospheric sampling by the probe/lander during entry, and terrain and atmosphere physical composition measurement for a period of about 1 day after landing.

Studies for this mission were predicated on the assumption that the atmosphere of Mars could be described as being within the range specified by NASA Mars Model Atmospheres 1, 2, 3 and a Terminal Descent Atmosphere of the document NASA TM-D2525. These models describe the surface pressure as being between 10 and 40 mb. For this surface pressure range a payload of moderate size can be landed on the planet's surface if the entry angle is restricted to be less than about 45 degrees.

Midway during the course of the study, it was discovered by Mariner IV that the pressure at the surface of the planet is in the 4 to 10 mb range, a range much lower than previously thought to be the case. The results of the study were re-examined at this point. It was found that retention of the direct entry mission mode would require much shallower entry angles to achieve the same payloads previously attained at the higher entry angles of the higher surface pressure model atmospheres. The achievement of shallow entry angles (on the order of 20 degrees), in turn, required sophisticated capsule terminal guidance, and a sizeable capsule propulsion system to apply a velocity correction close to the planet, after the final terminal navigation measurements.

Faced with these facts, NASA/LRC decided that the direct entry from the approach trajectory mission mode should be compared with the entry from orbit mode under the assumption that the Saturn V launch vehicle would be available. Entry of the flight capsule from orbit allows the shallow angle entry (together with low entry velocity) necessary to permit higher values of M/C_DA, and hence entry weight in the attenuated atmosphere.

It was also decided by LRC to eliminate the landing portion of the mission in favor of a descent payload having greater data-gathering capacity, including television and penetrometers. In both the direct entry and the entry from orbit cases, ballistic atmospheric retardation was the only retardation means considered as specifically required by the contract work statement.

Four months had elapsed at the time the study ground rules were changed. After this point the study continued for an additional five months, during which period a new design for the substantially changed conditions was evolved. For this design, qualification test programs for selected subsystems were studied. Sterilization studies were included in the program from the start and, based on the development of a fundamental approach to the sterilization problem, these efforts were expanded in the second half of the study.

The organization of this report reflects the circumstance that two essentially different mission modes were studied -- the first being the entry from the approach trajectory mission mode and the other being the entry from orbit mission mode -- from which two designs were evolved. The report organization is as follows:

Volume I, Summary, summarizes the entire study for both mission modes.

Volume II reports on the results of the first part of the study. This volume is titled Probe/Lander, Entry from the Approach Trajectory. It is divided into two books, Book 1 and Book 2. Book 1 is titled System Design and presents a discursive summary of the entry from the approach trajectory system as it had evolved up to the point where the mission mode was changed. Book 2, titled Mission and System Specifications, presents, in formal fashion, specifications for the system. It should be understood, however, that the study for this mission mode was not carried through to completion and many of the design selections are subject to further tradeoff analysis.

Volume III is composed of three books which summarize the results of the entry from orbit studies. Books 1 and 2 are organized in the same fashion as the books of Volume II, except that Book 2 of Volume III presents component specifications as well. Book 3 is titled Development Test Programs and presents, for selected subsystems, a discussion of technology status, test requirements and plans. This Book is intended to satisfy the study and reporting requirements concerning qualification studies, but the selected title is believed to describe more accurately the study emphasis desired by LRC.

Volume IV presents Sterilization results. This information is presented separately because of its potential utilization as a more fundamental reference document.

Volume V presents, in six separate books, Subsystem and Technical Analyses. In order (from Book 1 to Book 6) they are:

Trajectory Analysis
Aeromechanics and Thermal Control
Telecommunications, Radar Systems and Power
Instrumentation
Attitude Control and Propulsion
Mechanical Subsystems

Most of the books of Volume V are divided into separate discussions of the two mission modes. The Table of Contents for each book clearly shows its organization.

CONTENTS

CONTENTS (Cont'd)

CONTENTS (Concl'd)

ILLUSTRATIONS

ILLUSTRATIONS (Cont'd)

ILLUSTRATIONS (Concl'd)

TABLES

TABLES (Concl'd)

GLOSSARY

ACS	Attitude Control System
CC&S	Central Computer and Sequencer
DSN	Deep Space Network
DSIF	Deep Space Instrumentation Facility
EFAT	Entry from Approach Trajectory
EFO	Entry from Orbit
FC	Flight Capsule
FS	Flight Spacecraft
FSK	Frequencey Shift Keyed
IRS	Interial Reference System
LCM	Linear Chirp Modulation
MDF	Mild Detonating Fuse
MFS	Multiple Frequency Shift
MOS	Mission Operations System
TWT	Traveling Wave Tube
VHF	Very High Frequency
ΔV	Velocity Increment
$M/C_D A$	Ballistic Parameter

ACKNOWLEDGMENT

The principal study managers for this program were:

W. P. Neacy	-	Deputy Project Director
T. R. Ellis	-	Systems Engineering
R. Hanselman	-	Instrumentation
H. Hurwicz	-	Aeromechanics
J. J. Mahoney	-	Communications and Power
W. J. Schafer	-	Sterilization

Acknowledgment is made to principal subcontractors:

RCA Astroelectronics Division for communications assistance and Wilmot Castle Company for sterilization technology assistance.

Acknowledgment is also made to the Northrop Ventura Division for providing significant assistance in parachute technology.

J. A. Gautraud

J. A. Gautraud
Project Director

INTRODUCTION

This summary volume presents in abbreviated form the results for the entire study. The method of presentation adopted for this volume is:

Part A - Summary of the entry from the approach trajectory study.

Part B - Summary of the entry from orbit study.

In each Part, the arrangement of material is:

Summary

System Design

Subsystem Design

System and Subsystem Tradeoffs

Included under Part B are the summaries of Development Test Program and Sterilization studies.

A. PROBE/LANDER MISSION, ENTRY FROM THE APPROACH TRAJECTORY

1.0 STUDY SUMMARY

1.1 STUDY OBJECTIVES

The successful achievement of manned exploration of Mars can be enhanced by prior definition of the Mars environment by unmanned systems. This study has been performed to define the nature of a Mars entry vehicle system required to return significant planet data for the 1971 Mars opportunity.

As stated in the preface, the study underwent a major change at mid-point because of the significant reduction in surface pressure estimates resulting from the data received from Mariner IV. This section presents the original objectives of the study for the probe/lander mission using the entry from approach trajectory mission mode. Briefly stated, these objectives were the conceptual design of a non-lifting probe/lander (an entry vehicle to probe the atmosphere during entry, and to achieve a survivable landing) for the 1971 Mars opportunity and the growth potential of the vehicle for later, more elaborate, lander missions. By the term growth potential was meant the use of the same entry vehicle shell -- its structure and heat shield -- not only for the first mission in 1971, but for the more complex missions envisioned for the 1973 and 1975 opportunities as well. This shell definition was called the multi-mission shell concept.

Important collateral objectives of the study were the definition of procedures required to assure sterilization of the probe/lander and a comparison and definition of qualification procedures to be used to qualify the vehicle, including definition of the extent and value of Earth flight test programs.

1.2 STUDY GROUND RULES

The most important ground rules which were initially specified are the following:

a) Saturn IB-Centaur launch vehicle

b) Probe/lander separation on the approach trajectory

c) Flight spacecraft orbiter in 1971 and 1973, fly-by in 1975

d) Maximum probe/lander weight of 2500 lbs in 1971 and 1973; 4500 pounds in 1975

e) Ballistic entry as probe/lander retardation means

f) NASA Mars Model Atmospheres 1, 2, 3 (10, 25, 40 millibar)

g) Subsonic parachute for payload descent; full deployment at Mach 0.8, 15,000 feet

h) Hard lander -- 1000g maximum impact load

i) Short duration (a few hours to a few days) landed mission in 1971

j) Mission objectives:

Engineering data for future missions
Scientific data for design of future experiments.

k) Instrumentation/experimentation constraints:

No biological or television instrumentation
No mobility experiments.

l) Comparison of three basic probe/lander shell configurations for the multi-mission shell concept: tension shell, blunt cone, modified Apollo

m) Sterilization -- 10^{-4} probability of planet contamination by a flight capsule entering the atmosphere.

The first six of these ground rules essentially establish the M/C_DA and entry weight of the probe/lander. Items g - k determine the basic landing mode and the type and number of the data-gathering instrumentation. Item l describes the configurations over which an optimized design is sought. NASA's ground rule on planetary quarantine is reflected in Item m.

1.3 STUDY CHRONOLOGY

In the chronology that follows it will be seen that the major changes in study direction were occasioned by the necessity for developing a design with sufficient available payload weight to accomplish mission objectives. Intensive weight and subsystem analyses, associated system studies, test program development and sterilization studies were carried on throughout, and together represented the major effort involved.

The conceptual designs that evolved early in the study showed that it was impossible to achieve, adequate landed capsule weight in the Model 3 atmosphere at entry angles as steep as -90 degrees. The possible remedies for the critical weight situation were: 1) use of shallower entry angles, 2) increase of probe/lander diameter, 3) utilization of a supersonic parachute, 4) reduction of parachute opening altitude, 5) reduction of landed instrumentation requirements,

6) reduction of the probe/lander shell weight fraction. It was felt that adoption of the shallow entry angle condition, together with a strong effort to achieve a shell design of minimum weight, were the most practical first steps to take.

Several approaches to the achievement of minimum weight were followed. The first was to adopt minimum-weight shell materials (heat shield and structure) for each configuration, at the expense of manufacturing ease and cost. Thus, for example, the shell structure selected for the large angle cone -- a light-weight sandwich of stainless steel honeycomb bonded between beryllium face sheets -- was selected for its low weight, despite the fact that it required manufacturing development.

The second step was the examination of concepts for the entry shell which were lighter than the multi-mission shell, but less versatile. These concepts were:

1. <u>Multi-mission Structure and 1971 Heat Shield</u>

   The structure of this shell is the same as that for the multi-mission shell, but the heat shield is designed for the lower capsule entry weight of the 1971 mission. This concept has much of the mission flexibility of the multi-mission shell concept without the attendant severe heat shield weight penalty for the 1971 mission.

2. <u>1971 Entry Shell</u>

   The structure and heat shield are designed for the weight, entry and atmosphere conditions of the 1971 mission. This approach yields the minimum-weight shell that can be employed for this opportunity only.

3. <u>Model 3 Entry Shell</u>

   This shell is designed to accommodate the heavy capsule weights of future missions under the assumption that the Model 3 atmosphere is determined to be the reference atmosphere. Comparison of this shell weight with the multi-mission shell and structure allows determination of the potential weight penalty for future missions that the use of a multi-mission shell concept would engender.

Concept 1, above, was selected after an evaluation showed the multi-mission structure and 1971 heat shield to be sufficiently lighter than the multi-mission shell concept (because of the reduced heat shield weight) to warrant its selection. After analysis, the weight saving on Concepts 2 and 3 were deemed to be insufficient to warrant abandonment of the practical advantages a multi-mission structure would have.

At the time the shell concept was changed from that of a multi-mission shell to that of a multi-mission structure and 1971 heat shield the 40 millibar (Model 1) atmosphere was eliminated as a design requirement, based on early indications from Mariner IV. This had the effect of reducing the required heat shield weight, since operation in the densest atmosphere governs that weight.

Comparison of the tension shell, blunt cone and modified Apollo configurations after adoption of the weight-saving measures showed the blunt cone to have a small weight advantage over the tension shell and the modified Apollo shapes. While the weight difference was not sufficient to warrant selection of the blunt cone, the added advantages of better stability and greater flight experience led to its selection for the reference design.

The allowable entry weight of the system was further increased by restricting the maximum entry angle to -45 degrees thereby increasing the allowable capsule M/C_DA and hence payload.

The increased payload weight resulting from these several compromises in the capsule mission flexibility resulted in a barely feasible weight limited design.

In an attempt to recapture the reduction in allowable M/C_DA that attended the drop in surface pressure estimates, the use of a two-chute system (supersonic drogue parachute and subsonic main parachute) was examined parametrically, together with an assessment of the effect of reducing the parachute deployment altitude below the original design value of 15, 000 feet. These studies showed that while altitude reduction and use of the supersonic parachute were of great benefit, the benefits were not nearly enough to compensate for the effects of the reduction in the minimum Mars surface pressure from 10 to 5 millibars.

It was at this point that the study received major re-direction to the entry from orbit mode utilizing the Saturn V launch vehicle.

1.4 CONCLUSIONS -- ENTRY FROM THE APPROACH TRAJECTORY

The major conclusions for this portion of the study are:

1. For the currently assumed range of Mars surface pressures ($<$ 10 millibars) deployment of large payload capsules, dependent only on ballistic retardation, is not practical

2. For the previously assumed minimum surface pressure of 10 millibars, deployment of large payload capsules would be practical with the use of a supersonic parachute

3. Hard-landed capsules of the size necessary to meet the mission objectives of this study (approximately 600 pounds) would be difficult to develop and such development is not recommended for landed payloads of moderate complexity.

After analysis and evaluation of many hard-lander concepts, it has been concluded that the problems of developing a wide gamut of g-hardened instrumentation and, the relatively large crushup structures involved and the difficulty of multiple deployments of instruments, are sufficiently formidable to make the hard-landed concept unattractive as a fundamental design approach, unless it is necessary to develop this technique for future missions. It must be emphasized that this conclusion does not apply to a very simple landed capsule with one or two instruments, but only to those of the class called for by the objectives of this study.

2.0 SYSTEM DESIGN SUMMARY

This section and Section 3.0 summarize the design for the entry from the approach trajectory mission mode. In this design the ground rules are as listed in Section 1.2 except that: 1) the Model 1 atmosphere (40 mb) is eliminated as a specification, which leaves Models 2 (25 mb) and 3 (10 mb) as the design atmospheres, and 2) the multi-mission structure and 1971 heat shield concept is used in place of the multi-mission shell. (See paragraph 1.3.)

2.1 SYSTEM OPERATION

The flight spacecraft serves as a transport vehicle for the flight capsule until 12 days prior to encounter, when the two are separated and the capsule is deflected to a planet impact trajectory. From this time through the mission phases of ballistic entry, parachute descent, landing and a 24-hour surface mission, the flight capsule operates independently. Communications is by means of a relay link to the flight spacecraft during entry and a direct link to the DSN on Earth after landing.

After entry and ballistic retardation, and when a Mach number of 1.3 is reached, a parachute system is deployed to further reduce velocity at impact, At an altitude between 19,000 feet and 98,000 feet, depending upon atmosphere, the action of parachute deployment in a reefed condition separates the entry vehicle shell from the landed capsule which then descends on the parachute. The parachute is disreefed at 16,000 feet.

The landed capsule is of an oblate spheroid shape and is composed of an internal payload section completely surrounded by an omnidirectional passive impact attenuator which is employed to protect the landed equipment from impact velocities which can be as high as 130 ft/sec. These impact velocities can result from a postulated maximum wind velocity of 100 ft/sec in combination with an 80 ft/sec descent velocity. Under design conditions, the maximum impact load to be sustained by the landed capsule will be 500 Earth g.

After impact the attenuator is deployed by shaped charges to expose and deploy instrumentation. Since the oblate spheroid shape has two preferred landing orientations, the landed capsule is provided with duplicate instrumentation and antennas. The proper set to be activated is determined by a simple g-switch.

After deployment of instruments which primarily measure atmospheric properties, data are transmitted to Earth via an S-band direct link at about 2 bps whenever Earth is in view during the first day after landing.

2.2 DESIGN DESCRIPTION

For illustrative purposes the design is shown in several figures, each of which highlights one or more major subsystems.

2.2.1 Flight Capsule Launch Configuration

The flight capsule in the launch configuration is shown in Figure 1. Shown is a 60-degree blunt cone entry shell containing the oblate spheroid landing capsule. The significant features are the sterilization canister and flight capsule - flight spacecraft adapter. The sterilization canister consists of a lid that is jettisoned prior to flight capsule separation, and a base, which is attached to the flight capsule - flight spacecraft adapter. Each part of the canister is constructed of thin-sheet aluminum. The base has two main sections - an outer annulus conical section,and an inner circular section. These sections are welded together at their intersection with the flight capsule - flight spacecraft adapter. The base and lid are also welded together at the outer rim as the final step in the assembly. The result is a completely welded shell, providing a biological barrier for the sterile flight capsule.

Separation of the lid is accomplished by a flexible linear shaped charge housed in a ring on the outer rim of the canister.

A pressurization control device (located within the canister) maintains a small positive internal pressure (~ 1 lb/in^2) across the sterilization canister from assembly to just before separation to assure sterility of the flight capsule. Checkout of the flight capsule telecommunications subsystem prior to separation is accomplished through a parasite monopole antenna through the sterilization canister near the VHF antenna on the suspended capsule.

Separation of the flight capsule is accomplished by four pin-puller release mechanisms and eight springs located at the interface of the flight capsule - flight spacecraft adapter and the afterbody of the entry vehicle. The adapter is a monocoque structure with rings at both ends for mounting to the flight spacecraft and the entry vehicle via the separation mechanism. A backup separation system is also located on this adapter near the flight spacecraft interface to be used in case a failure occurs in the nominal separation sequence. The backup separation is required because spacecraft orbit injection is not possible with the additional weight of the flight capsule.

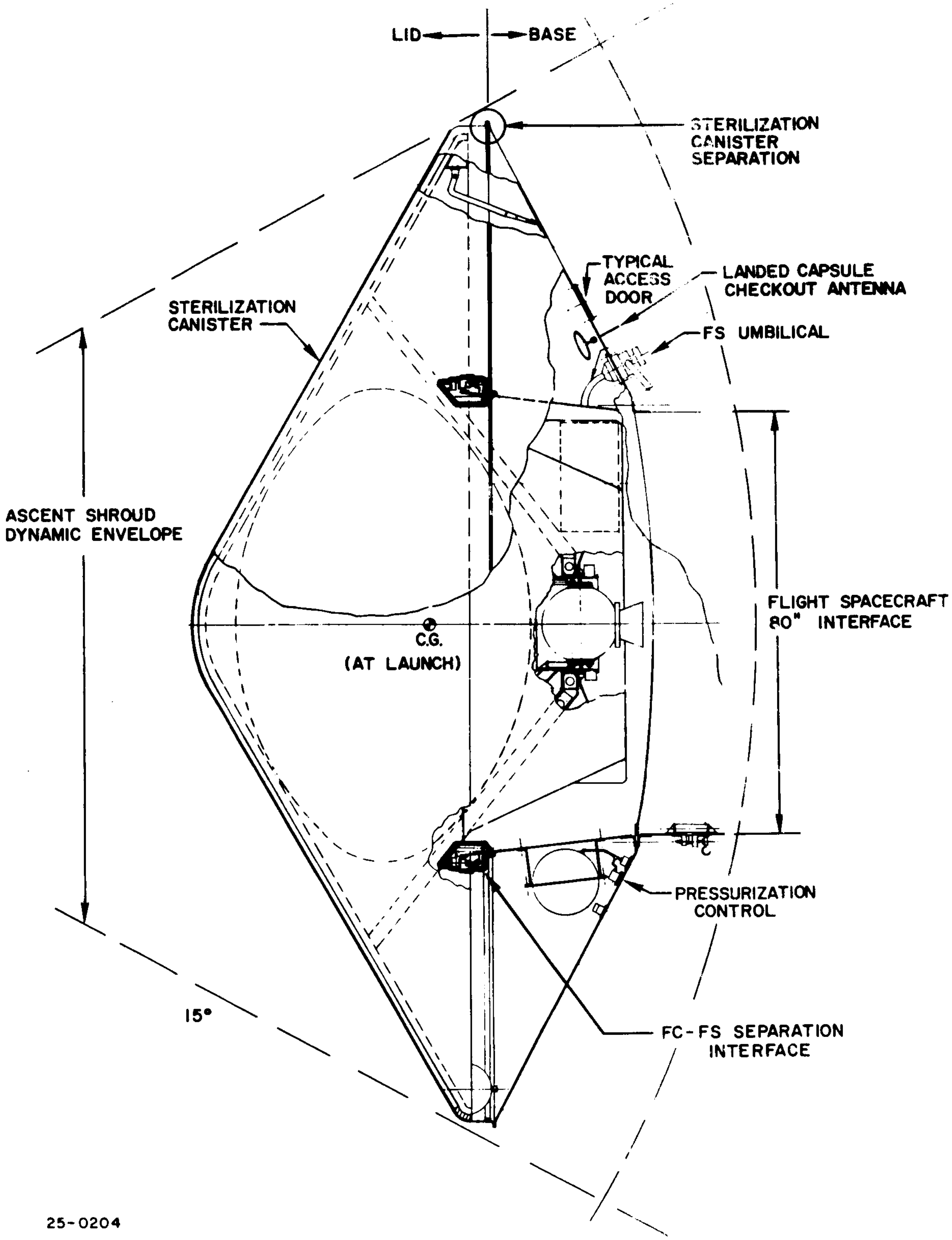

Figure 1 FLIGHT CAPSULE LAUNCH CONFIGURATION

The envelope constraints of the Saturn-Centaur ascent shroud and the specified flight capsule interface diameter of 80 inches are also shown in Figure 1.

2.2.2 Attitude Control and ΔV Propulsion Subsystems

Post-separation attitude maneuvering and thrust vector control of the flight capsule is accomplished by a cold-gas ACS system. This system uses 12 nozzles to produce attitude control torque in couples about each of the 3 axes. The nozzles are arranged in two independent systems fed by independent gas supplies and regulators. If either system fails, the other system can complete the mission. The location of this system is illustrated in Figure 2.

The cold-gas supply is maintained in two sets of spherical tanks located near the base ring of the entry shell. Each set of tanks (two spheres) feeds six nozzles. Although the two spherical tanks were originally employed in each set to reduce the projected area on the entry shell, additional redundancy is provided by this design feature. After ΔV thrusting, the flight capsule is maneuvered to the proper flight attitude for zero angle of attack at entry and spin stabilized (10 rpm) at that attitude by 2 spin rockets.

If an ACS failure is detected during the preseparation checkout, a flight spacecraft attitude maneuver is used rather than the flight capsule attitude maneuver. After the spacecraft has maneuvered to provide the appropriate thrust application direction, the capsule is separated and immediately spin stabilized at 40 rpm to provide thrust vector control during the application of ΔV propulsion. The capsule remains spinning in this attitude until entry. Eight despin rockets reduce the spin rate to about 10 rpm early during entry to avoid the destabilizing effect of large spin rates during entry. The spin and despin rockets are located around the periphery of the entry shell base ring as shown in Figure 2.

The ΔV propulsion rocket which is located on the suspended capsule afterbody is jettisoned, along with the ACS electronics, after final vehicle spin stabilization. A simple marmon clamp is used to release the package; four springs provide the required separation impulse.

2.2.3 Antenna Subsystems

Flight capsule antennas are required for telecommunications to the flight spacecraft and directly to the DSIF stations on Earth, and for the radar altimeters. The VHF relay communications link antenna is located on the suspended capsule afterbody as illustrated in Figure 3. This antenna is used for communications to the flight spacecraft from separation until impact. After impact S-band direct link communications antennas located within the landed capsule are used for communication directly to Earth.

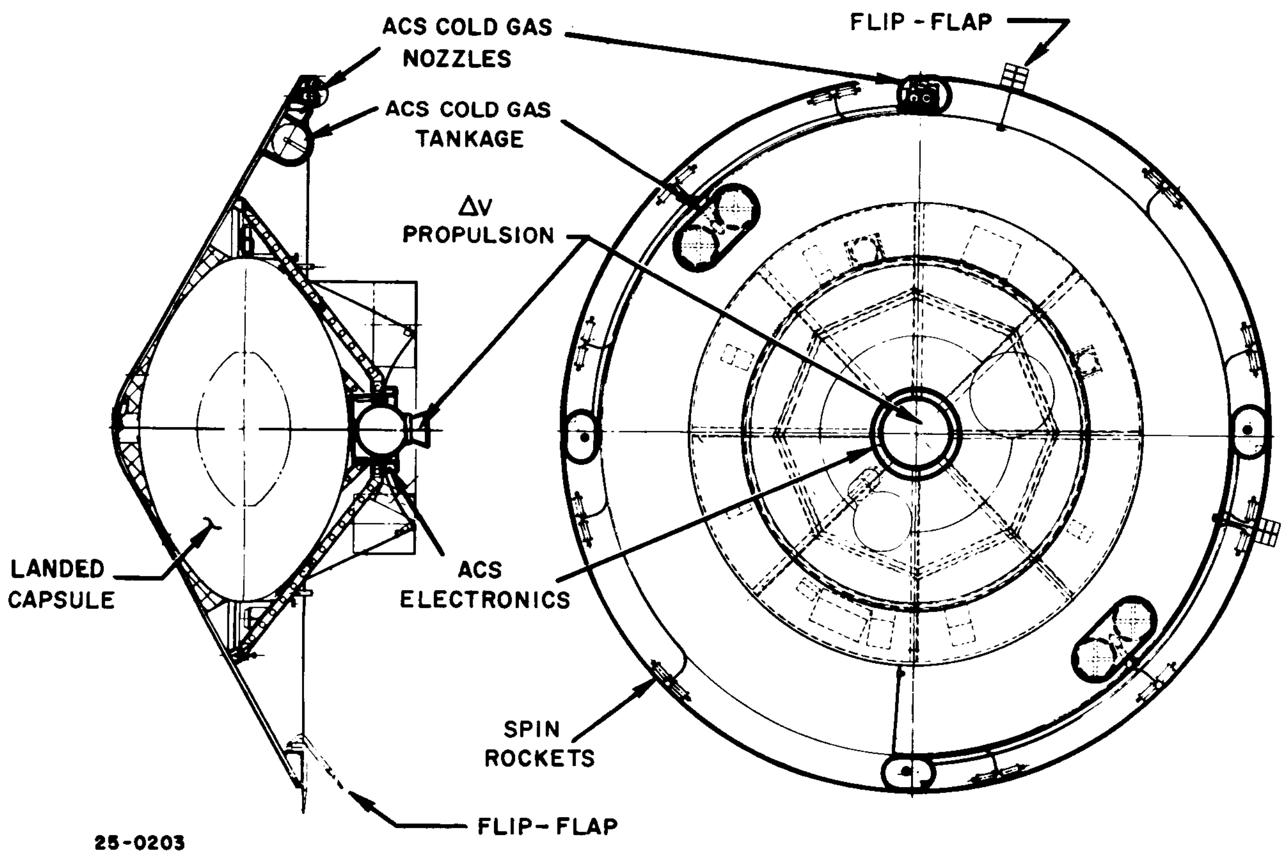

Figure 2 ATTITUDE CONTROL AND ΔV PROPULSION SUBSYSTEMS

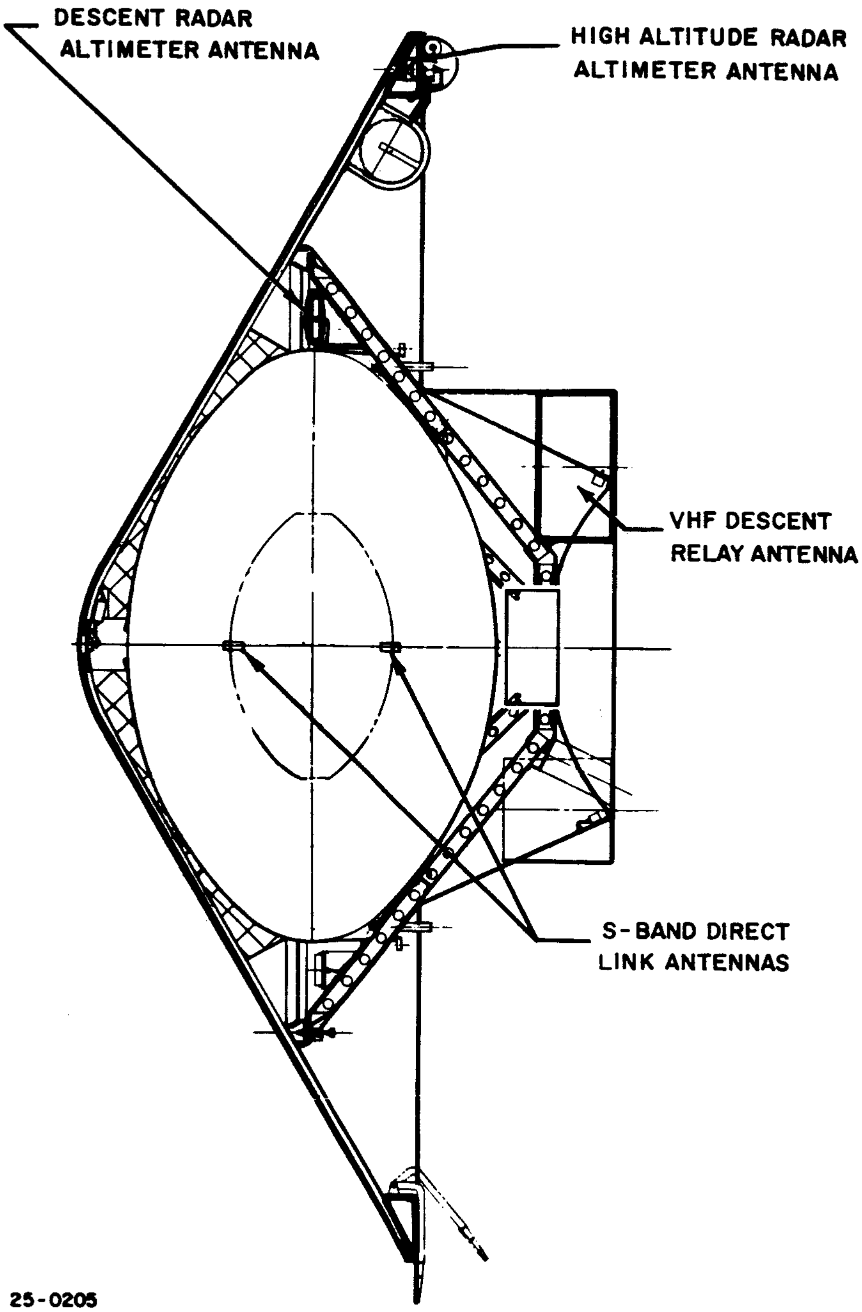

Figure 3 ANTENNA SUBSYSTEMS

Two altimeters are used on the flight capsule. One for high altitude measurement, prior to entry shell jettison, and one for low altitude measurements after entry shell jettison. The high altitude altimeter utilizes the entry shell structure as an antenna by exciting the outer ring. The low altitude altimeter uses a crossed slot cavity backed antenna located on the suspended capsule structure near the landed capsule. Both systems are used as altitude reference for the instrumentation and as event indicators for parachute deployment and instrumentation deployment.

2.2.4 Suspended Capsule Structural Arrangement

The basic suspended capsule structure consists of eight equally spaced radial beams reinforced by three rings at the entry shell separation interface, the flight capsule - flight spacecraft adapter interface, and the ΔV propulsion separation interface. These beams are covered by a thin shell coated with a cork heat shield for thermal protection from wake heating during entry. This arrangement is shown in Figure 4.

Protruding from the afterbody and mounted to the radial beams are the VHF antenna cavity and the parachute subsystem. Each is surrounded by a local nacelle for aerodynamic contouring and thermal protection.

The pilot parachute and main parachute containers are mounted together between a pair of radial beams. The main parachute harness is attached to four of the radial beams at the flight capsule - flight spacecraft adapter interface ring. The four harness straps are joined at a swivel joint to the main parachute riser line. The parachute opening shock loads are transmitted directly to the primary suspended capsule load carrying structure.

Four pin-puller release mechanisms, at the suspended capsule interface with the entry shell implement separation of the entry shell at peak parachute opening load. Eight straps located around the landed capsule provide the support for the landed capsule after entry shell jettison. During entry, a bearing pad on the entry shell supports the landed capsule. At approximately 500 foot altitude, these straps are released and the landed capsule is dropped on a tether line to minimize the possibility of the parachute enveloping the landed capsule at impact. The tether line is severed at landed capsule impact allowing the parachute to drift away.

The descent instrumentation, telecommunications and power supply equipment are located in the toroidal cavity formed by the radial beam network and the landed capsule.

The entry shell structure is a light-weight sandwich of stainless steel honeycomb bonded between beryllium face sheets. The honeycomb and face sheet thicknesses are 0.60 and 0.025 inches, respectively. Each face

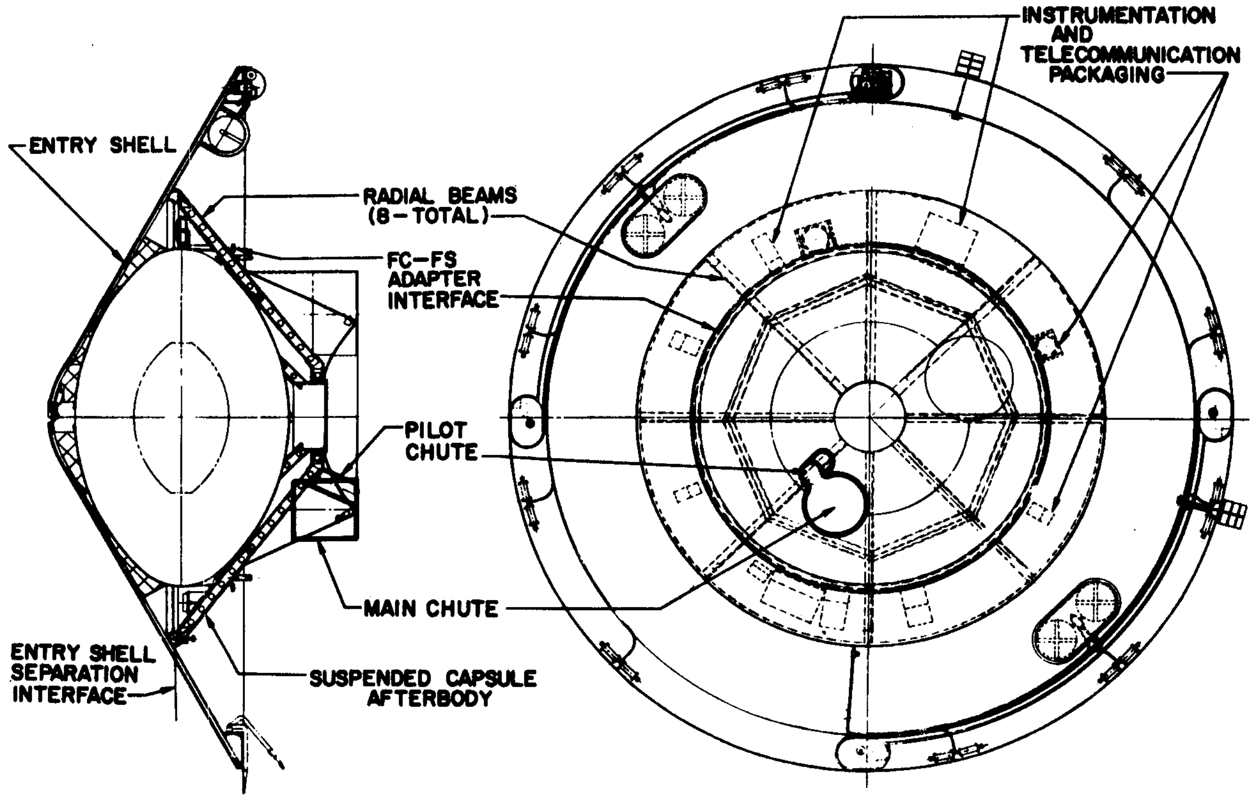

25-0207

Figure 4 SUSPENDED CAPSULE STRUCTURAL ARRANGEMENT sheet is divided into 18 radial gores. The entry shell is assembled by bonding two 3-gore face sheet sections to a radial section of honeycomb core. Six such sections are then welded together to form the complete entry shell. A stainless steel closeout ring is welded onto the main shell. The beryllium base ring is composed of extruded angles and flat sections riveted together and to the stainless steel closeout ring. An extruded angle suspended capsule mounting ring is also riveted directly to the entry shell through beryllium spacers previously mounted within the stainless steel core.

2.2.5 Landed Capsule

The functions of the landed capsule are to absorb the kinetic energy of impact, to deploy the instruments, and to measure and transmit engineering and scientific data. The oblate spheroid shape facilitates preferred orientation of the landed capsule after impact (two preferred rest orientations). The preferred orientation is desired to alleviate the problems of instrument deployment and antenna pointing associated with random orientation of the landed capsule after touchdown. The two probable orientations of the oblate spheroid are accommodated by providing duplicate instruments and antennas installed in opposing positions in the landed capsule. Only the set of equipment which is in the proper attitude after landing is used. The duplicate equipment is shown in the inboard profile of Figure 5.

A crushable material impact attenuator protects the landed capsule from the high velocity impact. The crushable material is reinforced fiberglass honeycomb with polyurethane foam-filled cells. The thickness varies from 15 inches on the flat faces to 23 inches on the torroidal edges to limit the impact loads to less than 500 Earth g. The impact attenuator is assembled in three layers of material bonded to thin fiberglass sheets. The honeycomb cells are radially oriented to provide maximum energy absorption. A thin layer of balsa wood is provided on the inside surface of the main impact attenuator to provide protection against sharp objects.

The central section of the landed capsule contains instrumentation, telecommunication and power supply modules. Each module, composed of selected equipment, is treated as an independent unit to facilitate assembly and checkout. Electrical connection to the suspended capsule is provided through one side of the landed capsule as shown in Figure 5. At landed capsule release from the suspended capsule this line is severed by a cable cutter. In the center of each face of the landed capsule, a small S-band V-horn antenna is provided for direct-link transmission to Earth.

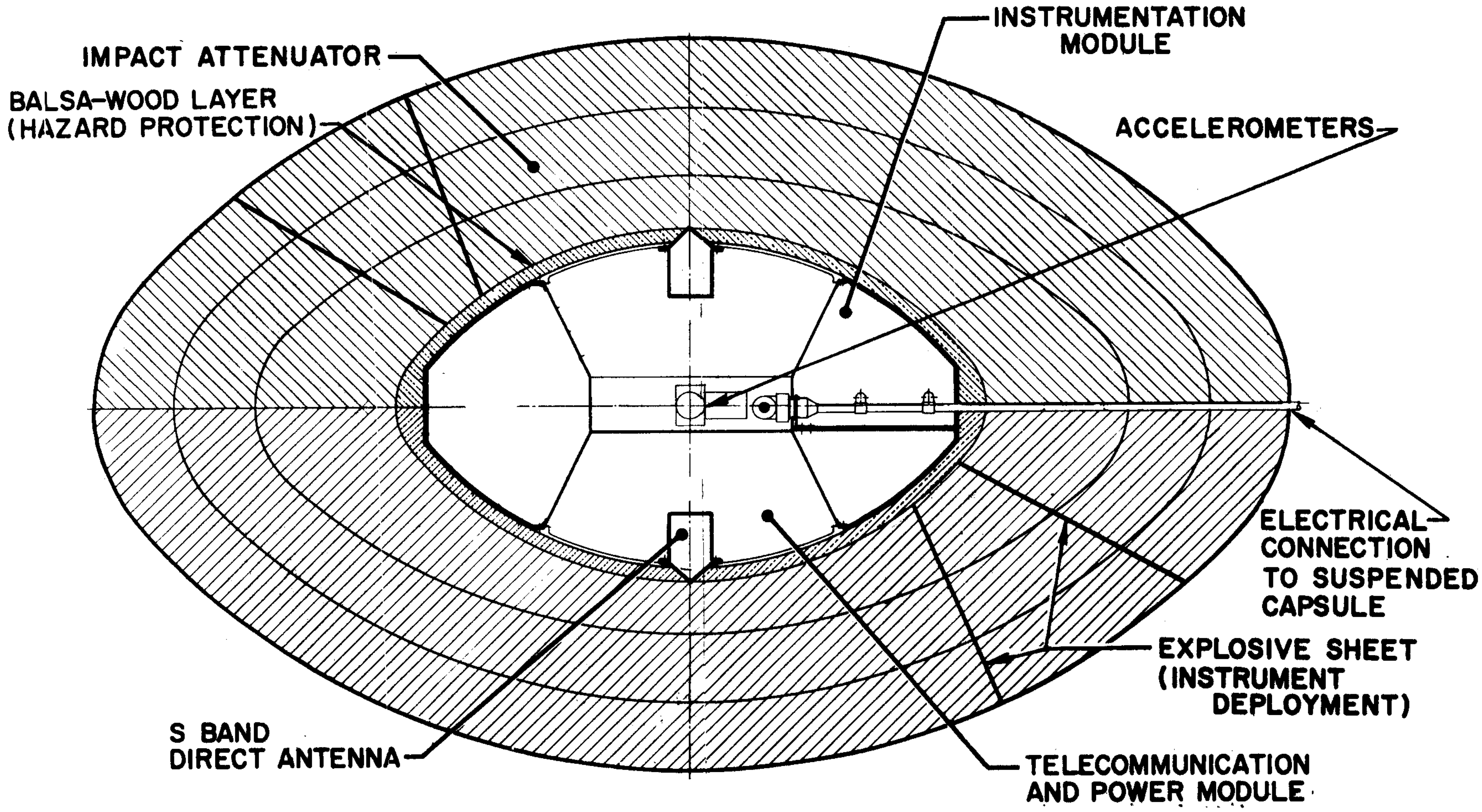

Figure 5 OBLATE SPHEROID LANDED CAPSULE

2.3 FLIGHT OPERATIONAL SEQUENCE

The flight operational sequence of the flight capsule for the interval from planetary encounter aboard the flight spacecraft to completion of the surface mission involves thirteen primary functional operations. The functional operations for entry into the Model 3 atmosphere are summarized below in order of occurence.

a) The sterilization canister lid is jettisoned

b) The entry vehicle is separated from the flight spacecraft

c) The entry vehicle is reoriented to the proper thrust application angle by the cold-gas ACS

d) Thrust is applied to place the entry vehicle on an impact trajectory using the cold-gas ACS for thrust vector control

e) The entry vehicle is again reoriented to the desired entry angle of attack (α_e = 0 degrees)

f) The entry vehicle is spun-up to 10 rpm by the spin rockets

g) The suspended ΔV rocket motor and ACS electronics package are jettisoned

h) After entry, the parachute deployment sequence begins at approximately 21, 000 feet --starting with mortar ejection of the pilot parachute which then deploys the main parachute in an 18 percent reefed condition

i) At peak opening shock-load of the reefed main parachute, the entry shell is released

j) At approximately 16, 000 feet,the main parachute is disreefed and descent operations begin

k) At an altitude of 500 feet the landed capsule is released on a tether

l) At impact the tether is released and the landed capsule rolls free

m) After coming to rest, the landed capsule impact attenuator is jettisoned and instrumentation is deployed to start surface operations.

The entire sequence is illustrated in Figure 6.

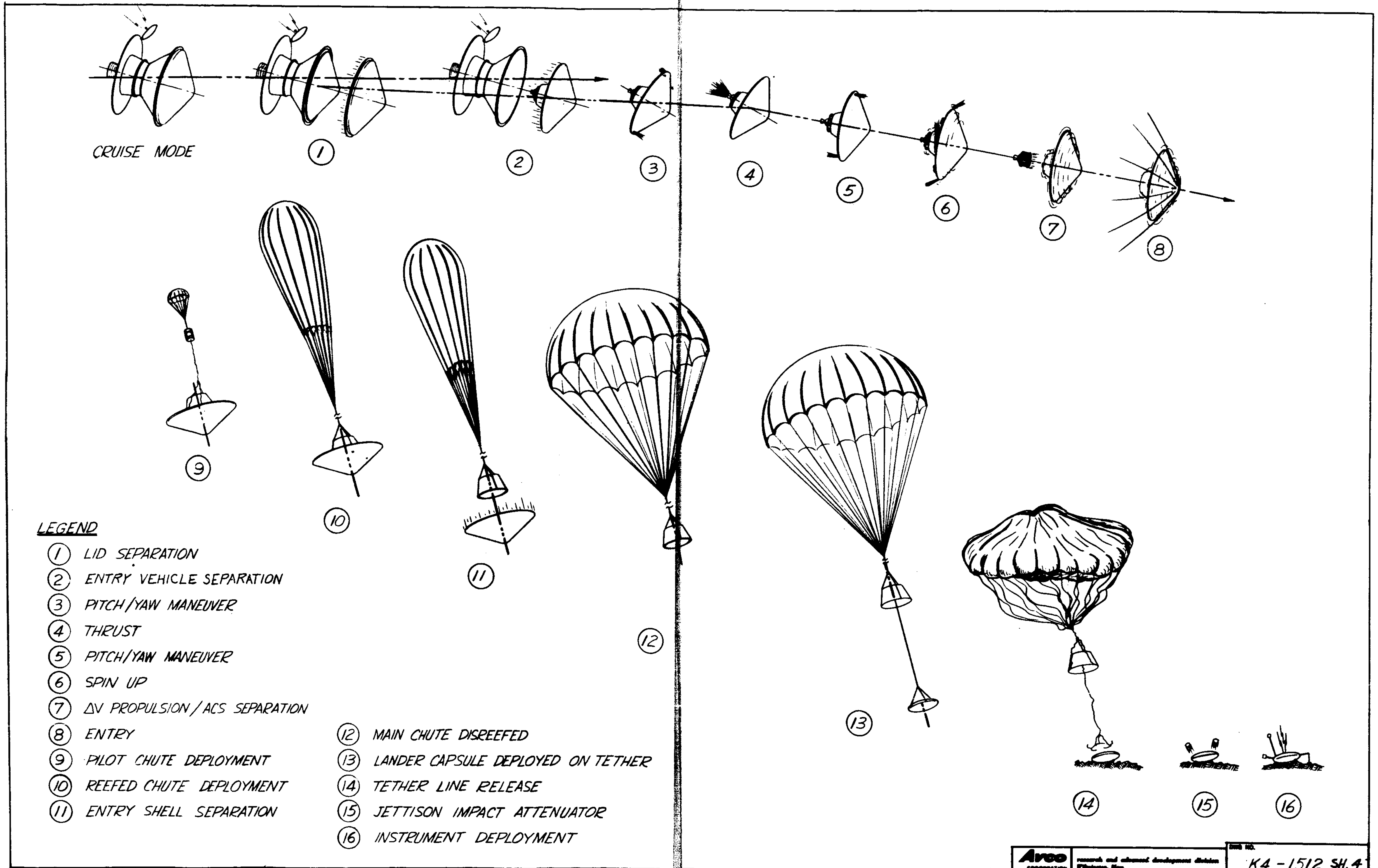

Figure 6 FLIGHT OPERATIONAL SEQUENCE

17-1

2

In case of an indication of ACS failure prior to initiation of the entry vehicle separation sequence, a backup sequence can be employed:

1) The sterilization canister lid is separated

2) The flight spacecraft is maneuvered to the proper entry vehicle thrust application attitude

3) The entry vehicle is separated

4) Immediately thereafter, the entry vehicle is spin-stabilized at 40 rpm for thrust vector control

5) Thrust is applied

6) After thrusting, the ΔV propulsion and ACS electronics packages are jettisoned.

7) The entry vehicle is despun to 10 rpm early during entry.

The remaining steps from entry to surface operation, are the same as the normal mode.

2.4 WEIGHT SUMMARY

The complete flight capsule weight summary is presented in Table I. Each major weight category represents the operational vehicle in a particular phase of the flight sequence. The separated vehicle represents the total weight at separation from the flight spacecraft. After jettisoning of the expended ΔV rocket motor and the ACS electronics package, the entry vehicle remains.

The majority of the entry vehicle weight is apportioned between the entry shell (the primary structure and heat shield), and the landed capsule (that portion landing on the surface). A 25 percent contingency factor is added to both the suspended capsule and landed capsule active payload weight. This factor will account for weight sources unpredictable at the level of analysis associated with a conceptual design.

The majority of the weight data presented in this summary were determined by analysis, however some weights for items such as, the electrical and mechanical connectors, thermal control coatings and several structural elements were estimated.

The weight summary shown in Table I allows little contingency weight for the entry shell and no weight available for growth of the flight capsule mission. As such, this design is marginal for use in the Model 3 (10 millibar) atmosphere. However, should a higher density atmosphere prevail, a vehicle of slightly higher ballistic parameter could be designed for the entry from approach trajectory mission mode with more than adequate weight margin.

TABLE I

FLIGHT CAPSULE WEIGHT SUMMARY
(OBLATE SPHEROID LANDED CAPSULE)

	Weight (pounds)		c. g. * (inches)	I_{xx} (slug-ft^2)	I_{yy}
Flight Capsule		2500.0	42.2	1259.1	861.3
FC-FS adapter	100.0				
Sterile canister	366.9				
Electrical and mechanical connectors	50.0				
Separated Vehicle		1983.1	38.0	809.5	561.6
ΔV propulsion	98.5				
ACS electronics	10.0				
Spin propellant	2.1				
Propulsion supports	10.0				
Miscellaneous	12.5				
Entry Vehicle		1850.0	35.6	808.9	526.3
Entry shell heat shield	290.0				
Entry shell structure	451.2				
Thermal control	25.0				
ACS nozzles, tanks, etc.	69.3				
Spin rockets and supports	10.0				
Electrical and mechanical connectors	55.5				
Contingency	23.0				
Suspended Capsule		926.0	41.6	139.3	140.7
Instrumentation	35.3				
Telecommunications	20.6				
Power	33.0				
Miscellaneous	4.6				
Contingency (25 percent on above)	23.1				
Parachute	74.0				
Structure	120.0				
Afterbody heat shield	21.0				
Landed Capsule		595.0	32.0	39.3	39.3
Impact attenuator	215.0				
Electrical and mechanical connectors	15.5				
Internal Weight		364.5			
Instrumentation	48.0				
Telecommunications	98.7				
Power	70.1				
Miscellaneous	2.0				
Contigency (25 percent on above)	54.7				
Thermal control	15.0				
Structure	76.0				

*Note: Center of gravity (c. g.) location is from the entry shell nose.

3.0 SUBSYSTEM DESIGN SUMMARY

3.1 COMMAND AND CONTROL

All flight capsule timing, sequencing and associated computational activities are performed by the central computer and sequencer subsystem (CC&S). This subsystem, comprised of an external CC&S and an internal CC&S, initiates events by providing properly sequenced outputs to the other flight capsule subsystems. The four sequences (separation, cruise, entry-descent, and landed) can be characterized by the mission phases they control as indicated in Table II.

The external CC&S, which controls all events occurring from 240 minutes before separation until impact, is located outside the landed capsule in the external payload. The cruise sequence, the main external CC&S sequence, is initiated by command from the mission operations system (MOS) through the flight spacecraft CC&S. The flight capsule external CC&S separation sequence is immediately initiated by the cruise sequence. The entry-descent sequence is initiated by a cruise sequence output nominally 5 minutes before entry at which time the entire entry-descent system is activated. The internal CC&S landed sequence is initiated by an impact accelerometer.

All sequences are also initiated by functionally redundant backup signals. During periods when functionally redundant initiation is not possible, a direct-link command from Earth is used as a backup. This capability, however, only exists during periods of the day when there is mutual visibility between the landed capsule and the DSN stations on Earth. These sequences are summarized in Table II which presents the major events in each sequence, and the prime and backup means of initiation.

3.2 SCIENTIFIC AND ENGINEERING INSTRUMENTATION

The scientific and engineering instruments for this mission, as presented in Table III, were selected to provide the data necessary for the design of future flight capsules (engineering objectives) and to provide the data required for the design of future experiments which would more fully define the nature of Mars, including its biological, geological, and meteorological phenomena both past and present (scientific objectives).

The ground rules governing the instrument selection required that: (1) no consideration be given to television experiments, active life detection experiments, and mobile landers; (2) all instrumentation survive the qualification and mission environments; and (3) all instruments be available for test in prototype form by 1 September 1966.

The most important objective of the mission was to measure the atmospheric density profile. This information is essential for the optimized design of entry

TABLE II

CENTRAL COMPUTER AND SEQUENCER SEQUENCES

Sequence	Event	Prime Initiation	Backup Initiation
A. External CC&S			
Separation	Pre-separation checkout Multiple ACS operations ΔV rocket control ΔV rocket ejection	Timer	Redundant timer
Cruise	Transmitter control Cruise checkout Entry subsystems activation	Timer	Redundant timer
Entry-descent	Data storage activation	Accelerometer	Lateral accelerometers
	Data mode switching	Inertial timer	VSWR monitor
	Parachute deployment and entry shell jettison	Accelerometer	Altimeter
	Altimeter switching	Entry shell separation loop	Entry shell redundant separation loop
	Landed capsule tethering Landed capsule release	Altimeter	Accelerometer
B. Internal CC&S			
Landed	Data mode switching Transmitter control	Timer	Direct-link command

TABLE III

SCIENCE AND ENGINEERING INSTRUMENTATION

Descent Instruments	Number Carried	Landed Instruments	Number Carried
Accelerometer	3	Force anemometer	2
Radar altimeter	1	Particle microphone	2
Atmospheric pressure probe	2	Water detector	1
Atmospheric temperature probe	2	Atmospheric temperature probe	2
Gas chromatograph	1	Atmospheric pressure probe	2
Acoustic densitometer	1	Gas chromatograph	1
Radiometer	1	Surface temperature	2
Mass spectrometer	1	Cosmic radiation	2
Beta scatter	1	Surface radiation	1
*R. F. probe	1	Alpha scatter	2
*Trapped radiation	1	Acoustic densitometer	1
		*Penetrometer	3
		*Impact accelerometer	3
		*Hot-wire anemometer	2

*Not included in reference payload.

vehicles without large design contingencies for atmospheric density uncertainties. Other important objectives included the measurement of near-surface wind velocity, of the chemical composition of the atmosphere (both major and certain minor constituents), of the physical character of the Martian surface, of surface chemical composition, of surface and atmospheric temperature, and of electromagnetic and particulate radiation fluxes. In addition, it was desirable to obtain at least preliminary data on the nature of the ionosphere, the magnetosphere and the planetary interior.

To meet these objectives the instruments shown in Table III were selected as a payload which would satisfy both the objectives and the ground rules without causing excessive flight capsule integration problems. The instruments are arranged in order of decreasing importance toward the satisfaction of the mission objectives. As the flight capsule design evolved it became apparent that weight limitations would require the removal of several instruments. The selection of the oblate spheroid shape for the landed capsule with its need for duplication of instruments requiring orientation relative to the local vertical, put further constraints on the number of instruments which could be carried. Those instruments in the table marked with an asterisk were not included in the final design. A possible shortcoming of the selected payload is that it does not contain experiments to measure directly the physical characteristics of the surface. The measurement of wind velocity and of wind-blown dust to some extent mitigate this deficiency. However, it is recommended that, in any further work on this mission concept, serious consideration be given to the inclusion of a lightweight penetrometer-type experiment. If necessary, the landed acoustic densitometer might be eliminated.

The descent and landed payloads, with the exception of the accelerometers, are physically separated and require duplication of those instruments which are to operate in both mission phases. The alternative to this weight penalty involves compromising the impact attenuation system on the landed capsule.

A quick analysis of the selected payload might lead to the conclusion that there was unnecessary redundancy in the atmospheric density and composition experiments. Actually, these experiments tend more to complement each other rather than provide pure redundancy. The state of the art in making many of the desired measurements is such that complete coverage frequently cannot be obtained with a single instrument over the desired breadth of range or components.

The major problem areas associated with the scientific and engineering instrumentation are the accelerated development schedules which will be required to have instruments ready for the testing programs, and the more general design problems associated with designing sensitive transducers to survive the high impact landing loads.

3.3 TELECOMMUNICATIONS

The telecommunications system consists of two independent data handling and data transmission systems: an external system, located outside the landed capsule and an internal system inside the landed capsule. The overall system is illustrated as a block diagram in Figure 7. The external system is used during the period between flight capsule separation and landed capsule impact on the planet's surface. It employs a VHF relay-link mode of data transmission. The internal system is used exclusively during the post-impact mission and uses a direct-link mode of data transmission. Since the external system is jettisoned at impact, interface between the two systems must be minimized. Accelerometers inside the landed capsule (near the entry vehicle center of gravity) provide information during entry and therefore must be connected to the external system. The use of the internal system direct link to provide redundant transmission of entry data after landed capsule impact requires connection between the internal and external telemetry systems.

The data handling function for each system is split into two data handling sections and one storage section. The data handling sections are the data-automation subsystem and the telemetry subsystem. The data automation equipment handles all scientific instrumentation, while the telemetry subsystem handles all engineering data, since the data acquisition requirements of the two data sources are dissimilar. The science-instrumentation package is also more susceptible to change than engineering requirements; therefore, a less complex interface results from use of two subsystems. A failure in either subsystem will not compromise operation of the other.

The external and internal radio subsystems are quite dissimilar. The external relay-link system operates at approximately 270 MHz, employs a 30 watt solid-state transmitter and utilizes a frequency shift keying (FSK) modulation technique. The internal direct-link system transmits at 2295 MHz, utilizes a 20 watt traveling-wave tube (TWT) and employs a multiple frequency shift (MFS) or linear chirp modulation (LCM). A command receiver is incorporated in the direct-link radio subsystem to allow landed capsule control flexibility during surface operation.

A brief resume of the telecommunications system salient design and performance characteristics is presented in Table IV.

3.4 POWER

The power subsystem consists of two independent battery-load voltage regulator systems -- an external system mounted on the suspended capsule structure and an internal system within the landed capsule. The external and internal systems are used before and after impact. In addition, a charge regulator, located in the flight spacecraft, controls charging of the flight capsule power supplies by the flight spacecraft power system. The power subsystem is illustrated in the block diagram in Figure 8.

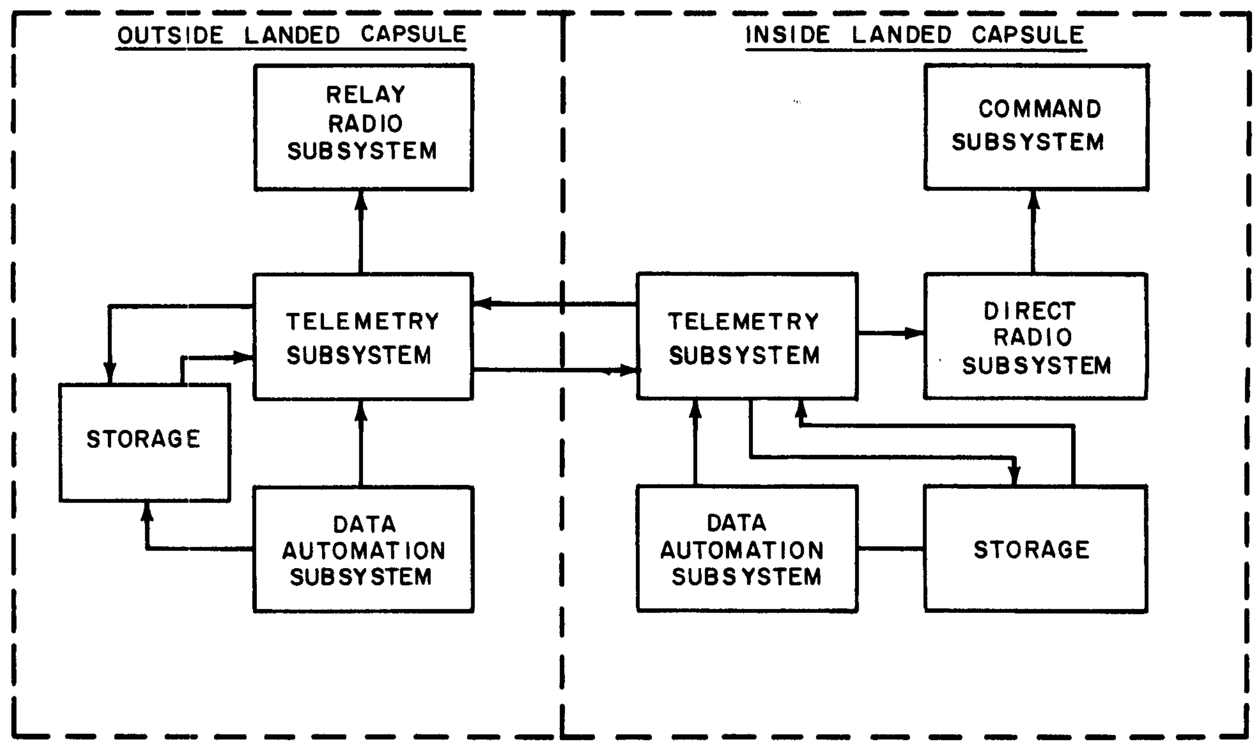

86-1638

Figure 7 TELECOMMUNICATIONS SUBSYSTEM

TABLE IV

TELECOMMUNICATIONS CHARACTERISTICS

External System	
Mode of transmission	Relay via flight spacecraft
Transmitter power	30 watts
Frequency	270 MHz
Modulation	FSK
FC antenna type	Spiral
FS antenna type	Helix (body fixed)
FS receiver noise figure	5 db
Data rate	64 bits per second
Internal System	
Mode of transmission/reception	Direct with Earth
Transmitter power	20 watts
Frequency	
Transmit	2295 MHz
Receive	2115 MHz
Modulation	MFS or LCM
Antenna Type	V Horn
Data Rate	2 bits per second

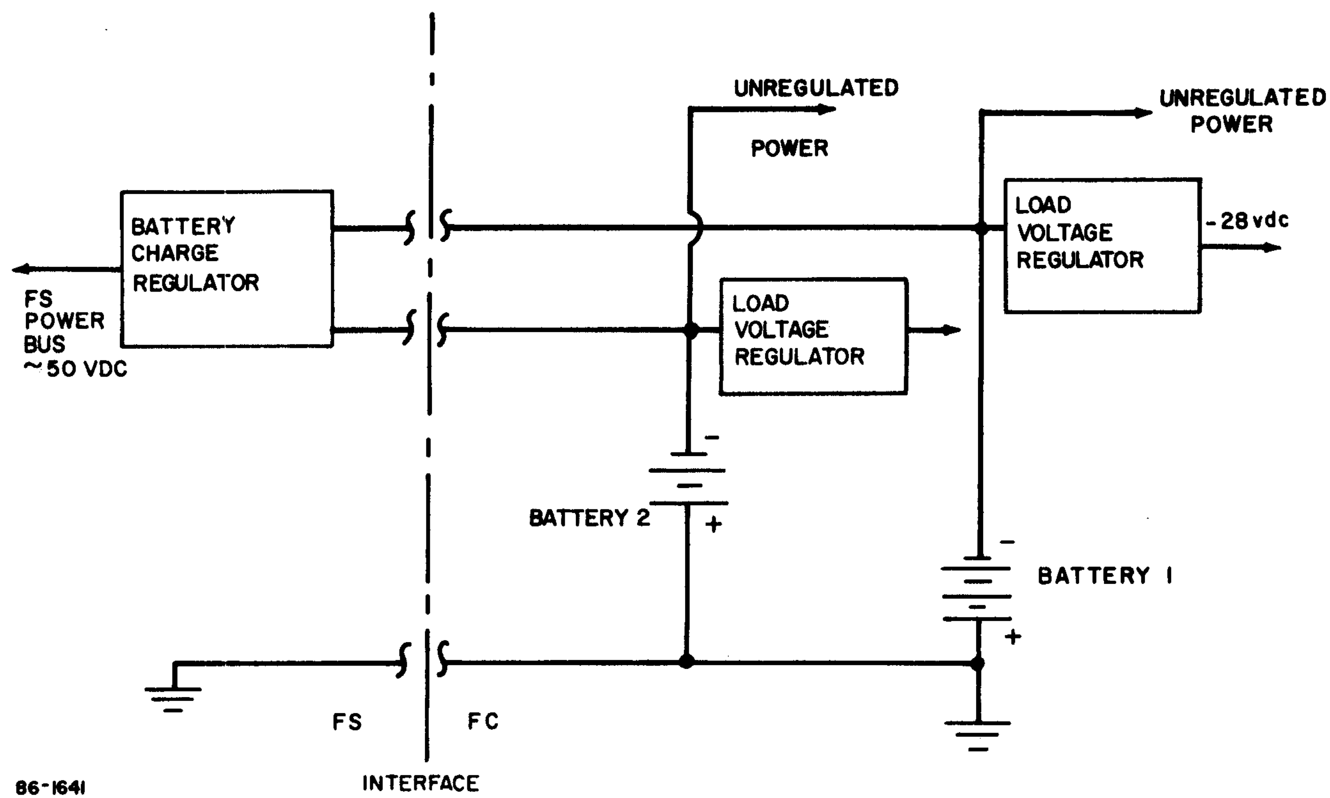

Figure 8 POWER SYSTEM CONFIGURATION--BEFORE SEPARATION

The recommended power source is two batteries each of which consist of 24 hermetically sealed nickel-cadmium connected in series. The cells are packaged in unsealed containers to facilitate mounting and thermal dissipation. Design capacity for the two batteries is 12.5 amp-hours (350 watt-hours) and 35.7 amp-hours (980 watt-hours). Output voltage limits before regulation are 25 to 33 vdc. The weight of the batteries is 116 pounds and the volume is 1.04 cubic feet. A nickel-cadmium battery was selected after study of available data on heat sterilization of silver-zinc cells, other battery types, an RTG and a fuel cell system. It is recommended that development of the lithium chlorine fuel cell system be given early attention because of the potential weight savings and other operational advantages.

Except for the radio transmitters, power to all users is voltage regulated dc. This is provided by two "buck-boost" load voltage regulators. These regulators are able to accept input voltages above or below the required output level allowing most of the battery capacity to be used.

Charge control is achieved by a simple continuous trickle-charge regulator arranged to provide an equivalent 100 hour charging rate. Provision is made for cutoff should the battery temperature exceed operating limits.

3.5 PROPULSION

The propulsion subsystem consists of a solid propellant rocket motor, which is fired to alter the flight capsule approach trajectory to impact the planet. The rocket firing is controlled by the flight capsule CC&S, which stores the start time and duration commands, updated as needed through the DSN-to-planetary vehicle-to-flight capsule communication link. After the attitude control subsystem has positioned the flight capsule in the correct firing attitude, at the prescribed time, the rocket is ignited by an electrical signal originated in the flight capsule CC&S. Thrust termination is controlled by a flight capsule integrating accelerometer which measures the ΔV attained. A backup control is provided by the flight capsule CC&S, when the proper burning time has been realized. Thrust termination is followed by the jettisoning of the expended motor.

A solid propellant rocket motor was selected over a liquid propellant system because of cost, reliability, sterilizability, ease of packaging, space storability, and the requirement for only a single firing.

The rocket motor is a modified Titan vernier motor (TE-M-345). The primary modification consists of replacing the present propellant with a sterilizable propellant (TP-H-3105). The motor has a total impulse capability between 255 lb-sec and 16,320 lb-sec because of its thrust termination feature. The required total impulse of 6100 lb-sec nominal results in a ΔV of 100 ft/sec, while the total impulse available results in a ΔV capability of 270 ft/sec. The stored total impulse capability may be reduced, if desired, to 137 ft/sec by off-loading propellant, which reduces the rocket motor total weight by approximately 30 pounds. The rocket motor operates at an average thrust level of 768 pounds with a specific impulse of 255 seconds.

The Titan vernier motor is spherical in shape, 13.5 inches in diameter, and 18.6 inches long, having a TH-1050 stainless steel case. The exhaust nozzle is partially submerged with an area ratio of 18.7, and is made of vitreous silica-phenolic. The nozzle is retained in the motor case by a split flange, which is held together by two explosive bolts. On receipt of an electrical signal the bolts are released, the flange separates, and the nozzle is blown free of the case resulting in a sudden drop in chamber pressure, which terminates thrust. The motor is mounted in the flight capsule using existing mounting flanges on the Titan vernier motor. The total loaded weight of the propulsion subsystem is 81.0 pounds, with a propellant mass ratio of 0.788.

3.6 ATTITUDE CONTROL

Attitude control is accomplished by a combination of an active cold-gas system together with spin stabilization. The active system uses body-mounted rate gyros for reference attitude information. After separation, the active system attitude-stabilizes the entry vehicle to remove the disturbances which occur during separation and then orients the entry vehicle to the thrusting attitude. The active system maintains this attitude during thrusting, and after thrust termination reorients the entry vehicle to the attitude desired at entry. After orientation to the entry attitude, solid propellant rockets are used to spin stabilize the entry vehicle for the remainder of its trajectory until entry.

The body-mounted gyros measure angular rates of the entry vehicle and the gyro outputs are electronically integrated so that angular position as well as angular rate is available. This information is used by the control logic to operate the valves of the cold-gas reaction control system. The reaction system provides 3-axis control torque in couples through 12 nozzles. Spin stabilization is provided by two groups of solid propellant rockets. Normally only one group of two rockets is required for spin stabilization at 10 rpm, but if the primary operational mode of the ACS fails, a second group of six spin rockets are used in addition to the primary group for the backup mode. (The backup mode requires that the flight spacecraft maneuver to the proper flight capsule thrusting attitude. Immediately after separation, the flight capsule is spun-up to 40 rpm for thrust vector control during engine firing. In this case it is necessary to despin prior to entry, and a third set of rockets is provided for that purpose.)

The ACS gyros and electronics will be turned on for warmup, checkout and drift-check prior to separation.

3.7 PARACHUTE

The parachute subsystem consists of a single subsonic main parachute, a pilot parachute, ejection equipment and an initiation device. The main parachute is an 85 foot diameter, ring-sail parachute deployed at Mach 1.3. Parachute size is based on a suspended weight of 924 pounds impacting at 80 ft/sec in the "terminal descent atmosphere". The parachute is reefed to 18 percent of the projected area at deployment to minimize opening shock loads and reduce parachute weight. The pilot parachute is a 9 foot nominal diameter ring-slot type, mortar ejected at 100 ft/sec. The main parachute is ejected from its canister by the drag of the pilot parachute. In the event that this method of main parachute deployment fails, a gas generator forces the main parachute from its canister at 30 ft/sec. The initiation system consists of an accelerometer and computer which trigger ejection of the pilot parachute at a variable time interval after peak entry deceleration. The time interval is a function of the peak deceleration magnitude which is correlated to initiate deployment at Mach 1.3 under nominal environmental and operational conditions. The main parachute is disreefed at an altitude of 16,000 feet. The total weight parachute subsystem is 74 pounds.

Various parachute systems were considered before selecting the reference system. The systems under consideration were: (1) a single main parachute without reefing (Mach 1.3 deployment), (2) a two parachute drogue-main system, and (3) a cluster of main parachutes. All four systems satisfy the design constraints, however, the single main parachute with reefing was chosen on the basis of tradeoffs which considered weight, reliability, performance and developmental risk. For advanced missions requiring larger payloads, a drogue-main parachute system would probably be necessary. This system permits an increase in vehicle ballistic coefficients (M/C_DA) and associated increase in payload weight.

3.8 IMPACT ATTENUATOR

The impact attenuator consists of crushable material which completely encapsulates the landed payload. The material crushes during impact, dissipating the impact energy in the crushing process. The material is a glass cloth reinforced plastic honeycomb with its cells filled with polyurethane foam. The configuration of the attenuator (and encapsulated payload) is an oblate spheroid. The thickness of the material on the major and minor axes is 23 and 15 inches, respectively. These dimensions were determined by the impact velocity (130 ft/sec) and the requirement that the internal package experience a maximum deceleration no greater than 500 g. The impact velocity is the result of the contractually specified vertical descent velocity of 80 ft/sec and horizontal wind velocities of 100 ft/sec. Omnidirectional protection is required because of the possibility of skip impacts. The impact attenuator weight is 30 percent of the total landed weight.

A number of impact attenuators such as alternate layers of air bags and alternative crushable materials were considered. In the velocity range considered air bags of current design are heavier and less reliable than crushable materials. Plastic honeycombs which are RF transparent were preferred to metal honeycombs. The latter would require post-impact jettisoning of the attenuator to permit radio transmission from the internal package. Balsa wood is a more efficient attenuator in terms of energy absorbed per weight of material but it involves large payload decelerations.

The most critical problem area encountered at the present time is the very low density required for the crushable material. This low density provides the optimum weight fraction for the impact attenuator protecting the landed payload. This low-density material may prove difficult to manufacture and may not perform as well as tests on higher density samples indicate. In this event, balsa wood, with its attendant higher impact loads may be the necessary alternative.

3.9 ENTRY SHELL

The entry shell is defined as the primary load carrying structure together with its external coating of heat shield material. Of the three configurations studied (tension shell, modified Apollo and blunt cone), the blunt cone was selected for the reference design because of a lower entry shell weight fraction and higher confidence in the aerodynamic performance of this configuration. While the design of a multi-mission entry shell was recognized as a desirable objective, tradeoff analyses showed the combination of a multi-mission structure with a 1971 heat shield to be a more desirable entry shell for a weight limited design.

The design requirements for the entry shell are based on the loads and heating on the shell during entry for the most severe atmosphere for either requirement. The loads and heating for the blunt cone are summarized in Tables V and VI.

The primary structure must maintain its structural integrity throughout its operating sequence; i.e., from manufacture to terminal sterilization to parachute opening shock loads in the Martian atmosphere. The structure is the multi-mission design; i.e., it is designed to operate at entry velocities up to 23,800 ft/sec, entry angles of -20 to -90 degrees, entry weights up to 4500 pounds, and in Model 2 and 3 atmospheres. The structure is a honeycomb sandwich shell utilizing beryllium face sheets with a stainless steel core, chosen because of the weight advantage over the other materials and concepts analyzed.

The heat shield provides thermal protection to the primary structure and internal components during the entry phase of the mission. The reference heat shield which is designed specifically for the 1971 mission, employs cork silicone as the reference material because it yields the minimum weight design.

TABLE V

LOAD SUMMARY OF THE BLUNT CONE -- MULTI-MISSION STRUCTURE

Entry Weight = up to 4500 pounds
Entry Velocity = 23, 800 ft/sec
Entry Angle = -90 degrees
Diameter = 15 feet
Model 2 Atmosphere

	Entry Weight (pounds)	Peak Dynamic Pressure (lb/ft^2)	Peak Axial Acceleration (earth g)	Peak Normal Acceleration (earth g)	Angle of Attack at Peak Loads (degrees)
Normal Entry $\alpha_E = 0°$	4500 ($M/C_DA = 0.42$)	1152	73.3	--	--
	1391 ($M/C_DA = 0.15$)	777	161	--	--
Failure Mode Entry $\alpha_E = 179°$	4500 ($M/C_DA = 0.42$	1426	91	7	16
	1391 ($M/C_DA = 0.15$)	1009	209	19	20

TABLE VI

HEATING SUMMARY OF THE BLUNT CONE -- 1971 HEAT SHIELD

W_E = 1391 pounds | Vehicle Diameter = 15 feet

V_E = up to 23,800 ft/sec | Model 2 Atmosphere

γ_E = -20 degrees | α_E = 0 degree

Peak Heating Rate at $\gamma_\epsilon = 20^\circ$ (Btu/ft^2/sec)		Total Integrated Heating at $\gamma_\epsilon = 20^\circ$ (Btu/ft^2)		
		Stagnation Point		Sonic Point
Convective	Radiative	Convective	Radiative	Convective
70	1	2798	19	803

3.10 THERMAL CONTROL

The thermal control system is required to maintain the various elements of the flight capsule within specified temperature limits during various phases of flight. The utilization of a passive system is a desirable feature and was used as a design objective. The thermal control analysis and design dealt largely with the investigation of critical conditions and the establishment of the limiting requirements.

Figure 9 presents the reference design for the thermal control system. The system consists of a low ϵ (0.05) thermal coating on the primary structure and secondary heat shield faces and a moderately low ϵ (a/ϵ = 1 - 3) coating on the afterbody to maintain the critical components within the allowable temperature range during the post-separation phase. The batteries require external heat to be supplied prior to separation to provide proper operating temperatures for the remainder of the flight capsule mission.

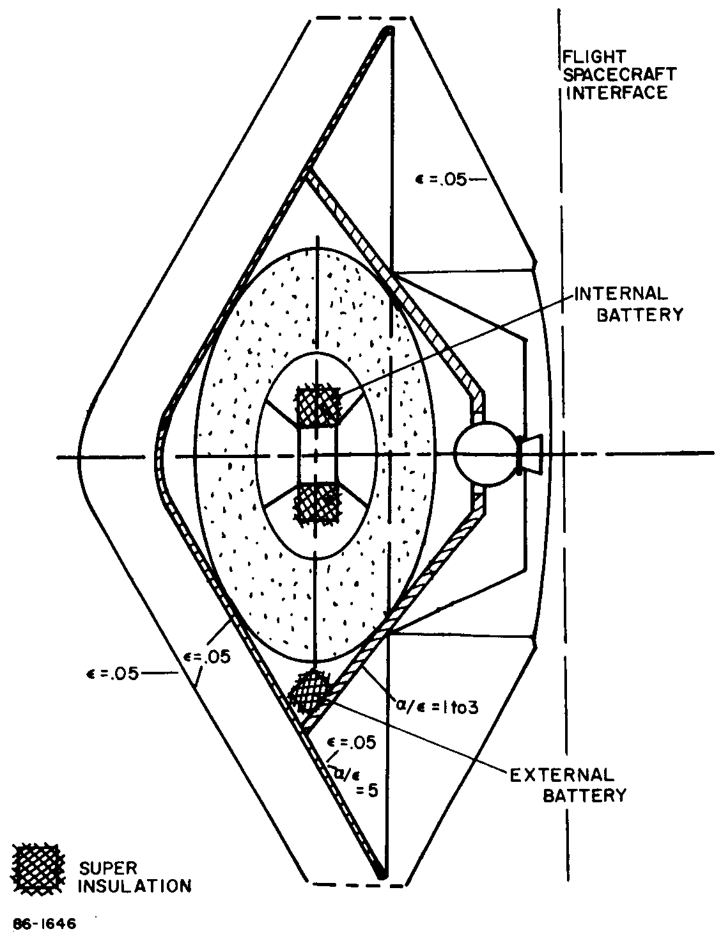

Figure 9 THERMAL CONTROL SYSTEM

4.0 SYSTEM AND SUBSYSTEM TRADEOFF SUMMARY

4.1 ENTRY SHELL CONCEPT SELECTION

One of the primary tradeoffs in this study was the comparison of several entry shell concepts to provide data from which a recommended shell concept could be selected. The entry shell concepts included:

a) Multi-Mission Entry Shell

This shell is designed to accommodate the requirements of Mars lander missions through 1975. The multi-mission shell is designed to enter any of the model atmospheres at entry velocities up to 23,800 ft/sec, entry angles from -20 to -90 degrees, at any M/C_DA up to 0.48 slug/ft^2.

b) Multi-Mission Structure -- 1971 Heat Shield

The structure of this shell is the same as that used in the multi-mission shell. The design of the heat shield is tailored for the 1971 mission.

c) 1971 Entry Shell

This shell, structure and heat shield are designed for the 1971 mission only. The entry vehicle M/C_DA is restricted to 0.15 slug/ft^2.

d) Model 3 Entry Shell

This shell is designed to accommodate a future mission if the model 3 atmosphere is determined to be correct. An M/C_DA of up to 0.53 slug/ft^2 was used.

Table VII summarizes the design conditions for the various shell concepts.

The multi-mission entry shell is a very attractive concept in that only one development program is necessary to develop a single entry shell capable of carrying any payload in the weight class being contemplated through 1975 and perhaps beyond. However, with its many cost and development schedule advantages, the multi-mission entry shell must still be capable of providing a practical payload capability for the severely weight limited 1971 mission in order to be feasible. The payload capability must also be considered for future missions, in the event that the Model 3 or a less dense atmosphere is correct.

Residual weights (entry weight less heat shield and structure weight) for the blunt cone configurations for the four entry shell concepts are presented in Table VIII. The largest residual weight is provided by the 1971 entry shell concept, however, all of the development and cost advantages of the multi-mission shell are lost. The example design makes use of the multi-mission

TABLE VII

SUMMARY OF DESIGN CONDITIONS FOR ENTRY SHELLS
(180-inch diameter)

Design Approach	Heat Shield	Structure
1. Multimission Structure plus 1971 Designed Heat Shield	M/C_DA for γ_e = -90 degrees Model 3, evaluate at γ_e = -20 degrees Model 2	M/C_DA for γ_e = -90 degrees Model 2, evaluate at γ_e = -90 degrees Model 2
2. 1971 Designed Shell	M/C_DA for γ_e = -90 degrees Model 3, evaluate at γ_e = -20 degrees Model 2	M/C_DA for γ_e = -90 degrees Model 3, evaluate at γ_e = -90 degrees Model 3
3. Model 3 Shell	M/C_DA for γ_e = -90 degrees, evaluate at γ_e = -20 degrees Model 3	M/C_DA for γ_e = -90 degrees Model 3, evaluate at γ_e = -90 degrees Model 3

TABLE VIII

SHELL DESIGN CONCEPT COMPARISON–BLUNT CONE
(residual weights, pounds)

Concept	Weight (pounds)
Multi-mission shell	1020
Multi-mission structure + 1971 heat shield	1131
1971 shell	1217
Model 3 shell	1216

structure-1971 heat shield entry shell concept. This concept retains most of the advantages of the full multi-mission entry shell while allowing more than a 100-pound increase in the residual weight. This selection represents a compromise between the payload capability of the 1971 flight capsule and the expense of a new structural capsule development program for each Mars mission.

4.2 ENTRY SHELL CONFIGURATION SELECTION

Three basic shell configurations were compared for utilization as the reference design. These were: (1) a modified Apollo configuration, the modification being to the toroidal corner to improve the Apollo drag coefficient; (2) a 60-degree half-angle blunt cone; and (3) a tension shell, one of a generic class of entry shapes designed to reduce structure weight.

The selection of a shell configuration can be based on entry shell efficiency if a definite trend can be established to show an optimum configuration for a specific purpose. However, such a clear cut optimization did not result and additional criteria were considered to select the best shell configuration.

The efficiency of the entry shell is measured by determining residual weights. Entry vehicles of each shape are designed for the same entry conditions. The one with the largest residual weight is the most efficient. The blunt cone exhibited the largest residual weight, however, comparison with the residual weights of the other configurations did not provide a sufficient difference to make weight a strong factor in the selection. Comparison of the dynamic stability of each entry shape revealed that the blunt cone was probably superior; however, the validity of available test data is questionable. The packaging versatility is a very important systems consideration. The modified Apollo presents the widest flexibility in allowable center of gravity position, thereby, the greatest packaging versatility. In conjunction with packaging versatility, the modified Apollo also has a payload accessibility advantage associated with its flat face. The blunt cone has a considerable advantage over the other shapes in the degree of design confidence in its aerodynamic performance. The blunt cone because of its single curvature surface is significantly easier to fabricate.

The final selection of the blunt cone entry vehicle configuration for the sample design is primarily based upon the level of experience which exists with blunt cone vehicles in Earth reentry, its ease of manufacture, and the slightly better entry shell efficiency achievable.

4.3 LANDED CAPSULE SELECTION

Two landed capsule configurations (flotation sphere and oblate spheroid) showed considerable promise for the surface operations of the 1971 mission, each with its own merits and limitations.

The primary advantage of the flotation sphere concept is the markedly superior performance capability, higher bit rate, and an instrument complex that more completely satisfies the mission objectives. However, the oblate spheroid represents the more conservative selection since its operation on the surface is nearly passive, requiring no re-erection prior to its operation.

Both landed capsule concepts are compatible with the selected entry shell (blunt cone), however, the more compact nature of the flotation sphere requires less suspended capsule structure to support it within the entry shell and during parachute descent. The required center of mass position within the blunt cone is easily satisfied by either landed capsule.

The primary advantage of the flotation sphere lies in its ability to achieve vertical orientation after impact, independent of the surface terrain slope. This allows the use of a narrower beam antenna since the pointing direction is known. A log spiral antenna is used for the relay link and a slot antenna, built into the log spiral antenna, is used for direct link communications. The relatively narrower beam width provides a -1db direct link gain over look angles of interest. The resulting power-gain product, with a 20 watt transmitter is sufficiently high to allow use of the proven PSK/PM modulation technique at a data rate of 8 bits per second directly to Earth. The knowledge of pointing direction also provides for better VHF relay link performance.

The oblate spheroid provides only general knowledge of post impact orientation. Either of the two flat sides may be facing up after the capsule comes to rest. Two S-Band direct link antennas are therefore required with the one facing upward selected for use once the capsule attitude is determined. This capsule is sensitive to the terrain slope; its final orientation could be as much as 45 degrees from the vertical, and requires a broader antenna beamwidth. A -7db antenna gain is realizable over the look angles of interest. The resulting power-gain product with a 20 watt transmitter forces the use of a noncoherent N-ary modulation technique. A data rate of only 2 bits per second by direct link to Earth can be achieved. No post-impact relay link is provided in the oblate spheriod design since there is insufficient weight available for its inclusion. The obvious advantage of such a link if the direct link should fail cannot be provided in this design.

The flotation sphere, being more compact and not so severely weight limited as the oblate spheriod, includes a more complete complement of instruments. Five additional instruments have been included in the blunt cone, flotation sphere design. Two external instruments, the trapped radiation detector and the RF probe for use during the preentry, and entry phases and three internal instruments, the penetrometer, impact accelerometer, and the hot-wire anemometer for surface measurements have been included.

The deployment of surface instruments which must sample the atmosphere is difficult for both designs, since at least a section of the protective crushable material must be deployed. The oblate spheroid deploys a section of crushable material around its maximum diameter and deploys instruments through the edge. The flotation sphere, since the relative orientation of the inner and outer spheres is completely random, must deploy the entire shell of crushable material. In addition, the outer flotation shell around the payload must be jettisoned to allow instrument deployment. The orientation of the deployed instruments is known for the flotation sphere. However, the oblate spheroid must carry two of each deployable instrument to ensure that one such instrument is properly oriented. The weight of the post-impact scientific instrument package for the oblate spheroid is higher even though it contains three fewer instrument types.

Thermal control for the flotation sphere is a more complex problem than for the oblate spheroid. The oblate spheroid can be provided with a low emmissivity thermal control coating over the entire capsule, except the region directly over the antennas, to limit the heat loss during the Martian night. However, the flotation sphere cannot be so coated since the region of the outer flotation sphere which will be over the antennas is not known a priori. The metallic thermal control coating could inhibit communications if it happened to cover the antennas. Additional batteries must be provided to heat the flotation sphere during the Martian night.

Both capsules employ crushable material impact attenuators which limit the impact loads to 500 Earth g. The oblate spheroid, because of its larger surface area to internal volume ratio, and the lower internal packaging density which can be achieved (2 slug/ft^3 as opposed to 3 slug/ft^3 for the flotation sphere) requires a significantly heavier impact attenuator. The optimum impact attenuator material density is also lower, in fact so much lower than the practicality of such materials is questionable. This may further increase the weight of the oblate spheroid impact attenuator.

The principle disadvantage of the flotation sphere is its total dependence upon re-erection after impact for successful operation. The oblate spheroid is semi-passive after impact and is therefore a much more attractive operational concept.

Selection between these two landed capsule configurations is therefore not clear-cut. The performance advantages of the flotation sphere are attractive for the weight-limited design. However, the less complex oblate spheroid is slightly preferable on the basis of design conservatism and has been incorporated in the preliminary reference design concept. Both landed capsule designs have been shown as alternatives in Volume II, Book 1, Section 3.

4.4 COMMUNICATIONS SYSTEM SELECTION

4.4.1 Relay-Direct Link Tradeoffs

During the entry and descent phases of the mission a relay link operating in the VHF band has a markedly superior data rate capability compared to that achievable by a direct capsule link to earth. The performance of a relay link far exceeds that of a direct link when each is constrained to the use of a wide-beam capsule antenna, as is required in the capsule design because of the extreme difficulty of incorporating a steerable directional antenna. On this basis the VHF relay link with a data rate capability of 64 bps has been selected for the reference concept for communications during entry and descent.

During the surface operation phase of the mission, there is not a sufficiently high probability of multiple line-of-sight contacts between the flight capsule and the flight spacecraft to warrant use of a relay link as the sole means of communications. Therefore, a direct link must be incorporated for surface operations. The use of a relay link as a backup is warranted if it were permitted by weight and volume constraints. Such is not the case for the example oblate spheroid design. The very large antenna volume required by operation at an optimum relay frequency results in an unacceptably large and heavy landed capsule, which is the result of primarily the increased size and weight of the impact attenuator. Increasing relay-link frequency sufficiently to reduce antenna volume, and consequently landed capsule size and weight, would degrade performance of a surface operation relay link to an unacceptable value. Therefore, the oblate spheroid design incorporates only a direct link for surface operations.

4.4.2 Relay Communications Considerations

Three flight spacecraft models have been used in analyzing the performance of the relay link. The significant characteristics of these models are presented in Table IX. The nominal system performance is based on model B, since this model allows a reasonable entry and descent mission which is adequate to define the vertical structure and constituents of the atmosphere, without unduly compromising the flight spacecraft mission objectives.

The rejection of the concept of post-landing relay transmission is due in part to the probable need for data playout by command from the flight spacecraft, as featured in model C. The dispersion in capsule and spacecraft position with time is so large as to require command control of the capsule transmitters to avoid a prohibitive battery requirement.

The long communications range (60,000 km) resulting from the 5-hour lead time in model A would significantly degrade the entry-descent mission, though it will provide additional time for MOS operations between the events leading to flight spacecraft orbit injection.

TABLE IX

SIGNIFICANT SPACECRAFT CHARACTERISTICS

	A. (Minimum Performance)	B. (Nominal Performance)	C. (Maximum Performance)
Communications Range at Entry	60, 000 km	35, 000 km	25, 000 km
Lead Time	5 hours	3 hours	2 hours
Receiving Antenna type and gain	Body Fixed 5. 5 db maximum gain	Body Fixed 10 db maximum gain	Steerable on PSP 10 db maximum gain
Receiver Noise Temperature	1450°K	1450°K	1450°K
Operating Frequency*	400 MHz	272 MHz	272 MHz
Down Link Data Rate **	<100 bit/sec	>1000 bit/sec	>1000 bit/sec
Command Capability	None	None	Yes
• Function	N/A	N/A	Landed capsule control turn-on capability
• Frequency	N/A	N/A	VHF
• Power	N/A	N/A	25w
Orbital Operation	No contact after orbit injection	No contact after orbit injection	Contact by command during period between 20-30 hours after entry
Orbit Geometry			
• Periapsis	N/A	N/A	4000 km
• Apoapsis	N/A	N/A	14, 000 km
• Inclination	N/A	N/A	40 degrees
Heading	N/A	N/A	South

*The operating frequencies were selected after analysis of the over-all relay problem and should not be considered as inferred constraints.

**Data rate from the flight spacecraft to Earth.

Further study will be required before the many tradeoffs between the flight spacecraft and flight capsule in the relay link analysis can be resolved in a mutually satisfactory manner. The use of the characteristics in model B, however, satisfies the flight capsule requirements.

4.4.3 Transmitter Power and Modulation Selection

Since the LRC study ground rule established a technology cutoff date* of September 1966, selection of direct-link transmitter power in excess of 20 watts would have been highly speculative. (Powers much less than 20 watts would result in data rates so low that the value of the mission would be questionable.) The moderately high risk associated with even a 20 watt unit when the impact shock is considered may well put the post impact mission below the threshold of feasibility. Thirty watts at 270 MHz represents the maximum power achievable using a solid-state design. The potential problems associated with gaseous breakdown, and possibly multipacting makes avoidance of high voltages (as required by vacuum tubes) desirable. In the absence of hard constraints regarding the flight spacecraft performance as a relay receiver, 30 watts appears to provide a reasonable compromise between system performance and equipment complexity.

Both the relay and direct link systems use noncoherent modulation techniques because of the large fraction of total power which would be required to provide a coherent reference. In the relay case, large loop bandwidths would be necessary to ensure rapid acquisition and to allow tracking during the high entry deceleration periods. In the direct link case, the very low effective radiated power resulting from the poor performance of achievable antennas would hardly be adequate to maintain lock with realizable DSIF receiver loop bandwidths.

For these reasons, the normally less efficient but more easily mechanized noncoherent FSK system proved better suited to the unusual environments during entry and descent and the 5-level MFS system or LCM system proved to be the best choice for the post-landing mission.

4.5 ATTITUDE CONTROL SYSTEM SELECTION

Several candidate attitude control systems were considered before the reference cold-gas spin system was selected. The final selection was strongly influenced by the stringent landing site dispersion requirement. This landing site dispersion requirement together with the necessary 3-hour communication lead time, require extremely accurate thrust vector alignment which can be accomplished only by an active thrust vector control system.

---

*A date at which there would be such a high level of confidence that the technology would permit the development of the specific components in question for inclusion in the 1971 capsule.

Particular attention was given to a spin-only system. This approach is attractive because of its simplicity but has two serious drawbacks. One is the requirement for a flight spacecraft maneuver to place the flight capsule in the proper thrust application attitude; the other is the poor thrust vector control accuracy of this system resulting primarily from tip-off errors at separation. The achievable thrust alignment accuracy of the spin system is about 0.4 degrees compared to the required accuracy of 0.25 degrees or better. If the communications lead time could be achieved by flight spacecraft slow-down rather than flight capsule speed-up, this thrust alignment accuracy would be acceptable and the spin-only system would be the preferred system.

A second candidate is the use of an active reaction control system using gyros on the capsule which are referenced to the flight spacecraft attitude before separation. This approach allows orientation maneuvers to be provided by the flight capsule rather than by the flight spacecraft. The achievable thrust alignment accuracy is acceptable with three hours communication lead time. It becomes marginal if the lead time is increased beyond three hours. The active attitude control system also permits orientation maneuvers between ΔV thrusting and entry to provide the desirable entry angle of attack.

A variation on the active attitude control system approach is the use of spin stabilization to maintain attitude from thrust termination until entry. This approach eliminates operation of the attitude control system in a limit cycle mode for several days, resulting in considerable saving in gas consumption and freedom from gyro drift. This active ACS-spin system is the selected reference design.

Still another candidate system with the potential of greater accuracy is the use of onboard celestial sensing to control the entry conditions by terminal guidance. This technique adds considerably to the weight and complexity of the flight capsule and its potentially greater accuracy is not warranted at least for early missions.

B. PROBE MISSION, ENTRY FROM ORBIT

1.0 STUDY SUMMARY

1.1 STUDY OBJECTIVES

The discovery by Mariner IV that the Martian atmosphere is more tenuous (5 to 10 millibars) than previously thought tended to vitiate the earlier technique of deployment of the capsule on the approach trajectory. When the implications of the very low surface pressure were evaluated by NASA, steps were taken to modify the study objectives and the guidelines for achievement of these objectives.

The principal modifications were:

1) Elimination of the landed phase of the mission

2) A greatly increased emphasis on obtaining Martian environment data, including surface characteristics, for use in the design of future missions

3) Elimination of the concept of multi-mission use of the entry shell and further comparison of shell configurations

4) Limitation of the study of qualification procedures to selected subsystems, rather than the entire system. These subsystems were the entry shell, parachute, attitude control, propulsion, sterilization canister and separation subsystems

5) Study emphasis was put on determination of development problems and development test procedures, rather than determination of formal qualification programs

6) Emphasis continued on the determination of sterilization techniques.

1.2 STUDY GROUND RULES

The new ground rules for the re-directed study specified the following:

1) Saturn V launch vehicle

2) Capsule separation from Mars orbit

3) Mars Model Atmospheres VM-3, VM-4, VM-7, VM-8 (10-5 millibar)

4) Ballistic entry as capsule retardation means

PRECEDING PAGE BLANK NOT FILMED.

5) Sixty-degree half-angle blunt cone entry shell configuration --

a) Emphasis to be placed on ease of manufacture rather than minimum weight

b) Allow reasonable system growth by selection of large shell diameter

6) Subsonic parachute for payload descent

7) No payload post-impact survival requirement

8) Primary mission objective to return engineering data for use in future missions

9) Consideration to be given to use of multiple capsules

10) Consideration to be given to incorporation of television and impact penetrometers in payload.

Several observations concerning the new ground rules may be made. The combination of the use of the Saturn V as the launch vehicle and separation of the capsule from the spacecraft in Mars orbit allows the achievement of reasonably high capsule weights despite the reduction of minimum Mars surface pressure estimates by a factor of 2 below the minimum assumed in the first part of the study. Second, the emphasis on engineering data requirements for future missions reflects the view that the objectives of early missions should be the definition of the environment to allow confidence in the design of future complex systems which will have scientific mission objectives. Finally, the elimination of the survivable landing reflects the view that this phase of the mission would return insufficient data of engineering use to warrant its incorporation.

1.3 STUDY CHRONOLOGY

With the new ground rules, three payload-classes were synthesized for comparison purposes. These were:

Payload 1 -- atmospheric properties measurements (but no wind measurement)

Payload 2 -- Payload 1, plus wind and terrain hardness measurements

Payload 3 -- Payload 2, plus terrain features measurements (by television).

Consideration of the value of these payloads relative to their cost led to the judgment that the data return of Payloads 1 and 2 was not sufficient to warrant their increased costs over that of simpler, nonparachute probes, but that the total data return of Payload 3 provided enough engineering information for the design of future missions to make it worth developing. Payload 3 was, therefore, selected for further design studies.

Conceptual capsule design studies and capsule-spacecraft integration studies, conducted in conjunction with the comparison of payloads, showed that it would be possible to incorporate, on each spacecraft, two capsules designed to carry Payload 1, but that only one capsule could be incorporated if it were to be designed to accommodate Payload 2 or Payload 3. Since Payload 3 was a strong choice for the reference design, incorporation of multiple capsules on each flight spacecraft did not prove to be possible.

After reaching these conclusions early in the study, and with LRC approval, the design proceeded on the basis of a single capsule designed to carry Payload 3.

1.4 CONCLUSIONS

Study in some depth has shown that a capsule of broad utility and conservative design can be developed to accomplish a 1971 mission. The selected diversified payload can provide the data return needed for the design of advanced systems, and which is of scientific value as well. The selected payload provides for the measurement of the composition and structure of the atmosphere by the use of a set of complementary instruments; the determination of the wind structure by several independent means; the measurement of terrain hardness at several locations; and the correlation of the hardness measurements with measurements of surface features and roughness obtained by television and radar.

This versatile payload and the capsule system can be developed in time for a 1971 mission if full-scale development is initiated in mid 1966. This assertion is predicated on the adoption of a sterilization approach similar to that set forth in this report. It should be noted that the elimination of the survivable landing phase of the mission makes early hardware development easier to achieve.

The more important characteristics of the conceptual capsule design are as follows:

1) The capsule system weight at launch is approximately 3000 pounds, the preseparation weight is approximately 2800 pounds and the entry weight is approximately 2000 pounds.

2) The capsule can deorbit from a wide range of orbits with a fixed total impulse solid-propellant rocket engine without thrust termination. For the reference design deorbit is possible from orbits with periapsis altitude (h_p) and apoapsis altitude (h_a) ranges of 700 km $\leq h_p \leq$ 1,500 km and 4,000 km $\leq h_a \leq$ 20,000 km.

3) Spacecraft orbit trim maneuvers before capsule separation are not required.

4) A spacecraft attitude maneuver is not required for capsule deorbit.

5) A simple fixed antenna can be used for the spacecraft relay link receiving antenna.

6) Television resolution of 1/4-ft/TV-line can be achieved even in the presence of high wind gust velocities.

7) The problems of flight capsule antenna pointing direction under the influence of the high wind velocities with the attendant multi-path transmission problems can be overcome by a combination of time and polarization diversity in the relay link communications system.

8) The capsule mission can be accomplished with a subsonic parachute.

9) The design is characterized by weight conservatism, provision for growth potential, and a high degree of redundancy.

Study of the required development test programs for the previously indicated six capsule subsystems has indicated that the parachute is the single feasibility problem in the capsule design. This question concerns the problem of parachute opening at low dynamic pressures. Comprehensive test programs for the parachute and other subsystems are presented in Volume III, Book 3.

A fundamental contribution of the study has been in sterilization technology and, in particular, in the conception and development of the burden analysis technique. This technique provides a quantitative basis for the sterilization problem and enables the comparative evaluation of various handling and decontamination methods. By means of this technique, it has been shown that parts can be manufactured under normal industry conditions, and that components can be assembled using essentially standard procedures. The development of the analytical methodology and the conclusion that a practical means of biological burden control is possible without severe economic penalty, are significant results.

2.0 SYSTEM DESIGN SUMMARY

This section and Section 3.0 summarize the design for the entry from orbit mission mode for the ground rules as listed in paragraph 1.2.

2.1 SYSTEM OPERATION AND DESCRIPTION

The Saturn V launch vehicle places two planetary vehicles (each consisting of a flight spacecraft and a flight capsule) on the desired interplanetary trajectory. The flight spacecraft serves as a transport vehicle for the flight capsule until after Mars orbit insertion. After orbit determination and possible landing site survey, the spacecraft and capsule are separated and the capsule is deorbited. An active, cold-gas reaction control system is used for maneuvering and a solid propellant hot-gas system is used for thrust vector control during thrusting. The flight capsule is capable of deorbiting from elliptical orbits ranging from 700 to 1500 kilometers periapsis altitudes and 4000 to 20,000 kilometers apoapsis altitudes, using a fixed impulse deorbit motor (ΔV = 1400 ft/sec).

After entry and ballistic retardation, a parachute system is deployed at a Mach number less than 1.2. The entry shell is jettisoned at this time to increase terminal descent time and to enable experiment data collection and transmission.

The instrumentation measures atmospheric structure and composition, terrain features, surface hardness and surface roughness. Terrain features are obtained by a 3-camera boresighted television system, mounted on a stable platform, and producing from 11 to 19 pictures (dependent upon the atmosphere encountered) with resolution from 0.25 to 30 feet. The wind measurements are provided by a three-leg doppler radar. Surface roughness is determined by two radar altimeters, which are also used for high and low altitude determination for initiation and altitude indexing functions. Surface hardness is measured by 4 penetrometers dropped at 3500 feet altitude and below.

Communications from the flight capsule to the flight spacecraft are provided by a redundant, 30 watt FSK, 18,000 bps relay system.

The entry shell design is based on the model atmospheres presented in Table X. The external (aerodynamic) shape of the entry shell is a 60-degree half-angle blunt cone having a real gas hypersonic drag coefficient of 1.63. The conical entry shell has a base diameter of 15 feet with a weight at entry of 2040 pounds, yielding an M/C_DA at entry of 0.22 slug/ft^2. The basic structure is aluminum honeycomb, thermally protected by an ablative heat shield of Purple Blend Mod 5.

TABLE X

MARS MODEL ATMOSPHERE PARAMETERS

Property	Symbol	Dimension	VM-3	VM-4	VM-7	VM-8
Surface pressure	P_o	millibars lb/ft^2	10.0 20.9	10.0 20.9	5.0 10.4	5.0 10.4
Surface density	ρ_o	$(gm/cm^3)10^5$ $(slug/ft^3)10^5$	1.365 2.65	2.57 4.98	0.68 1.32	1.32 2.56
Surface temperature	T_o	°K °R	275 495	200 360	275 495	200 360
Stratospheric temperature	T_s	°K °R	200 360	100 180	200 360	100 180
Acceleration of gravity at surface	g	cm/sec^2 ft/sec^2	375 12.3	375 12.3	375 12.3	375 12.3
Composition						
CO_2 (by mass)			28.2	70.0	28.2	100.0
CO_2 (by volume)			20.0	68.0	20.0	100.0
N_2 (by mass)			71.8	0.0	71.8	0.0
N_2 (by volume)			80.0	0.0	80.0	0.0
A (by mass)			0.0	30.0	0.0	0.0
A (by volume)			0.0	32.0	0.0	0.0
Molecular weight	M	mol^{-1}	31.2	42.7	31.2	44.0
Specific heat of mixture	C_p	cal/gm °C	0.230	0.153	0.230	0.166
Specific heat ratio			1.38	1.43	1.38	1.37
Adiabatic lapse rate	Γ_o	°K/km °R/1000 feet	-3.88 -2.13	-5.85 -3.21	-3.88 -2.13	-5.39 -2.96
Tropopause altitude	h_T	kilometers kilofeet	19.3 63.3	17.1 56.1	19.3 63.3	18.6 61.0
Inverse scale height (stratosphere)	β	km^{-1} $ft^{-1} x 10^5$	0.0705 2.15	0.193 5.89	0.0705 2.15	0.199 6.07
Continuous surface wind speed	$\bar{v}$	ft/sec	155.5	155.5	220.0	220.0
Peak surface wind speed	v_{max}	ft/sec	390.0	390.0	556.0	556.0
Design vertical wind gradient	$\frac{d\bar{v}}{dh}$	(ft/sec)/1000 feet	2	2	2	2

2.2 DESIGN DESCRIPTION

Configurational arrangement and design integration of the flight capsule system is discussed in the following paragraphs. Simplified versions of inboard profiles of the flight capsule are used to illustrate the subsystem design integration. These profiles may differ somewhat from the complete layouts presented in Volume III because different cross-sections were used to bring out certain pertinent details on a single profile. These profiles are divided into several major subsystem categories; (a) flight capsule launch configuration, (b) attitude control and propulsion subsystems, (c) antenna subsystems, (d) entry vehicle structures, and (e) instrumentation arrangement.

2.2.1 Flight Capsule Launch Configuration

The flight capsule, as mounted on the flight spacecraft in the launch configuration, is shown in Figure 10. Primary components indicated on this figure are the sterilization canister and the flight capsule-flight spacecraft adapter. Other pertinent features of this profile are the interfaces with the flight spacecraft such as the electrical umbilicals and the entry vehicle separation system.

The sterilization canister is a thin (0.030 inch) aluminum monocoque structure consisting of three major subassemblies; (1) the lid, which covers the entry shell and is jettisoned prior to flight spacecraft orbit injection, (2) the outer annulus section of the base, which houses the lid separation system (an elastomer encased mild explosive - metal shear), and (3) the inner circular section of the base, which provides the access door for assembly of the deorbit rocket system. All three subassemblies are welded together, including the semi-monocoque flight capsule-flight spacecraft adapter running through the canister.

The flight capsule separation system is located at the forward end of the adapter and consists of a V-clamp cable mechanism for tie-down. The flight capsule is released by four explosive bolts, any one of which will effect release. Electrical separation occurs simultaneously with, and is implemented by, mechanical separation. A pressurization system inside the canister maintains a slight positive pressure differential (1 psi) across the canister during the long period from terminal heat sterilization to Earth orbit injection. At this point the canister is vented prior to transfer orbit injection.

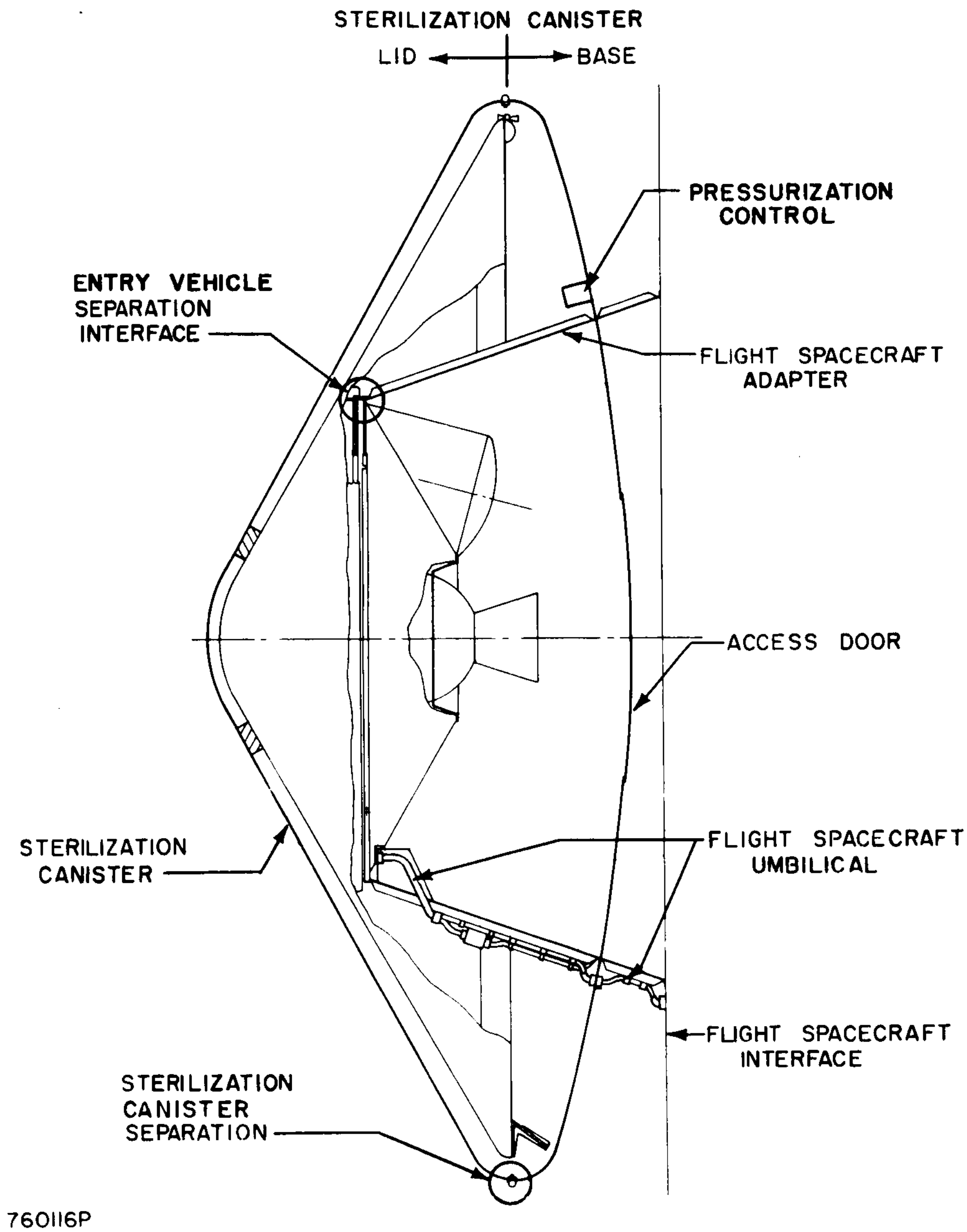

Figure 10 FLIGHT CAPSULE LAUNCH CONFIGURATION

2.2.2 Attitude Control and Propulsion Subsystems

The installation arrangement of the ACS and propulsion subsystems is shown in Figure 11. An active, cold-gas attitude control system (ACS) is used after separation for entry vehicle maneuver to the deorbit thrust attitude. An inertial reference system provides attitude reference during this period and throughout the preentry flight. The inertial reference system is also used in the parachute descent phase of the mission as a reference for a two-axis gimbaled platform upon which the television camera is mounted. A hot-gas, solid-propellant reaction control system provides thrust vector control during ΔV thrusting. Both the cold-gas reaction nozzles (12) and hot-gas reaction nozzles (8) are located on the outer periphery of the entry shell to provide a maximum thrust moment arm. The hot-gas generator is also located in this area to eliminate long lengths of hot piping. However, the cold-gas tanks and regulators are placed on the entry shell near the center line of the vehicle. This location eliminates the need for thermal protection and reduces the possible entry vehicle center of gravity shift which would occur if one tank supply was prematurely depleted.

The ΔV deorbit motor is located inside the suspended capsule assembly to minimize interference with the radiation patterns of the two relay antennas. The propulsion case and the Teflon-coated fiberglass nozzle are retained after thrust termination.

2.2.3 Antenna Subsystems

There are three antenna subsystems in the entry vehicle as indicated in Figure 12. They are: (1) two VHF relay antennas (272 MHz) for communication with the flight spacecraft, (2) two radar altimeter antennas for altitude and surface roughness measurements, and (3) two doppler antennas, providing a three-leg pattern*, for measuring wind velocity. Two redundant VHF relay communications systems are provided, including redundant antennas. These antennas are located diametrically opposite each other on the afterbody. They are tilted slightly inward to improve the overall antenna pattern.

Two radar altimeters are used, one at high altitudes and one at low altitudes. The high-altitude altimeter utilizes the entry shell structure as the antenna by exciting the outer ring at 19 MHz. At low altitudes, after parachute deployment and entry shell jettisoning, another antenna, mounted on the suspended capsule, is used for the altitude measurements at 324 MHz. This same antenna is also used as the penetrometer receiving antenna at 400 MHz.

---

*The two doppler radar antennas are mounted on the suspended capsule. One antenna is fed at two slightly different frequencies to produce two of the doppler legs. The other antenna provides the third doppler leg.

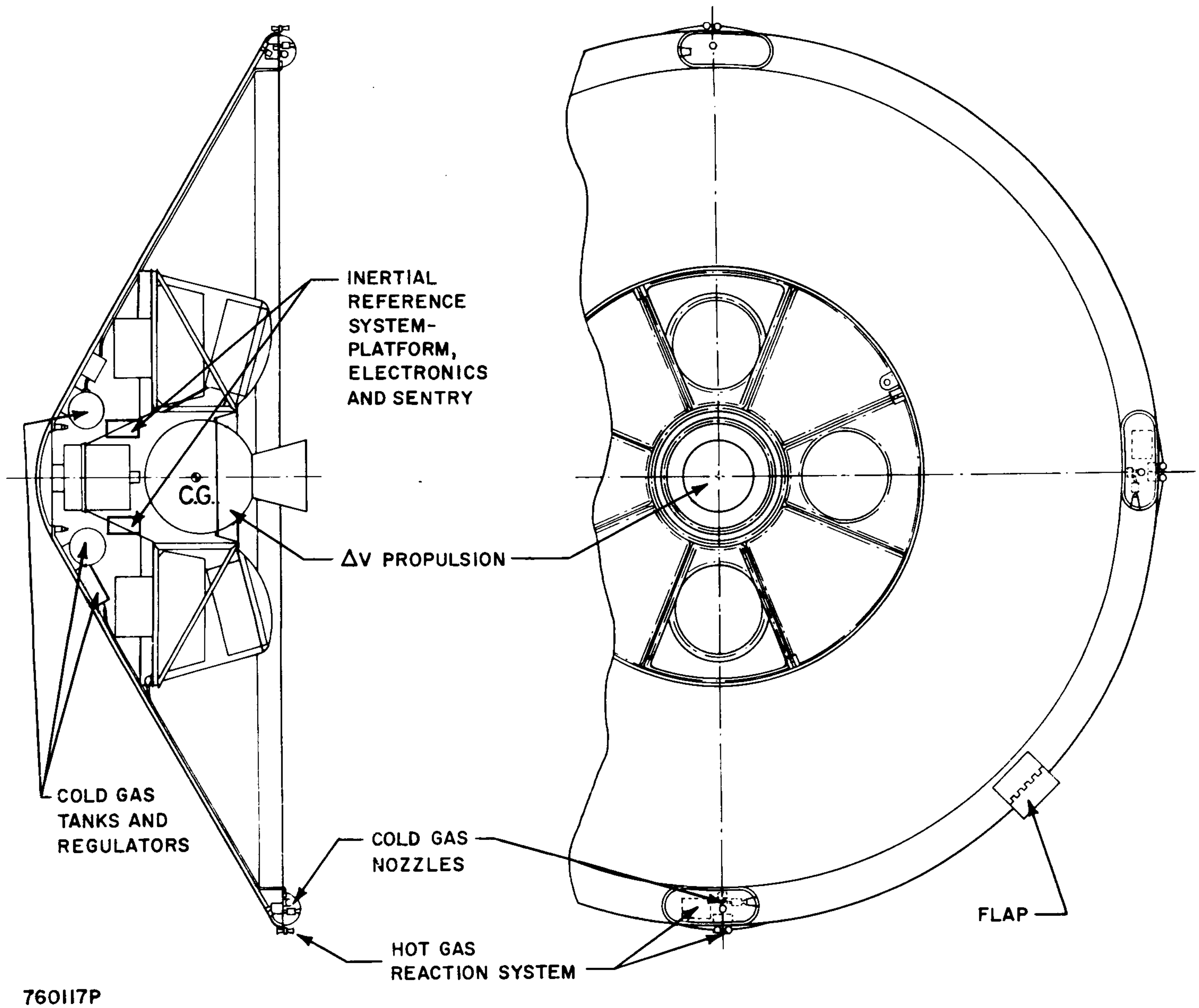

Figure 11 ATTITUDE CONTROL AND PROPULSION SUBSYSTEMS

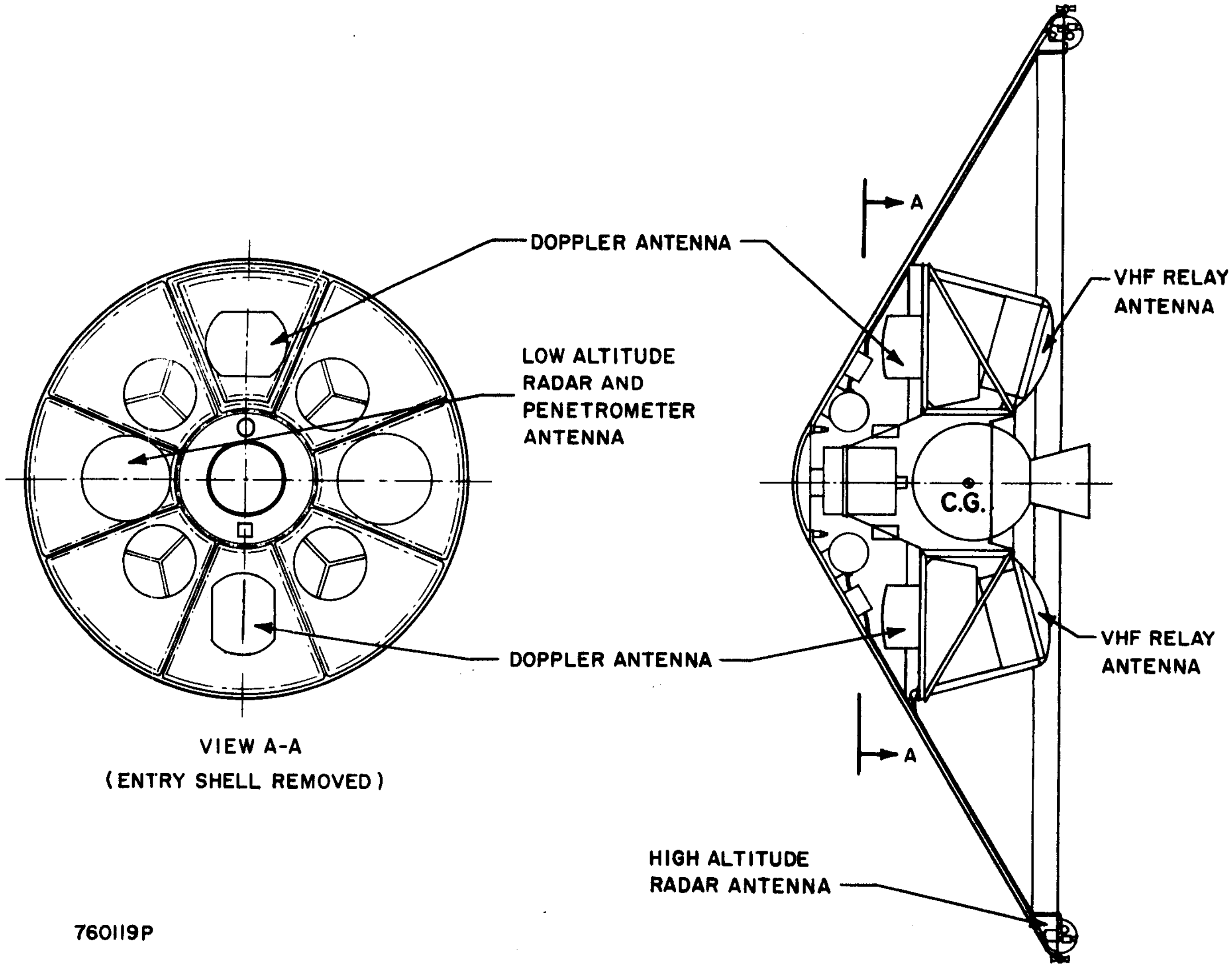

Figure 12 ANTENNA SUBSYSTEMS

2.2.4 Entry-Vehicle Structures

Two major structural elements constitute the primary load carrying system for the entry vehicle. These are the entry shell structure, which provides the aerodynamic configuration and supports the heat shield, and the suspended capsule structure, which provides the mounting and load carrying network for the majority of the equipment including the parachute. This breakdown is illustrated in Figure 13.

The entry shell is constructed on a bonded honeycomb sandwich, using aluminum for both face sheets and core. Because of the low stress-level of the entry shell both the face sheets and the core use minimum gage material (0.016 inch sheets and 5.7 lb/ft^3 core). Both the base ring and the suspended capsule mounting ring are riveted to this shell.

Purple Blend Mod 5 heat shield material ($\sim$0.3 inch thick) is bonded to the forward side of the entry shell and a thin layer ($\sim$0.050 inch) of the same material is bonded on the aft side, for protection against wake heating and inadvertent rearward entry.

The suspended capsule structure is composed of two semi-monocoque structures, one forming the afterbody contour (60-degree truncated-cone) and the other a cylindrical section around the ΔV propulsion. These two structures are held together by a ring at the aft end, and eight radial beams and the entry shell mounted ring at the other end. The majority of the equipment is mounted on the eight radial beams in the front portion of the suspended capsule. The longerons joining the eight radial beams form the primary load path system for the ΔV propulsion thrust and for parachute opening loads. Parachute harness lines run from four points at the mounting ring to a central swivel joint from which a single riser line attaches to the parachute. The parachute system, including the pilot parachute, is housed near the front of the structure and is deployed from its housing on the side of the afterbody.

2.2.5 Instrumentation Arrangement

The physical location of the pertinent instrumentation is shown in the inboard profile of Figure 14. This figure also shows the telecommunications and power supply locations. The numerous diagnostic instrumentation distributed over the entire vehicle is not shown.

Three platform-mounted, boresighted television cameras are located on the center line of the flight capsule, a short distance from a deployable nosecap. The television platform is gimbaled, with two degrees of freedom

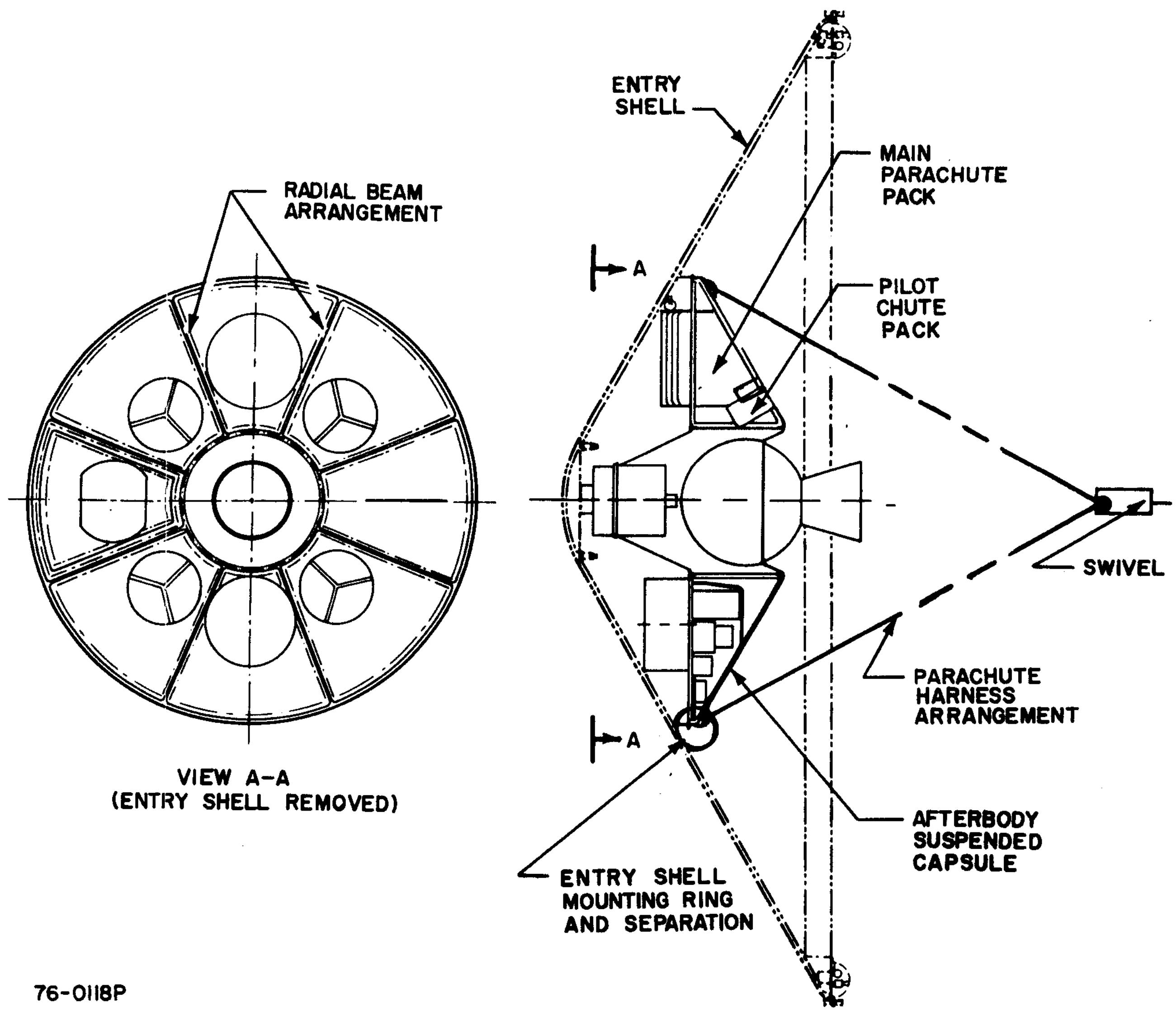

Figure 13 ENTRY VEHICLE STRUCTURES

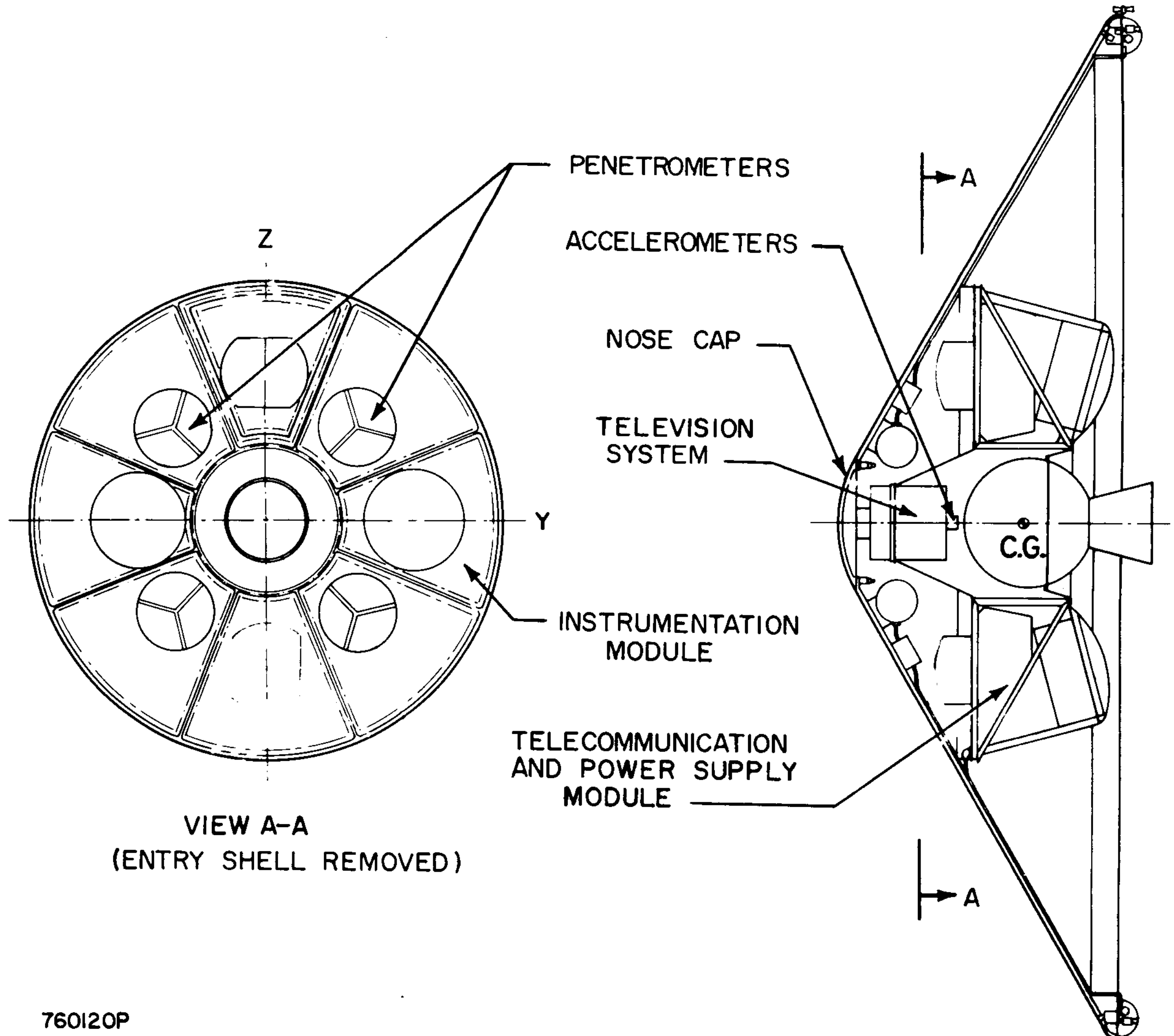

Figure 14 INSTRUMENTATION ARRANGEMENT

and is slaved to the inertial reference system to provide television stabilization along the local vertical in the presence of capsule swing on the parachute. In case the entry shell fails to separate, the nose cap is jettisoned, so that some television pictures may still be obtained.

Four penetrometers are located in the forward end of four bays of the suspended capsule structure. Engineering instrumentation, telecommunications equipment, and power supplies are located in modules in three bays. Two of the modules, located directly over the doppler-radar antennas and directly below the VHF relay antennas, contain identical telecommunications and power supply subsystems. The other module (located above the low-altitude radar antenna) contains the instrumentation for atmospheric measurements. This form of modular packaging was devised in order to ease assembly and checkout procedures during installation.

2.3 OPERATIONAL FLIGHT SEQUENCE

The operational flight sequence which consists of the flight spacecraft preorbit-injection maneuvers, orbit injection, orbital maneuvers and the flight capsule deorbit sequence to entry is illustrated in Figure 15. At planet approach, the sterilization canister lid is jettisoned, and the canister base remains attached to the flight spacecraft-flight capsule adapter. The flight spacecraft is subsequently maneuvered into retrothrust attitude for orbit injection. After the several days in orbit required for orbit-parameter determination and possibly for flight capsule landing site survey, the entry vehicle is separated from the flight spacecraft. The ACS orients the entry vehicle to the deorbit thrust altitude. Separation could occur anywhere in orbit but should be fairly close to the entry vehicle deorbit point to reduce entry vehicle power consumption and thermal control complexities. If entry vehicle deorbit thrusting were performed too close to the flight spacecraft,rocket plume interference or contamination of the flight spacecraft would result. Therefore, at least one kilometer separation between the entry vehicle and flight spacecraft is provided before deorbit thrusting.

Thrust vector control is provided by a solid propellant hot-gas reaction control system. After burnout, the entry vehicle is maintained under active attitude control with the cold-gas system until entry. Additional entry vehicle attitude maneuvers can be made, depending on the flight spacecraft orbit, to provide proper communication look angles and to provide a near-zero entry angle of attack. Roll control, provided by the ACS, is utilized throughout entry to facilitate minimum spin rates at parachute deployment.

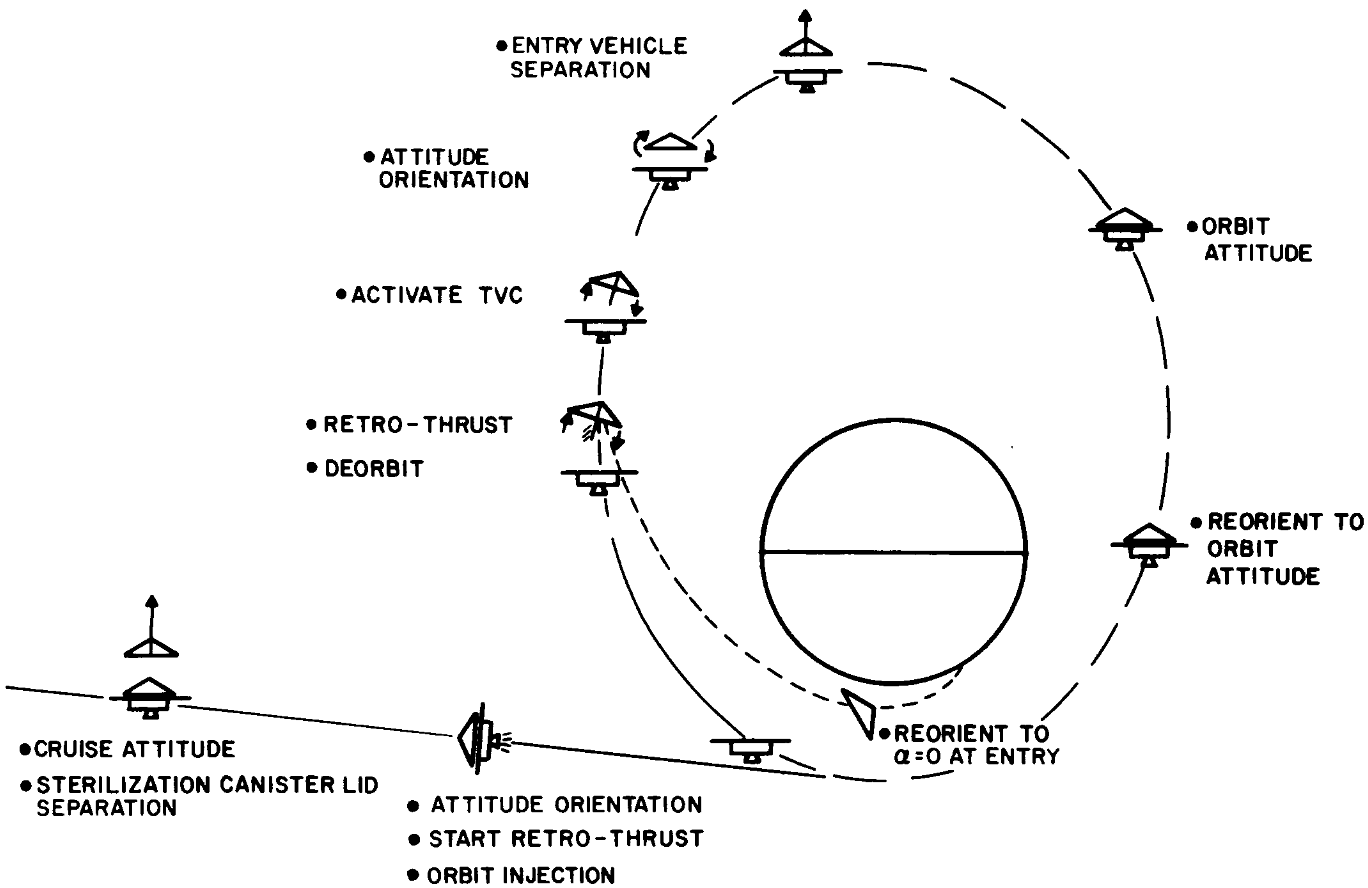

25-0997

Figure 15 DEORBIT SEQUENCE

Figure 16 depicts the terminal descent phase of the flight capsule mission starting with the parachute deployment sequence. Parachute deployment is initiated by the radar altimeter at 27,500 feet interlocked by a peak-g switch and timer that nominally indicates a Mach number of 1.2. If the entry vehicle velocity at 27,500 feet is greater than Mach 1.2, deployment is delayed until that Mach number is reached. The initiation signal mortars out a nine-foot diameter ring-slot pilot parachute which pulls the main parachute out of the parachute canister. The 81-foot ring-sail main parachute is fully deployed by the time it reaches the end of the riser line. The entry shell separation system is initiated at peak parachute opening loads by a load cell in the riser line. The load cell deployment signal is backed up by onboard accelerometer signals. If the entry shell fails to separate, the nosecap is then jettisoned to allow some television pictures to be taken. At an altitude of approximately 3500 feet, penetrometer deployment starts and continues at intervals of 2 seconds until all four penetrometers are deployed. The flight sequence and failure mode provisions are summarized in Table XI. Also included in this table are the general failure mode effects on the overall mission.

2.4 WEIGHT SUMMARY

The flight capsule weight summary is presented in Table XII. Each major weight category represents the operational vehicle in a particular phase of the flight sequence. For example, the sterile canister is jettisoned and the pressurization gas is expelled prior to orbital injection. The sum of these weights is subtracted from the flight capsule weight to arrive at the flight capsule pre-separation weight.

The total entry weight of 2040 pounds is based on an M/C_DA of 0.22 slug/ft^2 and a diameter of 15 feet. The diameter was selected to allow conservatism in design and provide growth margins for factors such as expanded mission goals or unanticipated failure-mode effects. The entry weight consists of two major categories: (1) the entry shell and associated attachments (that portion jettisoned at parachute deployment) and (2) the suspended capsule (that portion suspended on the parachute, including the parachute).

A contingency factor of 20 percent is included in most of the entry shell weight categories to account for elements which cannot be established at the preliminary design level.

The instrumentation weight indicated in Table XII includes both mission experiments and diagnostic instruments. The radar altimeters and the doppler radar are listed separately although they supply experimental data as well as performing other functions. The telecommunications weight includes all of the relay communication link subsystems as well as the data handling and storage subsystems. All subsystem weights indicated in the table include the weight of necessary associated hardware, packaging containers, wiring and fasteners. All other bracketry, interconnecting cabling, and miscellaneous hardware are included separately as an estimated 15 percent of the suspended capsule weight.

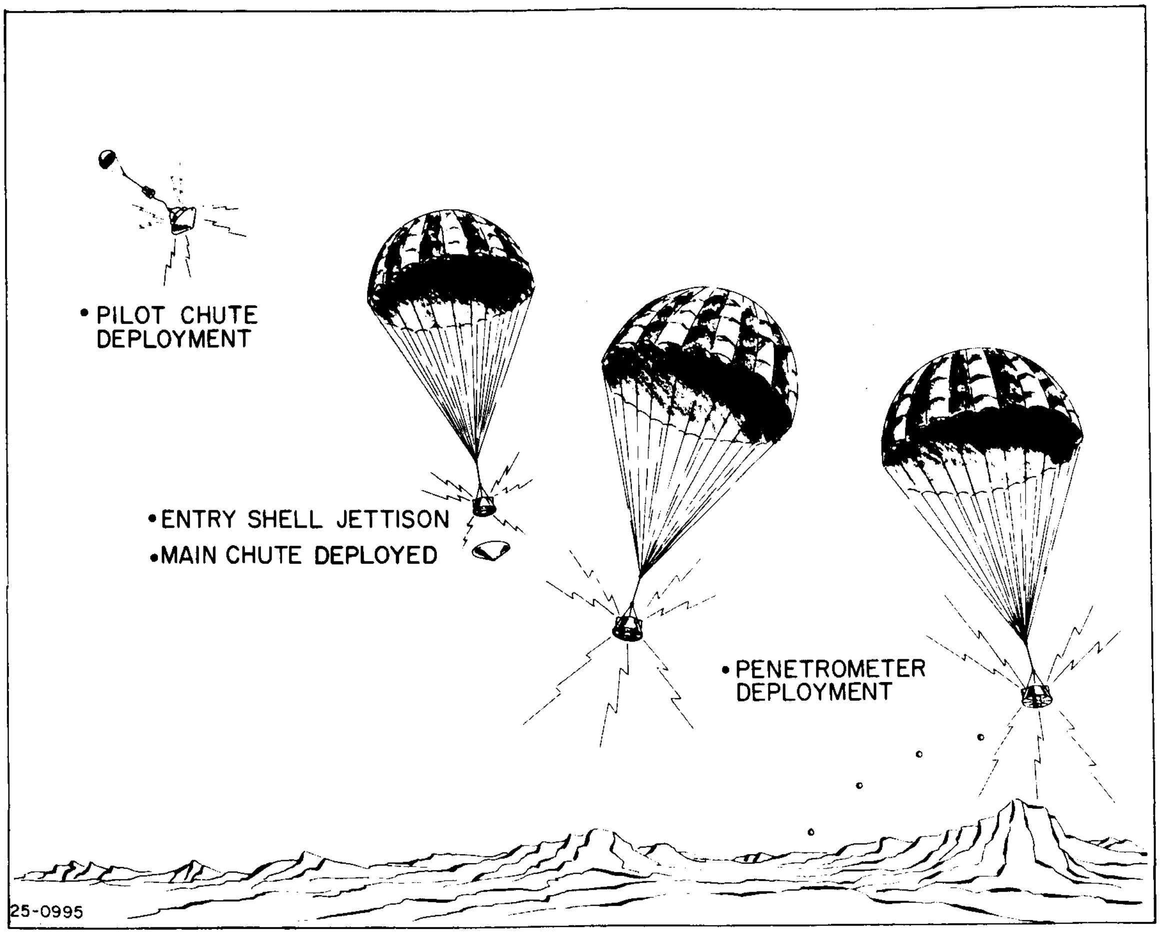

Figure 16 THERMINAL DESCENT SEQUENCE

TABLE XI

ABBREVIATED FLIGHT SEQUENCE

Event	Time	Failure Mode Provisions	Effect on Mission
Jettison sterilization canister lid	Approach Trajectory	Jettison flight capsule	Flight capsule mission failure
Planetary vehicle orbit -- inject	~Periapsis	None (?)	PV mission failure
Initiate relay communications	Preseparation	Redundant power, communication antennas	No effect
Separate flight capsule	In-orbit	Backup separation joint	Flight capsule mission failure
Orient flight capsule	Postseparation	Redundant reaction control system	No effect
Thrust vector control	Post-orientation	Redundant TVC system	No effect
Thrust -- ΔV propulsion	Post-orientation	None	Flight capsule mission failure
High altitude radar information	250,000 ft to 25,000 ft	G-switch for parachute deployment	None $\longrightarrow$ minor
Deploy parachute Jettison Entry Shell	27,500 ft or Mach 1.2 (whichever is lower altitude)	Jettison nosecap to accommodate TV	Fewer TV pictures No wind measurement No penetrometers
Low altitude radar information	Entry shell jettison	Doppler radar	No surface roughness
Doppler information	Entry shell jettison	Low altitude radar	Possible wind measurement degradation
Atmospheric information	Entry shell jettison	Complementary measurements	Minor
Initiate picture-taking	Entry shell jettison +5 seconds	Three-camera design	Minor $\longrightarrow$ No TV
Drop penetrometers	Start 3,500 ft (one every 2 seconds)	Multiple penetrometers	Minor $\longrightarrow$ no hardness measurement

TABLE XII

FLIGHT CAPSULE WEIGHT SUMMARY

	Weight (pounds)	cg* (inch)	Ixx (slug-ft^2)	Iyy (slug-ft^2)
Flight Capsule	2922.1	33.2	1367	780
Sterile canister lid	125.0			
Pressurization gas	15.0			
Preseparation	2782.1	33.2	1262	720
Sterile canister base	163.0			
Pressurization nozzle, valves	6.0			
FC - FS adapter	125.0			
Hwd., bkts., cables	29.5			
Separated Vehicle	2458.6	30.0	1042	581
Propulsion propellant	400.0			
ACS gas expelled	1.0			
TVC gas expelled	17.6			
Entry Vehicle	2040.0	29.5	1036	575
Entry shell heat shield	370.7			
Entry shell structure	343.0			
Thermal control	30.0			
ACS-reaction control	42.4			
TVC-reaction control	48.5			
Hwd., bkts., cables	83.5			
Available for growth	96.9			
Suspended Capsule	1025.0	26.8	131	97
Instrumentation	205.6			
Radar subsystem	56.9			
Telecommunications	117.4			
Programming and sequencing	23.6			
Power supply	178.0			
Parachute	84.0			
Inertial reference system	21.6			
Propulsion case	49.0			
Structure	96.0			
Afterbody heat shield	36.0			
Hwd., bkts., cables	131.0			
Available for growth	25.9			

*Measured from the nose cap of the Entry Vehicle structural contour.

The inertial reference system must be located in the suspended capsule since it provides the orientation reference for the television camera platform. Similarly, the ΔV rocket case weight is included in the suspended capsule weight since the case is retained after burnout.

2.5 ORBIT COMPARISON

The flight capsule has been designed to operate over the entire range of orbits considered, 700 to 1500 kilometer periapsis altitude and 4000 to 20,000 kilometer apoapsis altitude. Flight capsule requirements, therefore, do not restrict the selection of orbital altitude or the operational flexibility of the mission. The design orbit can be determined entirely by the flight spacecraft requirements. However, if there are no strong flight spacecraft requirements for selection of a particular orbit, there is a moderate preference for a high periapsis altitude-low apoapsis altitude orbit on the part of the flight capsule. Table XIII presents the preferred altitudes for several primary and secondary design considerations. The selection of orbital altitudes can be made to favor any of these considerations. The table is also helpful in flight spacecraft-flight capsule tradeoffs involving selection of orbital altitude.

The range of orbital inclination used in the design studies is 40 to 60 degrees. This range of inclinations allows good flexibility in planetary mapping from the flight spacecraft as well as access to any of the desired landing sites for the 1971 mission. (See Vol. III Book 1, Section 9.0.)

TABLE XIII

ORBIT COMPARISON

Primary Considerations	Favors	
	Periapsis (kilometers)	Apoapsis (kilometers)
Allowable suspended capsule swing angle on parachute	1500	4000
Required periapsis adjustment	1500	--
Secondary Considerations		
Entry angle of attack (requirement for maneuver)	700	--
Entry angle dispersion	1500	4000
Range extension capability	--	4000
Sensitivity to deorbit timing	1500	20,000

3.0 SUBSYSTEM DESIGN SUMMARY

3.1 COMMAND AND CONTROL

All flight capsule timing, sequencing and associated computational activities are controlled by the central computer and sequencer (CC&S) subsystem. This subsystem initiates events by providing properly timed outputs in appropriate sequence to the other subsystems.

The seven sequences provided by the flight capsule CC&S are:

1. Checkout Sequence

This sequence is employed before launch, during interplanetary cruise, and just before separation in orbit to electrically checkout all the flight capsule subsystems. Upon receipt of a discrete command from the flight spacecraft, a sequence of 13 time-based events is initiated. The entire checkout sequence requires 90 minutes with a one minute time base and is used as required to ensure proper operation of the flight capsule.

2. Electrical Stimulation Sequence

This sequence is a subsequence of the checkout sequence and as such is used whenever the checkout sequence is used. This detailed sequence exercises both altimeters, the inertial reference system, the ACS reaction control system (no gas is expelled), the accelerometers, and the gyros. A 1-second time-base is used for this sequence composed of 17 time-based events. The sequence requires 2 minutes.

3. Separation Sequence

This sequence of three time-based events is initiated by a discrete command from the master sequencer. This sequence controls the events starting 1 minute before separation for 66 seconds with a 1-second time base.

4. Master Sequence

This sequence of 27 time-based events controls the operation of the flight capsule from before separation until 3 minutes before entry. This sequence has a one-minute time base. Both the separation sequence and electrical stimulation sequence are initiated during this period by the master sequencer.

5. Entry Sequence

The entry sequence consists of nine events which are not time based. This sequence is controlled by computations performed on inputs from the accelerometers, the high altitude altimeter, and the parachute riser line load cell and controls the events during entry and parachute descent. The parachute and penetrometer deployment sequence and the television shutter control sequence are initiated by this sequence.

6. Parachute and Penetrometer Deployment Sequence

This 5 event time-based sequence deploys the parachute and penetrometers at the appropriate altitudes. It is initiated by the entry sequence. The primary parachute deployment signal is part of the entry sequence. This sequence provides the backup parachute deployment signal.

7. Television Shutter Control Sequence

This sequence controls the operation of the television cameras at appropriate times to avoid dead-air-time in the relay communications link. An override inhibit from the camera stable platform prevents shutter operation if either of the platform gimbal angles exceed 45 degrees.

3.2 ENGINEERING INSTRUMENTATION

The engineering instrumentation for the entry from orbit mission was selected to provide data similar to that desired for the entry from approach trajectory mission. However, there were several changes made in emphasis and in ground rules. A heavier weight was to be given to experiments that would provide data useful for the design of future flight capsules. The elimination of the survivable landing requirement obviated the use of several of the instruments requiring close proximity to the surface. The lower entry velocities and decelerations associated with entry from orbit, as well as the absence of the requirement to survive landing shock decelerations, reduced some of the transducer design problems. The prohibition of television experiments was eliminated, and the cutoff date for experiment development was relaxed to a more general availability requirement.

The payload selected for the entry from orbit case is shown in Table XIV. With the exception of one deletion and four additions, it is identical to the entry from approach trajectory payload. The radiometer experiment has been removed because at the lower entry velocities anticipated for this mission the temperature in the shocked region ahead of the stagnation point is too low to provide adequate emission intensities from the desired lines. The added experiments are: (1) the television cameras, which will provide between 11 and 19 pictures of varying resolution during the parachute descent, (2) the penetrometers, which will be released at about 3500 feet and telemeter back to the suspended capsule, the decelerations experienced at impact, (3) the doppler radar, which will provide an estimate of wind velocity by measuring the horizontal velocity of the suspended capsule, and (4) the water detector, which will measure the atmospheric water concentration with a sensor specifically designed for the task. This payload can provide most of the information which a small, impact attenuator-protected landed capsule can provide with the exception of growth-type life detection experiments, surface chemical composition, and meteorological experiments over a diurnal cycle. The first of these is partially compensated by the high resolution television pictures, and the second by the much wider coverage obtainable from electromagnetic reflectance (from radar to ultraviolet frequencies) studies of the surface from the flight spacecraft.

TABLE XIV

ENGINEERING INSTRUMENTATION

Instrument	Number Carried	Major Mission Phase
Radiation detector	1	Deorbit to parachute
Accelerometer	3	Entry to parachute
Radar altimeter	1	End Blackout to impact
Mass spectrometer	1	Parachute to impact
Acoustic densitometer	1	Parachute to impact
Gas chromatograph	1	Parachute to impact
Pressure gage	2	Parachute to impact
Temperature probe	2	Parachute to impact
Television	3	Parachute to impact
Beta scatter	1	Parachute to impact
Water detector	1	Parachute to impact
Doppler radar	1	Parachute to impact
Penetrometer	4	3500 feet to impact

One additional experiment was included in the design until almost the end of the study. This was a set of smoke bombs to be released from the suspended capsule at about 20, 000 feet. Each bomb would release puffs of smoke at timed intervals after impact. These smoke puffs would travel with the surface winds and the distance between the puffs would give an estimate of surface wind velocities. The actual inter-puff distance would be measured by the third and fourth sets of television pictures. Although it was demonstrated that the probability of seeing the smoke puffs was high (almost 50 percent under worse-case conditions), the converse problem of having significant portions of the high resolution pictures obscured by the smoke could not be resolved, and the experiment was deleted.

Although no single experiment in the entry from approach trajectory had a dominant role in various system and subsystem tradeoffs, in the entry from orbit mission the television experiment clearly had such a role. It has an important influence in command and control, data handling and storage, telecommunications, power, attitude control, parachute, entry shell, and thermal control tradeoffs, in addition to requiring detailed study as an experiment in its own right. Although the feasibility of performing a television experiment of considerable engineering and scientific value has been clearly demonstrated, further work should be done to determine the value of carrying out an ultrahigh resolution imaging experiment and to clarify several instrumentation problems.

3.3 TELECOMMUNICATIONS

The telecommunications concept features two totally redundant systems which incorporate the time diversity to ensure data retrieval even under the most adverse fading conditions experienced during the mission. As shown in the simplified block diagram of the telecommunications subsystem (Figure 17) all engineering and diagnostic data is fed to the corresponding data handling equipment in both subsystems. Rather than modulate radio subsystem No. 1 entirely from data handling subsystems No. 1 and radio subsystem No. 2 entirely from data handling subsystem No. 2, it is more advantageous to sequence the data alternately to the RF subsystems from each data handling subsystem. This technique results in the recovery of all data for any single failure and recovery of half the data for any two nonredundant failures. The alternating data sequence also provides the desired time diversity. The data from both data handling systems are not synchronous; different data is being transmitted from each RF subsystem at any given time. If signal fading occurs during the initial transmission, it is highly probable that the data will be recovered later when it is repeated.

The selected data format scheme interlaces 34 lines of television data with frames of non-television data every 2.5 seconds as shown in Figure 18. The radar, engineering, diagnostic, and penetrometer frames shown in the first 2.5 second interval of radio subsystem No. 1 via data handling subsystem No. 1 are repeated 2.5 seconds later; but this time, over radio subsystem No. 2 via data handling subsystem No. 2. The data frames transmitted over radio subsystem No. 1 during the first 5-second interval are entirely from data handling subsystem No. 1 and those transmitted over radio subsystem No. 2 are entirely from data handling subsystem No. 2. During the next 5-second interval, each of the two data handling subsystems feed data to the alternate radio subsystem. In this way, no data are lost in the event of a single failure of any subsystem.

The television transmission sequence is similarly shown in Figure 19. Each television camera has two redundant memories except the A camera which has four memories. After a set of three television pictures is taken, each picture

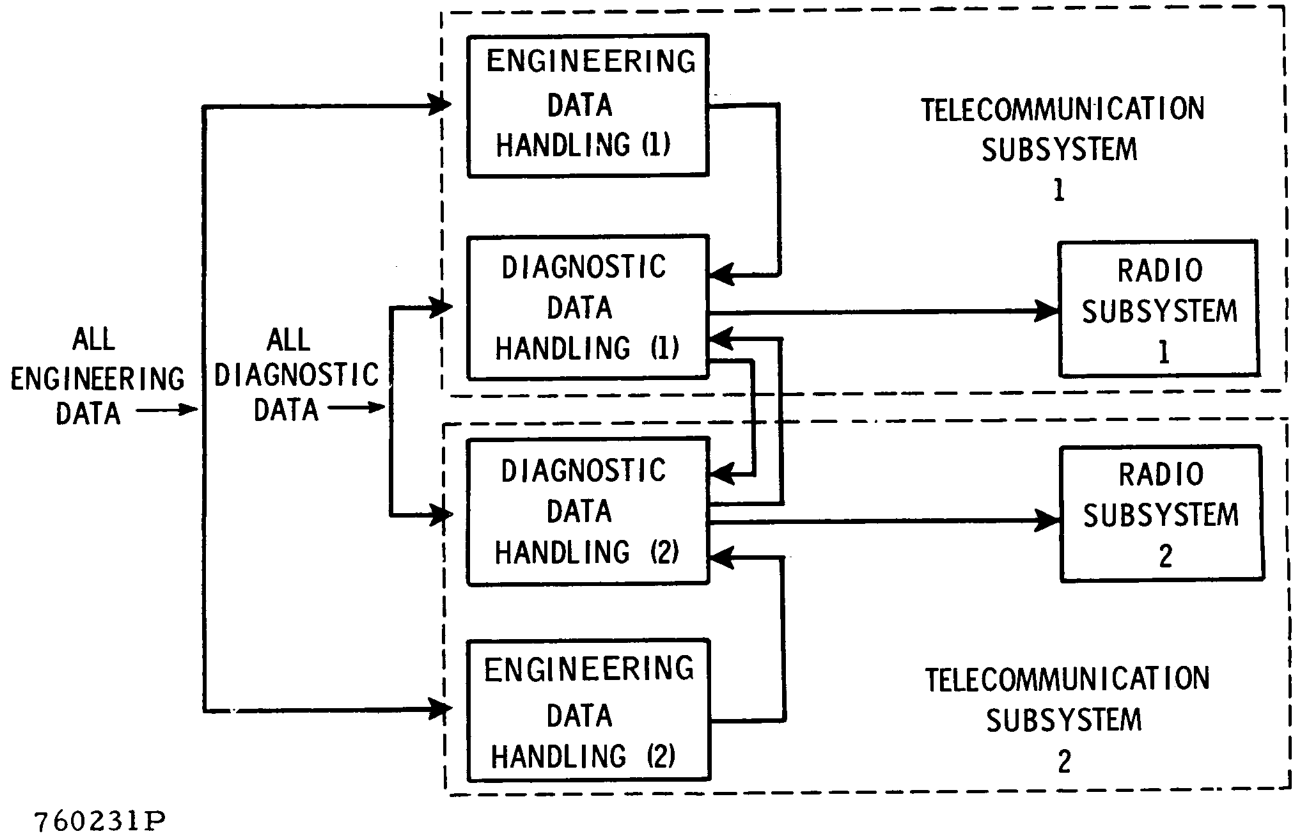

Figure 17 TELECOMMUNICATIONS SUBSYSTEM MECHANIZATION

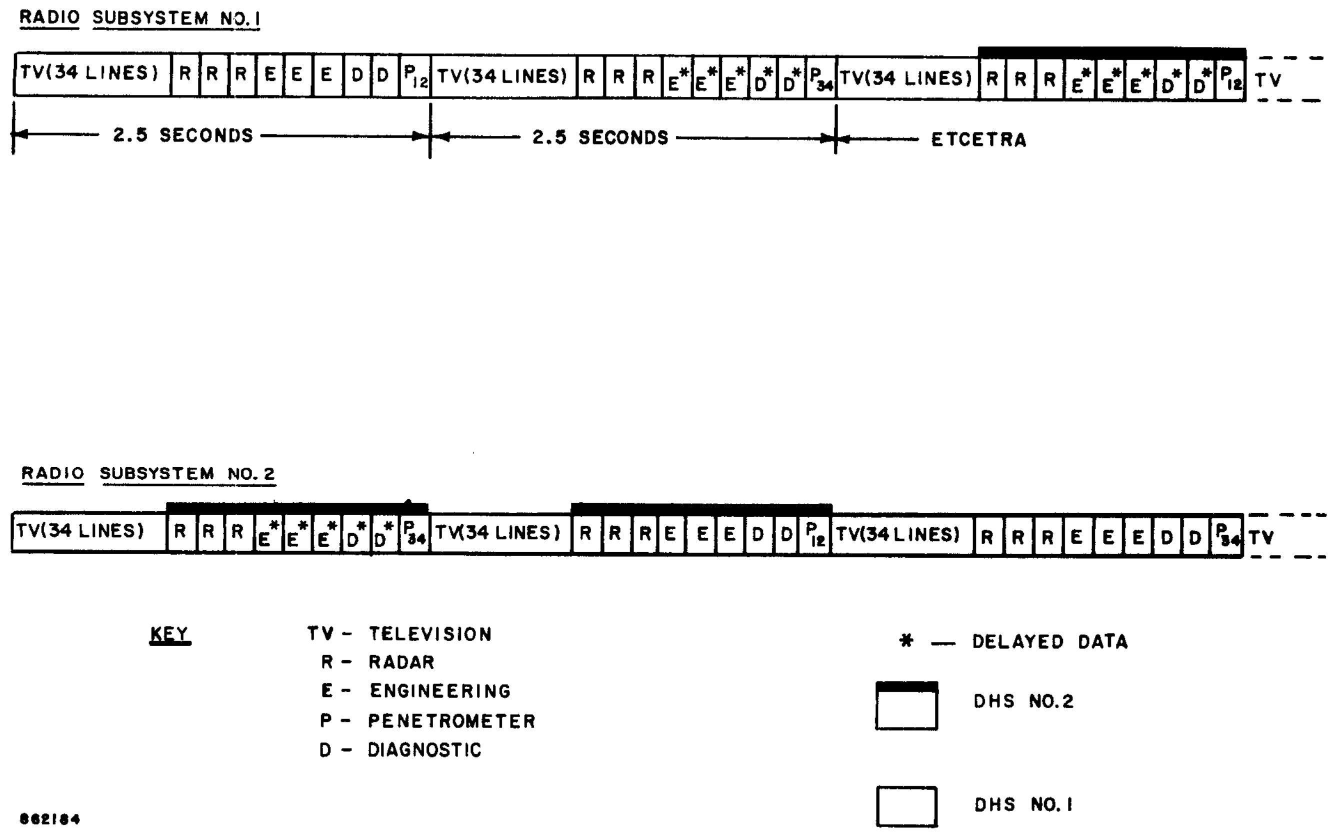

Figure 18 DATA TRANSMISSION SEQUENCE

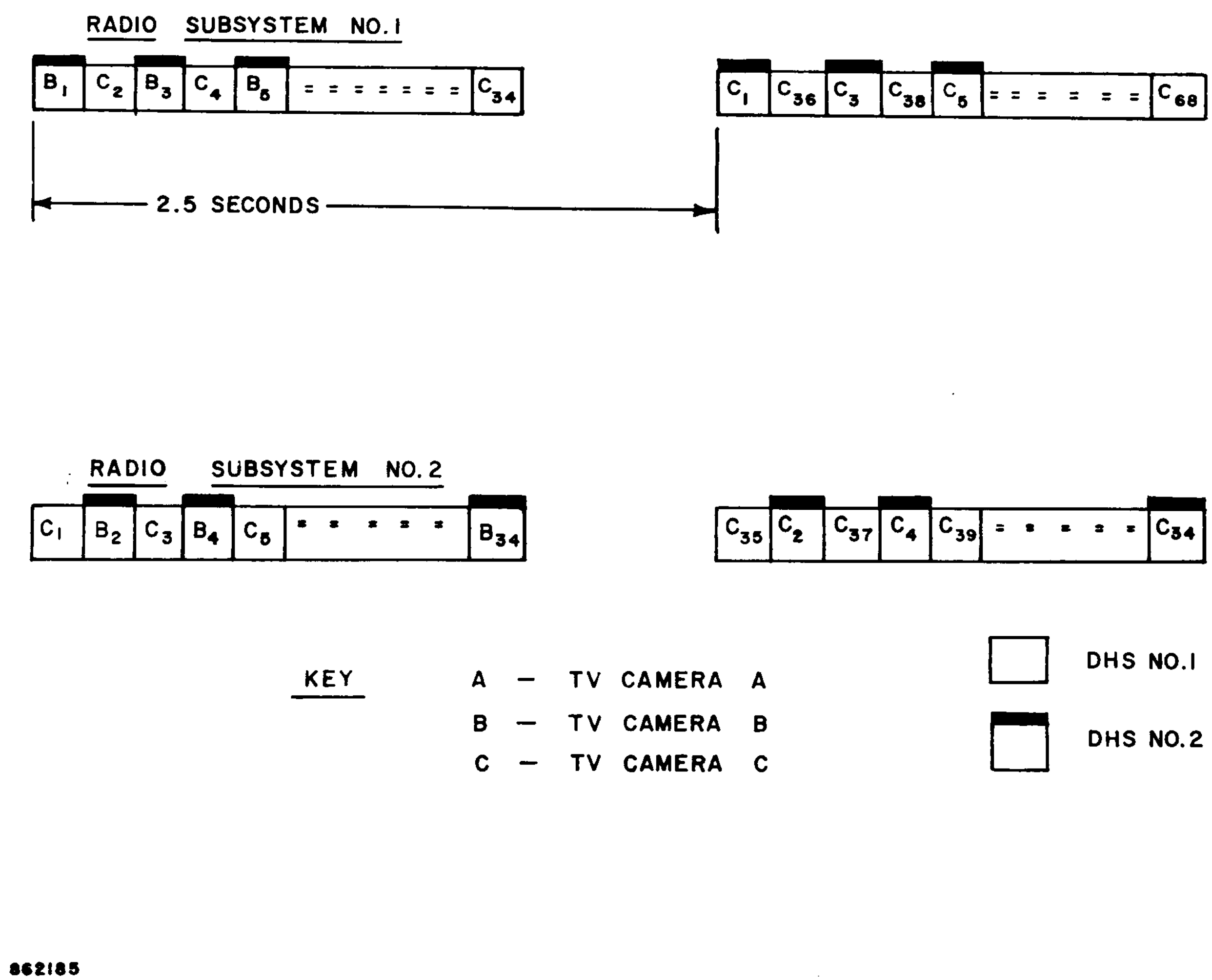

Figure 19 TELEVISION TRANSMISSION SEQUENCE

is read into both memories for that camera. The picture transmission sequence is C, B, A. Camera A has four memories to allow the next set of pictures to be taken before all the stored data of the first Camera A picture has been transmitted. The second set of Camera A memories is used to store the second Camera A picture while the first Camera A picture is still being transmitted. As shown in Figure 19 radio subsystem No. 1 transmits even numbered lines of the Camera C picture from the prime Camera C memory via data handling subsystem No. 1. This data is repeated 2.5 seconds later from the redundant Camera C memory via data handling subsystem No. 2 providing the 2.5 seconds of time diversity. Alternately, odd lines of the Camera C picture are transmitted first over radio subsystem No. 2 from the prime Camera C memory via data handling subsystem No. 1 and then 2.5 seconds later over radio subsystem No. 1 from the redundant Camera C memory via data handling subsystem No. 2. The second block of 34 lines of Camera C data are interleaved in the second block of 34 television lines transmitted to be repeated redundantly in the third block of 34 television lines and so on. Each block of 34 television lines is thus transmitted twice with complete redundancy, and with 2.5 seconds time diversity except the first 34 lines of Camera B which are transmitted first interleaved with the Camera C data in the first block of 34 television lines and redundantly 14 seconds later. This was done to eliminate transmitter dead-air time otherwise occurring every other frame in the first 2.5 second interval.

The salient features of the telecommunications subsystem which is characterized by conservatism are summarized in Table XV. When alternatives existed, the approach taken was the one involving the least technical risk. A transmitter power level of 30 watts was selected to remain within the state-of-the-art of solid state devices to avoid the design risk associated with high voltages required in vacuum tube amplifiers.

The selected frequency (270 MHz) is sufficiently close to the standard telemetry band (215 to 260 MHz) to allow Earth entry tests to be conducted with only slight modifications to mission equipment. Noncoherent frequency shift keying is the modulation choice, precluding the necessity for an automatic tracking receiver in the flight spacecraft. Since the payload is not weight limited, total redundancy is incorporated, maximizing the probability of successful data recovery. Data mode switching during entry is avoided by the use of a record-retransmit system for blackout data collection. The use of low gain, broad beamwidth flight capsule antennas make precision attitude control unnecessary during cruise, entry and terminal descent.

3.4 POWER SUBSYSTEM

A schematic diagram of the power subsystem is shown in Figure 20. The subsystem contains a dual set of power equipment providing parallel inputs to all users. Each battery, power control switch, and regulator is capable of carrying the entire load at any time; this assures complete block redundancy. The parts of the subsystem are interconnected to minimize the effect of failure of any component.

TABLE XV

TELECOMMUNICATION CHARACTERISTICS

FLIGHT CAPSULE	
Frequency	267 - 273 MHz/band
Bit rate	18,000 bits/sec
Transmitter power	30 watts
Modulation	FSK
Range	1,700 km maximum
Antenna type	Log spiral
Weight (total)	89.6 pounds
Power consumption	183 watts
Ancillary features	Redundant systems
Delay Memory Prevents	Loss of Data in Blackout
FLIGHT SPACECRAFT	
Antenna type	Body fixed turnstile
Receiver noise figure	5 db

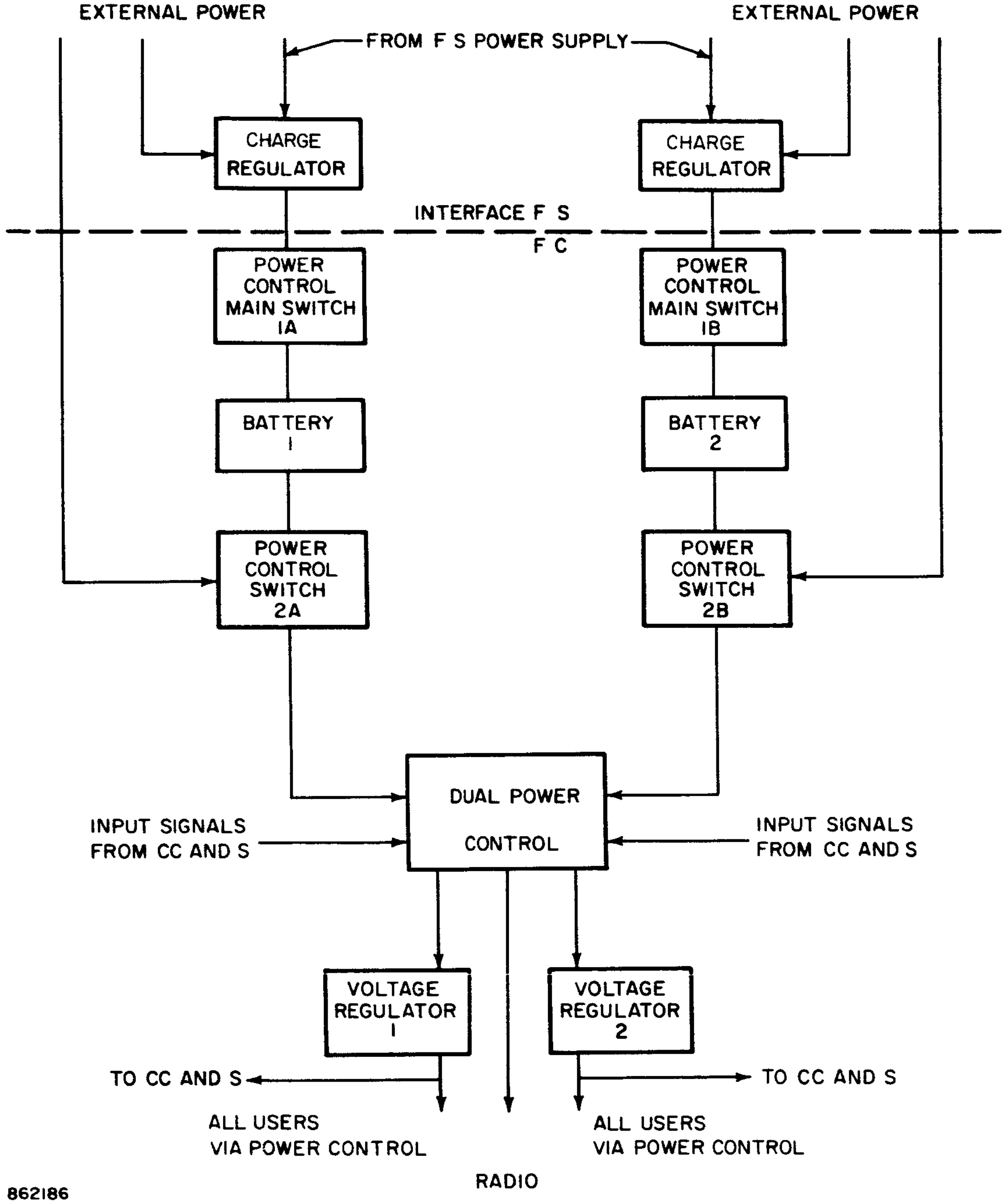

Figure 20 POWER AND CONTROL SUBSYSTEM SCHEMATIC DIAGRAM

Each battery power source consists of 24 series-connected hermetically-sealed, nickel-cadmium cells and is capable of providing the entire power profile. Each battery is rated at a nominal capacity of 740 watt-hours at +40° F and a 1-hour rate. Each battery weighs 53 pounds and occupies 0.46 cubic feet. Other types of power sources, such as silver-zinc batteries, were considered but, the nickel cadmium battery is the only proven heat sterilizable battery presently available.

"Buck-Boost" load voltage regulators are used to provide regulated dc to all power users. These regulators accept input voltages above or below the output voltage allowing more of the battery capacity to be used. The load voltage regulator supplies a rated load of 560 watts with 100 percent intermittent overload. The input voltage can range from 22 to 35 vdc; the output voltage is 28 vdc. The charge regulators are located on the flight spacecraft and are disconnected from the flight capsule just prior to separation. Each charge regulator is capable of providing both fast charge or trickle charge. The trickle charge is applied during interplanetary cruise. After the preseparation checkout, the fast charge mode is used to quickly recharge the batteries before separation. The charge regulator provides trickle charge rates from 50 to 250 milliamp and a fast charge rate of 3 amperes.

Each power control unit consists of solid state switches, blocking diodes, fuses, and mechanical switches. These units switch power to the users upon receipt of signals from the CC&S. Each unit has 35 solid state switches and 2 mechanical relays. The power capacity is 560 watts continuous.

3.5 PROPULSION

The propulsion subsystem consists of a solid propellant rocket motor, used to deorbit the flight capsule after separation from the flight spacecraft. The rocket motor is a new design, but the design concept is similar to the Surveyor main retromotor. The propellant (TP-H-3105) is sterilizable, and the motor total impulse is 101,600 lb-sec. This impulse will provide a velocity decrement of 1400 ft/sec. The rocket motor operates at an average thrust level of 3000 pounds for 33.5 seconds with a specific impulse of 254 seconds.

The motor is spherical in shape, 22.3 inches in diameter, and 24 inches long (including the nozzle), 432 pounds, with a propellant mass fraction of 0.925.

The primary exhaust nozzle is submerged except for 2 inches with an area ratio of 18.7 and is made of vitreous silica phenolic. An exhaust nozzle extension has been added to the basic motor to facilitate exhaust gas ducting away from the structure and other equipments. The extension is made of dielectric materials to prevent antenna attenuation. This extension is 11 inches long, mounted to the motor nozzle exit, and continues the existing exhaust nozzle contour. The extension structure is fiberglass coated with Teflon on both the interior and exterior surfaces. This unit with mounting attachment weighs 9 pounds.

A solid propellant rocket motor was selected over a liquid propellant system because of reliability, sterilizability, ease of packaging, space storability, the requirement for only a single firing, and cost.

3.6 ATTITUDE CONTROL

Attitude control is accomplished by a combination cold-gas and hot-gas reaction control system. The system actively provides the proper orientation from separation to entry using cold gas, except during the period when the propulsion system is operating. During that time the hot-gas system, with its higher thrust levels, controls the pitch and yaw attitude of the separated vehicle.

Commands to control the operation of the nozzle valves are generated in the inertial reference system (IRS) which includes a computer and a four-gimbal inertial platform. Inertial reference is established prior to separation. These command signals are a function of vehicle angular error and its time rate of change.

The cold-gas reaction control system provides 3-axis control in couples by means of 12 nozzles. Eight hot-gas nozzles supplied by solid propellant hot-gas generators provide control over the disturbing torques in pitch and yaw arising during the thrusting mode. Roll disturbances during this phase are handled by the cold-gas roll nozzles. Upon completion of the thrusting phase, the ACS maintains the attitude of the entry vehicle with the cold-gas system. It may reorient the vehicle to optimize communication performance. An orientation will be performed prior to entry to an attitude which minimizes the entry angle of attack.

During early entry, the reaction control system pitch and yaw control will be disabled and roll control will be used only to limit roll rates. The IRS will remain operative and will provide acceleration data during the entry phase for the purpose of event control and also for entry wind velocity and atmospheric density measurements. Upon parachute deployment, the IRS will send local vertical reference signals to the television gimbal system which maintains the cameras optical axis along the local vertical.

The IRS also includes a sentry system consisting of body mounted rate gyros which deactivate the reaction control system in the event of an inertial platform failure of a type which produces excessive angular rates (above 6 deg/sec). The roll-rate gyro is also used as the sensor for roll rate limiting during entry.

Both the hot-gas and cold-gas systems are completely redundant, so that failure of a single component in either system will not jeopardize the mission.

3.7 PARACHUTE

Descent time is the primary design criterion for sizing the parachute descent system in the entry from orbit mission mode impact velocity is of little consequence. The parachute descent system must satisfy both a minimum and maximum descent time requirement. A minimum descent time of 160 seconds is required for data acquisition and playout. The maximum descent time must be limited to 360 seconds, the time duration in which the flight spacecraft is within the region of acceptable communication look angles.

Neither a two parachute system (drogue-main) nor main parachute reefing is necessary to accomplish the intended mission under the design constraints. The selected descent system is therefore a conventional single stage ring-sail parachute which is deployed at a maximum Mach number of 1.2 (selected as the upper limit for reliable deployment and operation). An 81-foot nominal diameter parachute is required for operation in the VM-8 atmosphere based on the minimum descent time requirement of 160 seconds and a suspended weight of 1025 pounds. However, deployment of such a parachute at Mach 1.2 in the VM-3 atmosphere would occur at approximately 75,000 feet for the range of trajectories considered. The descent time would be 680 seconds, 320 seconds greater than the maximum limit. This problem was eliminated by using an initiation system which in effect applied altitude limiting to the $M = 1.2$ deployment. The system consists of a radar altimeter, accelerometers, timer and computer circuits. The Mach number, $M = 1.2$, is not measured directly, but is correlated with a time interval after peak deceleration for the various atmospheric models and entry trajectories.

The accelerometer detects the peak deceleration and the timer and computer circuits execute the necessary time delays and correlation computations. The system initiates parachute deployment when the altitude is less than 27,500 feet and the Mach number is less than 1.2. This will satisfy the minimum and maximum descent time requirements.

The total parachute system weight is 70 pounds including the main parachute, pilot parachute, mortar and gas generator assemblies. A 9-foot diameter ring-slot pilot parachute is mortared out at approximately 100 ft/sec which, in turn, pulls the main parachute out of its canister in a fully-deployable condition. In the event the mortar fails to fire the pilot parachute, a gas generator ejects the entire main parachute assembly from its canister at approximately 30 ft/sec.

3.8 ENTRY SHELL

The variation of entry shell design conditions with entry mode is significant although the entry from orbit conditions are not as severe as those previously studies for entry from the approach trajectory. Since the entry shell must be designed for the most severe conditions that could be encountered, failure mode analyses were performed to determine the most critical of these conditions. It was determined that a failure of the inertial reference system could result in the flight capsule entering at a random angle of attack and tumbling at about 0.1 rad/sec about any axis. Using this condition as a worst case, the reference design load and heating were developed and are presented in Table XVI and XVII.

The entry shell structure is a light weight aluminum honeycomb sandwich which supports the ablative heat-shield material, provides the desired aerodynamic loads to the remainder of the flight capsule. For the reference design, the structural shell weight was 268 pounds, including a safety factor of 1.25. Minimum weight of the structure was a desirable goal but not a rigid requirement because of the basic design conservatism provided by selection of a large vehicle diameter.

The requirements imposed on the heat shield paralled those of the structure throughout the entire mission from manufacture to mission completion. Again, minimum weight was not the overriding consideration. The reference design consists of a Purple Blend Mod 5 ablator, backed up by a ply of fiberglass with stiffening loops for added mechanical integrity. The calculated weight for the primary (forebody) heat shield not including contingency, but accounting for manufacturability, mounting pads and bond is 253.5 pounds; the secondary (aft side of forebody) heat shield weighs 55.4 pounds.

3.9 THERMAL CONTROL

The thermal control system maintains the various elements of the flight capsule within specified temperature limits during the various phases of the mission. The tradeoff studies performed for the reference design and a typical mission sequence revealed that the critical consideration governing the selection of the thermal control system, and thus the power required from the flight spacecraft, is the thermal interface between the flight capsule and flight spacecraft. The critical thermal control phase occurs after removal of the sterilization canister-lid some time prior to Mars orbit injection.

The reference thermal control system is illustrated in Figure 21. The system consists of low emissivity ($\epsilon = 0.05$) coatings on the external surfaces of the sterilization canister-base (facing the flight capsule afterbody and facing the flight spacecraft). The face of the primary heat shield is also coated with the same material ($\epsilon = 0.05$). The face of the secondary heat shield and the afterbody surface will receive no special thermal control coating, since the emissivity of the material used in these areas is adequate. In addition to the coatings specified, heaters are imbedded in the heat shield substructure to maintain the required temperature levels. Additional heaters in the subsystem compartments of the flight capsule are used to elevate subsystem temperatures to operating levels prior to flight capsule-flight spacecraft separation.

TABLE XVI

LOAD SUMMARY

α_E = 179 degrees   P = 0.1 rad/sec

V_E	15,200 ft/sec
γ_E	-16 degrees
Atmosphere	VM-8
Maximum X/W	
Axial load factor	15.9 (Earth G)
Normal load factor	0.61 (Earth G)
q_∞	114.6 lb/ft^2
α_E	10.3 degrees
$\dot{\alpha}_E$	1.63 rad/sec
$\ddot{\alpha}_E$	15.0 rad/sec^2
Maximum N/W	
Axial load factor	15.7 (Earth G)
Normal load factor	0.71 (Earth G)
q_∞	113.2 lb/ft^2
α_E	13.8 degrees
$\dot{\alpha}_E$	1.53 rad/sec
$\ddot{\alpha}_E$	9.8 rad/sec^2

TABLE XVII

HEATING SUMMARY

V_E	15,200 ft/sec
γ_E	-14 degrees
Atmosphere	VM-7
Q_s	2227 Btu/ft^2
Max q_s	1705 Btu/ft^2 sec
Max q_s at max. diameter	24.0 Btu/ft^2 sec

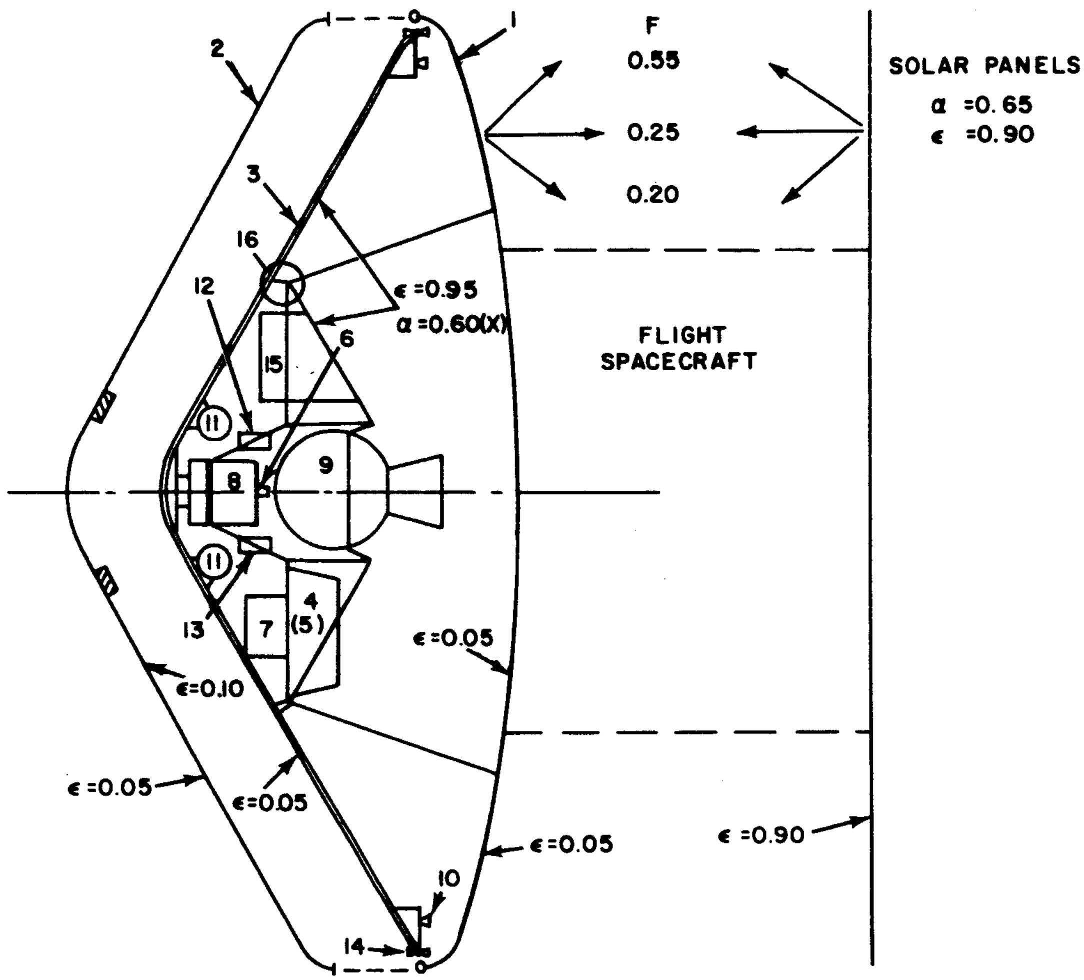

1. CANISTER BASE
2. CANISTER LID
3. ENTRY SHELL
4. TELECOMMUNICATIONS AND POWER MODULE (2)
5. INSTRUMENTATION MODULE
6. ACCELEROMETERS (3)
7. PENETROMETERS (4)
8. TELEVISION
9. ΔV PROPULSION
10. ACS REACTION NOZZLES (12)
11. ACS COLD GAS TANKS (2)
12. ACS ELECTRONICS
13. ACS SENTRY GYRO
14. TVC REACTION SUBSYSTEM (4)
15. PARACHUTE
16. ENTRY SHELL SEPARATION MECHANISM

X. PURPLE BLEND, UNCOATED

86 2191

Figure 21 THERMAL CONTROL SYSTEM

4.0 SYSTEM AND SUBSYSTEM TRADEOFF SUMMARY

4.1 GROWTH POTENTIAL AND DIAMETER SELECTION

A design diameter of 15 feet has been selected for the entry vehicle. This design diameter is somewhat in excess of that required for the particular engineering mission under consideration; however, it is preferable at this stage of design to decouple the entry shell design from the particular payload design. In the upper curve of Figure 22, the entry weight available at the required $M/C_D A$ is presented as a function of flight capsule diameter. The two lower curves present the weight required for the reference flight capsule configurations as a function of diameter. The lowest curve is the weight of the design excluding all contingency factors discussed in paragraph 2.4. The middle curve represents the weight required if these contingency factors are incorporated. This curve represents conservative preliminary design weights.

An additional weight is allowed in the actual design, over and above the required weight, to allow for growth in the system to the hardware stage and for possible moderate increases in instrumentation capability. The diameter selection of 15 feet gives approximately 6 percent of the total weight available for growth which is thought to be sufficient; the calculated weights shown are somewhat on the conservative side.

4.2 FIXED ΔV SELECTION AND ORBIT FLEXIBILITY

In the selection of a deorbit philosophy, mission and system constraints from many sources must be considered. The deorbit method should not limit the flexibility of orbit selection nor unduly constrain the mission by requiring orbit trim maneuvers for expected orbit injection errors. The deorbit method must allow flexibility in the selection of a landing site while retaining the capability to land at the proper time of day to ensure sufficient shadowing of surface features for television purposes. The deorbit method must also provide for proper communications geometry.

Four deorbit methods have been considered:

1) Fixed ΔV for all orbits

2) Fixed ΔV for each orbit, the ΔV selected for minimum entry angle dispersion

3) Fixed ΔV for each orbit, the ΔV selected for minimum ΔV magnitude

4) Variable ΔV, fixed entry angle.

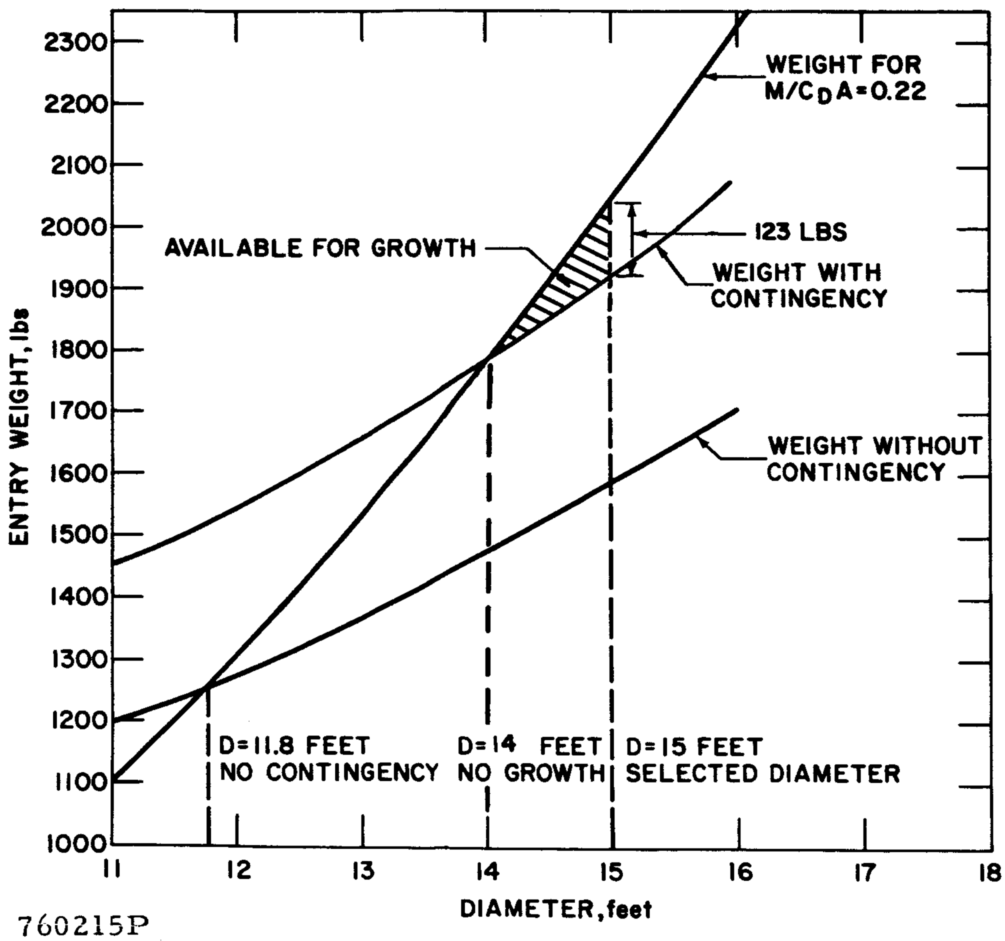

Figure 22 DIAMETER SELECTION AND WEIGHT AVAILABLE FOR GROWTH

These deorbit methods were selected to achieve various desireable system objectives such as: (1) a single fixed impulse engine for any orbit, (2) minimum entry angle dispersion; (3) minimum engine size and weight, and (4) mission flexibility for landing site selection from any orbit.

Figure 23 compares the four deorbit methods. The two techniques which employ a fixed ΔV, which is selected for each orbit, have the serious disadvantage of either requiring the development of a number of different engines if a range of orbits is to be maintained as optional, or the early selection of one orbit if only one engine development is pursued. These approaches are also significantly more sensitive to dispersion in the achieved orbit.

The performance of the concept employing a fixed ΔV for use on all orbits and the variable ΔV concept are roughly comparable. The variable ΔV concept, however, requires that thrust-termination capability be designed into the engine. Also, the engine must be jettisoned prior to entry since, depending on the particular orbit, significant propellant may be left after thrust termination. If the engine were not jettisoned, the resultant penalty on entry weight and suspended capsule weight would be prohibitive. The additional event sequences and the engine jettison requirement lead to undesirable failure modes which significantly detract from this approach.

The use of a fixed ΔV for all orbits is simple, flexible, meets all major requirements, and therefore, has been selected as the reference design.

At any deorbit true anomaly, there are an infinite number of ΔV magnitude and thrust application angle sets to achieve a specific entry angle; however, only one of these sets (for spacecraft central angle traversal < 360 degrees) also produces the optimum spacecraft-capsule communications geometry during capsule descent. For the orbits under consideration, Figure 24 shows the deorbit velocity requirements, as a function of deorbit true anomaly, with the condition understood that the thrust application angle is such as to produce the proper communications geometry.

From the figure it can be seen that a constant deorbit velocity of 1400 ft/sec will ensure optimum communications for the entire range of orbits considered. The achievement of a constant deorbit velocity requirement results in considerable engine simplification while retaining orbit selection flexibility.

At the selected deorbit velocity of 1400 ft/sec, the deorbit true anomaly is about 265 degrees, the range of true anomalies required to cover the entire range of orbits being very small ($\sim$ 17 degrees). The resulting deorbit, cruise, and entry conditions are very similar over the entire range of orbits. The sensitivity of these parameters to dispersion in the achieved orbit is, therefore, greatly reduced.

	Fixed ΔV All Orbits	Fixed ΔV Each Orbit		Variable ΔV Fixed γ_E
		Min $\Delta\gamma_E$	Min ΔV	
• Engine Design to Provide Orbit Flexibility				
Single engine fixed total impulse	X			
Many engines fixed total impulse		X	X	
Single engine thrust cut-off				X
• Entry Angle Dispersion	Fair-Good	Good	Poor	Good*
• Entry angle of attack (requirement for maneuver)	Fair-Good	Fair	Poor	Good*
• Time to entry (Battery Weight)	Good	Fair	Poor	Good*
• Sensitivity to orbital dispersion (requirement for orbit trim)	Good	Fair	Poor	Good*
• Periapsis location adjustment (efficiency of orbit injection)	Good	Fair	Poor	Good*
• Engine Size	Fair	Fair	Good	Poor
• Failure Mode				
Engine ejection required (propellant remaining)	Good	Good	Good	Poor
Thrust cut-off required (landing site miss)	Good	Good	Good	Poor

*All "Good" entries cannot all be achieved simultaneously in this technique.

Figure 23 DEORBIT METHOD SELECTION

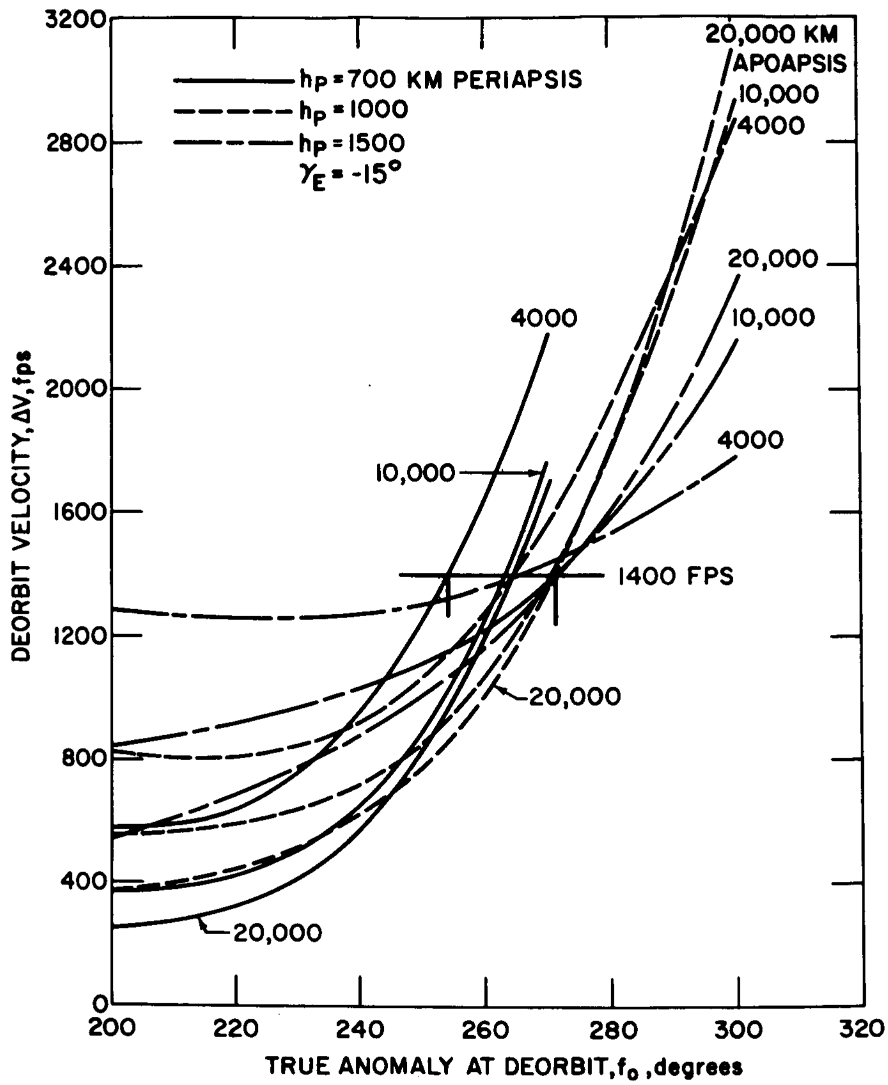

760147P

Figure 24 DEORBIT VELOCITY REQUIREMENTS

A weight optimization between the engine case weight and the required battery weight as a function of true anomaly has been performed for several orbits. The engine propellant has not been considered in this tradeoff since it is entirely burned prior to entry and is not chargeable to entry weight. The battery system considered is a totally redundant nickel-cadmium battery which operates the entire system from separation to deorbit (30 minutes) and thereafter, until impact. For true anomalies near apoapsis, the time of flight from deorbit to entry is long, thereby increasing the battery weight requirement. For true anomalies near periapsis, the required ΔV increases, thereby increasing engine case weight. The sum of the battery and engine weights are at a minimum at some deorbit true anomaly between apoapsis and periapsis. The optimum true anomaly range for all orbits corresponds quite well with the deorbit true anomalies (255 to 272 degrees) that result from the selection of a 1400 ft/sec velocity decrement.

Figure 25 shows the flight capsule entry velocity-entry angle map. The boundaries of the map labeled, "Nominal V_E-γ_EMap", represent the three-sigma entry angle dispersion limits about a nominal entry angle.

A range extension V_E-γ_E map is also shown. This boundary extends the range of entry angles to lower values constrained by the dynamic skipout contour at all velocities. With the fixed- ΔV deorbit concept, it is possible to extend the impact point by using shallower entry angles.

The impact true anomaly can be extended by slightly reducing the entry angle and adjusting the deorbit true anomaly and thrust application angle to maintain optimum communication geometry. This range extension capability is very significant, since it relaxes the orbit orientation requirements (argument of periapsis) or increases in number of deorbit opportunities by tending to cancel the apsidal line regression.

For the orbital range considered, the range extension capability is strongly dependent upon apoapsis altitude as shown in Figure 26, since increased apoapsis altitude results in increased entry velocity. Since the skip-out entry angle boundary increases with increasing entry velocity, smaller reductions in entry angle (less range extension) are permissible with increasing apoapsis altitude.

Figure 27 shows the number of landing passes that can be obtained over Syrtis Major after orbit injection, for the fixed-ΔV method of deorbit from a specific orbit. The natural periapsis is shown and the required periapsis location that must be achieved during orbit injection is also shown. All periapsis locations for subsequent passes over Syrtis Major consider the effect of nodal line precession and apsidal line regression. A fourth landing pass is possible, for this orbit, by use of the range extension capability. All passes shown have the proper landing time of day for proper television lighting.

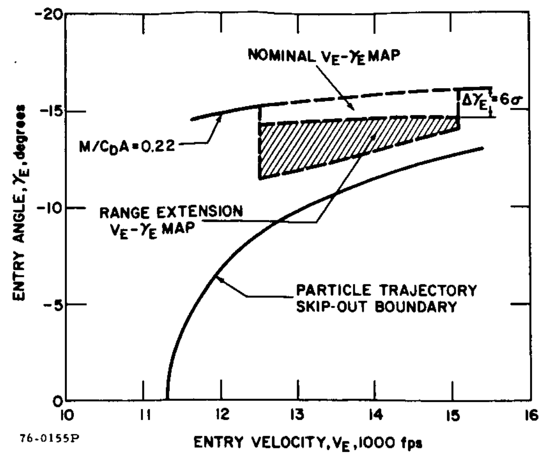

Figure 25 DISPERSION, RANGE EXTENSION, AND M/C_DA SELECTION

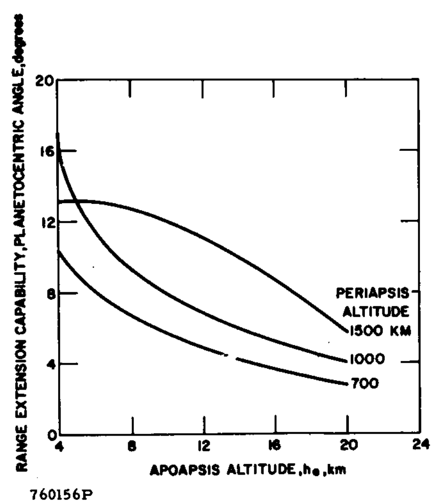

Figure 26 RANGE EXTENSION CAPABILITY

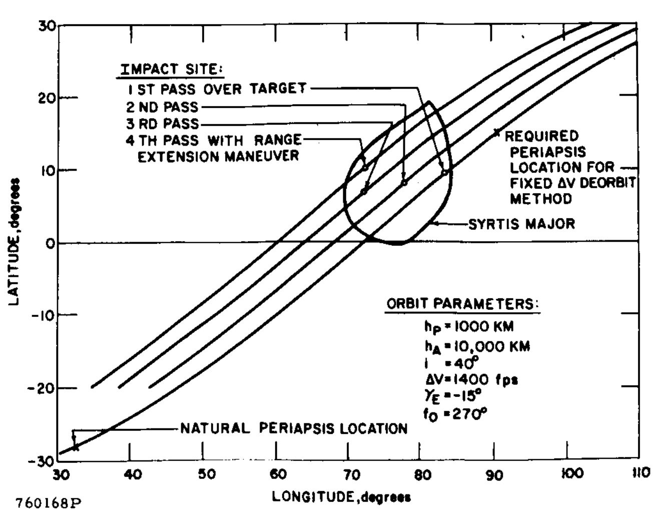

Figure 27 PERIAPSIS LOCATION AND IMPACT SITE ACHIEVEMENT

4.3 EXPERIMENT SELECTION

The general approach taken in the selection of experiments for the entry from orbit mission was first to develop a set of engineering and scientific objectives to be satisfied, second, from a study of the objectives to derive a list of candidate experiments which could be used to satisfy these objectives, and finally to select from this list a payload which would tend to minimize interface requirements, complexity, development problems, and integration difficulties while providing a high probability of achievement of the mission objectives. The candidate experiment list is given in Table XVIII. It is divided into those experiments which were included in the payload and those which were not.

The reasons for the inclusion or rejection of experiments are diverse, but fall into fairly small number of categories. Virtually all of the included experiments satisfy more than one of the mission goals and in addition are functionally redundant with at least one other experiment. They tend to complement other experiments. They exist today as flight qualified hardware, although not perhaps in the precise form required for the Mars mission or are under advanced development. With the exception of the television they do not place demands of great magnitude on the other flight capsule subsystems. In carrying out the tradeoffs which led to the rejection of experiments, the impact of a given experiment on the other experiments or other flight capsule subsystems was very carefully examined. The smoke bombs, surface transponder, impact accelerometer, and magnetometer experiments were rejected primarily on these grounds. A second sensitive criterion was the probability of obtaining ambiguously interpretable data or the probability of obtaining no meaningful data at all. Problems, in this area were raised with the radiometer, the surface transponder, the impact accelerometer and the rf probe. Experiments which provided single points of information were rejected in favor of more versatile ones, as is evident in the rejection of the oxygen, argon and carbon dioxide detectors and the particle microphone. Finally, experiments with serious development problems, such as the gamma scatter and the surface transponder, were avoided.

4.4 TELEVISION SYSTEM SELECTION

The prime objectives of the flight capsule television experiment are based on providing engineering and scientific data required for the future exploration of Mars. In fulfilling this objective, the television experiment must provide data unique to itself -- such as the generation of high resolution images for surface object hazard assessment -- and it must complement experiments performed with other elements of the instrumentation payload of the flight capsule and flight spacecraft.

In designing the television experiment, it has been assumed that the flight spacecraft will utilize both high and low resolution camera systems and that the high resolution system will map the region in which the flight capsule lands.

TABLE XVIII

CANDIDATE EXPERIMENT LIST

Selected Experiments	Rejected Experiments
Radiation detector	Smoke bombs
Accelerometer	Gamma scattering
Radar altimeter	Surface transponder
Mass spectrometer	Impact accelerometer
Acoustic densitometer	Oxygen detector
Gas chromatograph	Argon detector
Pressure gage	Carbon-dioxide detector
Temperature probe	RF probe
Television	Radiometer
Beta scatter	Particle microphone
Water detector	Magnetometer
Doppler radar	
Penetrometer	

The resolution which can be obtained from the flight spacecraft high resolution camera is assumed to be 10 to 100 meters/TV line.

The primary objectives of the flight capsule television experiment include generating imagery data to:

a) Assist in future flight capsule design through improved knowledge of surface object distributions, slopes, and bearing strength

b) Assist in the design of future image experiments from the surface through knowledge of local albedo and photometric properties

c) Assist in the interpretation of the lower resolution flight spacecraft images used to map larger segments of the Martian surface

d) Support other flight capsule experiments such as improving the interpretation of penetrometer results, wind measurements, atmospheric measurements, and radar surface roughness measurements.

Television images from the flight capsule will be used to generate engineering data through the analysis of topological statistics, the measurement of surface roughness, the identification of discrete surface object hazards, the generation of topographical maps to provide slope information, and the identification and description of geological features in larger maps. The desired image resolutions, nesting requirements, and solar elevation angles -- a key aspect of flight spacecraft-flight capsule trajectory selection -- are determined by considering each of these sub-experiments. In addition, the image characteristics required to effectively support wind measurements, atmospheric measurements, radar roughness measurements, and penetrometer bearing strength measurements are also reflected in generating the image requirements summarized in Figure 28.

The deorbit (preentry), entry, and parachute-descent regions of the capsule trajectory have been examined to determine the most advantageous period during which to take television pictures. The flight capsule has two major advantages over the flight spacecraft -- range to the surface and less potential atmospheric deterioration of images. The television experiment must use both of these advantages to achieve the high resolutions required for support data for future flight capsule operations. The parachute-descent phase has been selected as the best region for flight capsule image experiments, although it has certain limitations. The primary advantages are long duration at low altitudes and an unobstructed view of the surface from near vertical orientation. The major limitations of on-parachute television pictures are the relatively small total area covered and the effects of parachute dynamics.

PURPOSE	SURFACE RESOLUTION (FT/TV Line) MAX.	MIN.	NESTING DESIRABLE	LOCATION IN F/S IMAGES DESIRABLE	WIDE AREA COVERAGE DESIRABLE	TWO-COLORS DESIRABLE	DESIRED SOLAR ELEVATION ANGLE
Roughness and Object Hazards	0.1*	1.0			X		20^0-40^0
Topological Statistics	1	100		X	X		10^0-30^0
Experiment Support	3	30			X	X	20^0-40^0
Photometric Topography	3	100	X	X	X		20^0-30^0
Geological Mapping	10	100	X	X	X	X	20^0-60^0

*Desired Resolution Increased From Previous Value of 1 FT/TV Line Based on Luna IX Results

OTHER CONSIDERATIONS:

Lowest Resolution FC TV Should be no Worse Than 3:1 Better Than FS TV
Highest Resolution FC TV Should Meet Object Hazard Resolution Requirement
Steady Winds Prevent Picture Nesting by Means of Altitude Change
Nested Images Must Have no Worse Than 3:1 Resolution Relationship
At Least 32 Grey Levels Are Required
Cameras Should Operate at Minimum Surface Brightness of 30 Ft-Lamberts

760153P

Figure 28 TELEVISION IMAGE REQUIREMENTS

The use of relatively low sensitivity vidicon tubes -- in accordance with Langley Research Center direction -- necessitates long camera exposure times. Image smear because of flight capsule dynamics during exposure limits achievable resolution to 3 to 10 ft/TV line. The television cameras are mounted on a two-axis gimballed platform to minimize the effect of flight capsule dynamics, yield higher resolution images, and render the television experiment performance less sensitive to wind and gusts, and parachute/hardness design. The platform, slaved to the inertial reference system platform maintains camera look angles within 1 degree of local vertical and reduces pitch and yaw rates to less than 0.001 deg/sec.

A three-camera system with boresighted optical axes was selected to satisfy image resolution and nesting requirements during parachute descent. The cameras are designed with boresight resolutions in a 9:3:1 ratio and identical 200 X 200 element formats. They are exposed simultaneously to generate a nested set of three images. The 200 X 200 image format has been chosen as the best compromise -- in the light of solid-state data transmission limitations -- between area coverage and the variety and number of images required to achieve the experimental objectives. At least 11 pictures can be taken and transmitted during parachute descent even in the most tenous atmosphere. In denser atmospheres, additional images may be taken to increase the total number of samples. The pictures are taken at altitudes between 24,500 feet and 1400 feet to yield a resolution range of 36 to 0.25 ft/TV line. Figure 29 illustrates image format and area coverage.

The television experiment yield, tabulated in Figure 30, is dependent upon the atmosphere encountered during parachute descent. Both the number of images transmitted and the altitudes at which images are taken (hence their resolution) are different in each model atmosphere. In all cases, the highest resolution is adequate for the detection of object hazards and the lowest resolution for locating flight capsule pictures in the flight spacecraft pictures. The shutter logic is designed such that active video data is transmitted during the entire descent interval (beginning immediately after the first image set is exposed). The picture playout order -- Camera-C, Camera-B, Camera-A -- assures that the highest resolution image of each set is transmitted first.

Physical characteristics of the three-camera television system using standard state-of-the-art 1-inch vidicons are presented in Figure 31. In general, the Camera-A and -B are similar in many respects in Mariner IV and Ranger cameras. The Camera-C is closest to design limits. Double-blade mechanical shutters are contemplated to satisfy the short exposure time requirements (0.93 to 3.7 milliseconds). The requirements for a minimum detectable signal of 30 ft-Lamberts is based upon the assumed Martian surface photometric function and the desirability of maintaining as high a signal-to-noise ratio as possible to permit contrast expansion. Two color filters are used on the Camera-A, since it is the only one with sufficient signal energy to accommodate filter losses.

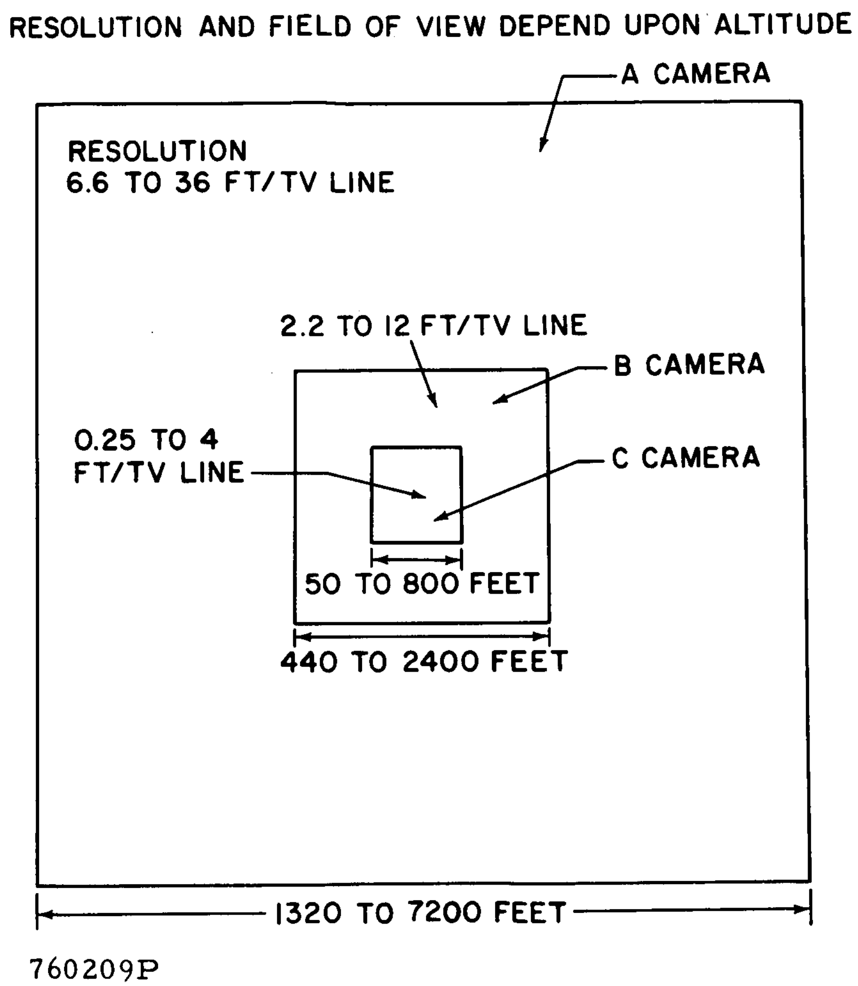

Figure 29 TELEVISION IMAGE FORMAT

	ATMOSPHERE			
	VM-3	VM-4	VM-7	VM-8
Number of Pictures	16	22	11	12
Altitude Range (1000 Ft.)	24.3-2.8	24.5-1.4	23.9-5.3	18.3-5.4
Resolution Range (FT/TV Line)	36-0.5	36-0.25	36-0.9	28-0.9

SEQUENCE: First Picture Set Taken Less Than 10 Seconds After Chute Deployment;
Subsequent Sets at 43 Second Intervals.

760182P

Figure 30 ANTICIPATED TELEVISION PICTURE YIELD

- Image Tubes — 3 Boresighted 1" Vidicons Mounted on 2-Axis Slaved Platform
- Optics

	A Camera	B Camera	C Camera
Field	24^0	8.2^0	2.7^0
Focal Length	0.4"	1.1"	3.3"
Relative Aperture	f/l	f/1.6	f/1

- Sensitivity — Unity SNR at Surface Brightness of 30 Ft-Lamberts
- Weight — 60 Lbs. Including Platform, Power Supply, Camera Electronics
- Power — 27 Watts
- Pictures
  - 3 Sets of 3 Nested Images/Set Minimum
  - 200 x 200 Lines
  - 32 Grey Levels
  - 2-Color Filters on A-Camera

760187P

Figure 31 TELEVISION SUBSYSTEM CHARACTERISTICS

4.5 ATTITUDE CONTROL SYSTEM SELECTION

Several alternatives were considered in the design of the ACS. The simplest is a spin-only system in which the separated vehicle is oriented to the thrusting attitude by the flight spacecraft and is spin stabilized after separation for thrusting and cruise. The vehicle must be despun prior to entry to minimize communications loss and to reduce problems of parachute deployment and entry shell jettison. This approach was rejected because of the requirement for a flight spacecraft maneuver. A second choice which eliminates the flight spacecraft maneuver is the use of an active ACS on the separated vehicle for orientation to the thrust attitude. Spin stabilization is then used for thrusting and cruise, with despin at entry. Although this approach permits either a flight spacecraft or separated vehicle maneuver, it does not permit post-thrust maneuvers to improve communications and lacks growth potential for use in later, more demanding missions. However, the use of spin is a highly reliable, proven technique. A third possibility is the use of active attitude control from the time of separation until entry. This approach would use cold-gas reaction control for all phases including stabilization while thrusting. As a result of high ACS thrust levels required to overcome the disturbance torques attributed to the deorbit rocket thrusting, the total impulse requirements make system weight excessive. An alternative is to use engine gimballing on an auxilliary hot-gas reaction control system for thrust vector control. Engine gimbals are heavy, complex, and less reliable. A hot-gas system using solid propellant gas generators can be highly reliable and light in weight. Because of its efficiency, large c.g. offsets and thrust vector misalignments can be tolerated, thus easing concern over variations in these parameters during the heat sterilization process. For these reasons, it is the system selected for the reference design.

4.6 TELECOMMUNICATIONS SUBSYSTEM SELECTION

4.6.1 Transmitter Power and Modulation

The short communication ranges associated with the entry from orbit mode allow a high data rate to be achieved with relatively low transmitter power. As in the case of entry from approach trajectory, a 30 watt solid-state transmitter was selected for the design. Higher power would necessitate the use of vacuum tubes, require a high voltage dc-to-dc converter, and possibly introduce problems of gaseous breakdown. The use of a noncoherent modulation technique still appears attractive. The complexity of the required auto-acquisition phase lock receiver coupled with the high probability of loss of lock during wind gusts overshadow the apparent advantages possible with a coherent system.

4.6.2 Influence of Parachute Size

A number of interesting tradeoffs can be made between the telecommunications system, the flight spacecraft, and the parachute. The response of the suspended capsule-parachute system to wind gusts is a prime factor in the design of the communications system. The resulting system swing angles determine the antenna beamwidth, and introduce severe multipath problems which influence the selection of the modulation technique and introduce the need for time diversity in the data formating. The selected parachute size of 81 feet is comfortably within the present state-of-the-art but further studies may conclude that a further reduction in size is desirable. A summary of these tradeoffs is presented in Figure 32.

4.6.3 Diversity Reception and Redundancy

The necessity to design for successful operation under severe wind gust conditions suggests the incorporation of features to combat fading. Of the various diversity techniques considered, time diversity offers the best chance for total data recovery.

In the absence of a weight constraint the incorporation of total redundancy is desirable; independent of fading. The benefits accrued when one utilizes this redundancy to obtain time diversity are considerable and impose virtually no additional penalty.

To minimize data loss in the event that one of the telecommunications systems fail, polarization diversity has been incorporated in the design. This measure, however, introduces additional equipment in the flight spacecraft receiver and may require further study to determine whether the failure mode which makes it desirable is sufficiently probable to warrant the additional equipment required.

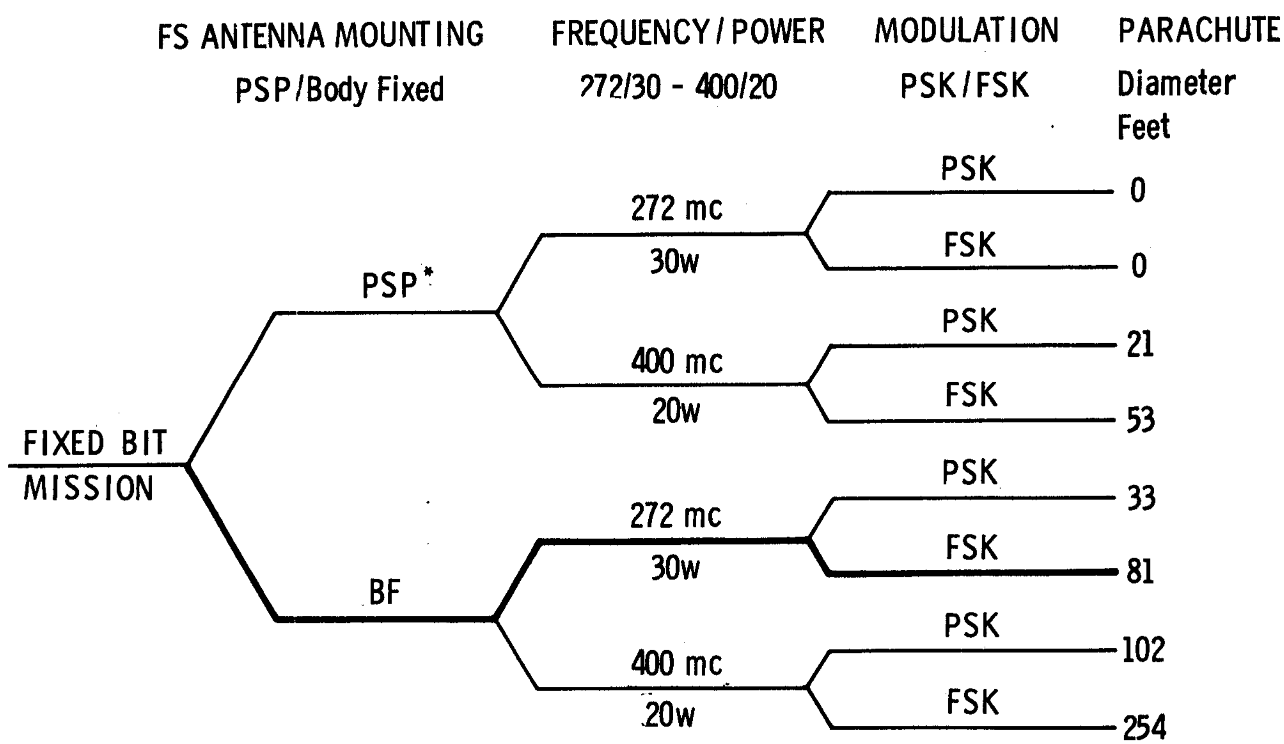

* Assumes communications during entry only

760232P

Figure 32 COMMUNICATIONS/PARACHUTE TRADEOFFS

5.0 DEVELOPMENT TEST PROGRAMS

5.1 INTRODUCTION

Development test requirements have been established for selected subsystems of the entry from orbit probe. The scope of the study was contractually restricted to the vehicle subsystems: structure and heat shield, sterilization canister, separation subsystems, parachute, attitude control and propulsion. The payload subsystems (communication, power supply, and instrumentation) were excluded. In addition, the ground test evaluation was limited contractually to the critical development problems to the exclusion of an extensive programming of routine tests.

In evaluating test requirements and candidate testing techniques, ground testing was considered the more desirable approach. Where these techniques proved inadequate, the potential of flight testing was examined. Results of the study indicate that flight testing was required for three subsystems: 1) parachute, 2) heat shield, and 3) separation subsystems. It was also determined that flight tests would augment rather than replace ground testing in these three cases. Of all the subsystems examined, only one (the parachute) was found to require technological development. Consequently, early pre-Voyager flight testing is recommended for this system.

The ground-test program is summarized in paragraph 5.2 and the flight-test program in paragraph 5.3.

5.2 GROUND TESTS

5.2.1 Entry Vehicle

5.2.1.1 Aerothermodynamics

Aerothermodynamic analyses provide the environment in terms of the imposed thermal and structural loads as well as the vehicle stability and performance. This involves determining pressure and heating distributions and aerodynamic coefficients. The development testing should be aimed at filling basic information gaps and investigating critical areas.

The velocities associated with entry out of orbit are such that radiative heating does not contribute significantly to the environments; thus only convective heating need be investigated. A significant reduction in the development test program can be realized if the ground tests are restricted in the extent to which atmospheric composition is varied. Considerable data have already been obtained on the effect of atmospheric composition on convective heating. Thus, it is recommended that the ground tests be conducted on the reference configuration in air with the data presently available being utilized to account for composition effects.

In particular, the desired information should be established under real gas conditions, the relevant parameter in this case being the stagnation point density ratio, ρ_s / ρ_∞ which is a measure of the effective specific heat ratio as well as the shock standoff distance. The simulation of ρ_s / ρ_∞ is necessary to ensure adequate determination of the performance and environments.

The aerothermodynamic testing has been divided into three elements: 1) the afterbody, 2) the forebody, and 3) the entry configuration comprising the afterbody and forebody.

The afterbody development is critical in terms of the overall system requirement. Its primary function of ensuring only one stable trim point, can result in significant penalties not only in weight but in terms of other system interfaces such as the ΔV-rocket location. The early phase of the program would determine if a minimum afterbody is justified and if auxiliary destabilizing devices such as asymmetries or flaps are needed.

Primary emphasis for the forebody is on the generation of basic design information, such as pressure distributions and heating distributions. Included in these tests are the effects of protuberances and cavities, which will be examined on the reference configurations to ensure the proper local flow environments and obviate the need for possible parametric studies.

The configuration performace and stability development will require a complete Mach No. variation as well as testing in a gas other than air to determine the possible effects of density ratio on the vehicle aerodynamic coefficients.

Table XIX summarizes the aerothermodynamic development requirements and tests. The simulation requirements are shown in Figure 33 where flight conditions at various critical phases are delineated.

5.2.1.2 Thermal Protection

The thermal protection system (TPS) consists of the composite of an external layer of heat shielding material bonded to the load carrying structure. The performance of the heat shield and its response to the environment depends not only on the basic properties of the material itself but also on the environment it is exposed to. While it is relatively easy to predict analytically the effect of the substructure on the

TABLE XIX

AEROTHERMODYNAMIC DEVELOPMENT

	Element	Mission Phase of Concern	Design Analysis Problem Area or Requirement	Test Objectives	Test Description	Desired Test Conditions	Typical Test Facilities
(A)	Afterbody	Early entry and entry	Heating and stability	Determination of: 1. Rearward stability 2. Need for and effectiveness of flaps and/or asymmetries 3. Heating distributions and local aggravations	1. Static force and moment measurements in wind tunnels and ballistic range 2. Wind-tunnel measurements of heating and aggravations	1. Hypersonic Mach Nos. (greater than 10) 2. Low Reynolds Nos. (less than 10^5)	1. Ames Hypersonic Blowdown Tunnel 2. JPL Hypersonic 3. NOL Ballistic Range
(B)	Forebody	Entry	1. Heating 2. Pressure Distributions	Determination of: 1. Pressure/Distributions 2. Low Reynolds No. effects on heating 3. Angle of attack effect on heating and loads 4. Local aggravations	Wind-tunnel measurements of heating and pressures	1. Hypersonic Mach Nos. (greater than 10) 2. Reynolds Nos. between 10^4 and 10^6 3. Density ratios as high as possible	1. Ames Hypersonic Blowdown Tunnel 2. Cornell Wave Superheater 3. Langley Hypersonic
(C)	Entry Configuration	Early entry Entry and post-entry	Performance and stability	Determination of: 1. Static and dynamic stability derivatives 2. Force derivatives 3. Composition effects	Force and Moment Measurements in Wind Tunnels and Ballistic Range	Complete simulation of Mach and Reynolds Nos. variations and density ratios extent as well as angle of attack	1. Eight-Foot Transonic Tunnel Langley 2. Unitary Wind Tunnel 3. Ames Hypersonic Blowdown Tunnel 4. NOL Ballistic Range 5. BRL Ballistic Range
(D)	Parachute Flight Test Vehicle	Post-entry	Transonic stability and performance	Determination of: 1. Static and dynamic stability derivatives 2. Force derivatives at transonic speeds	Force and Moment Measurements in Wind Tunnel	Transonic Mach. Nos. at moderate Reynolds Nos.	Eight-Foot Transonic Wind Tunnel Langley

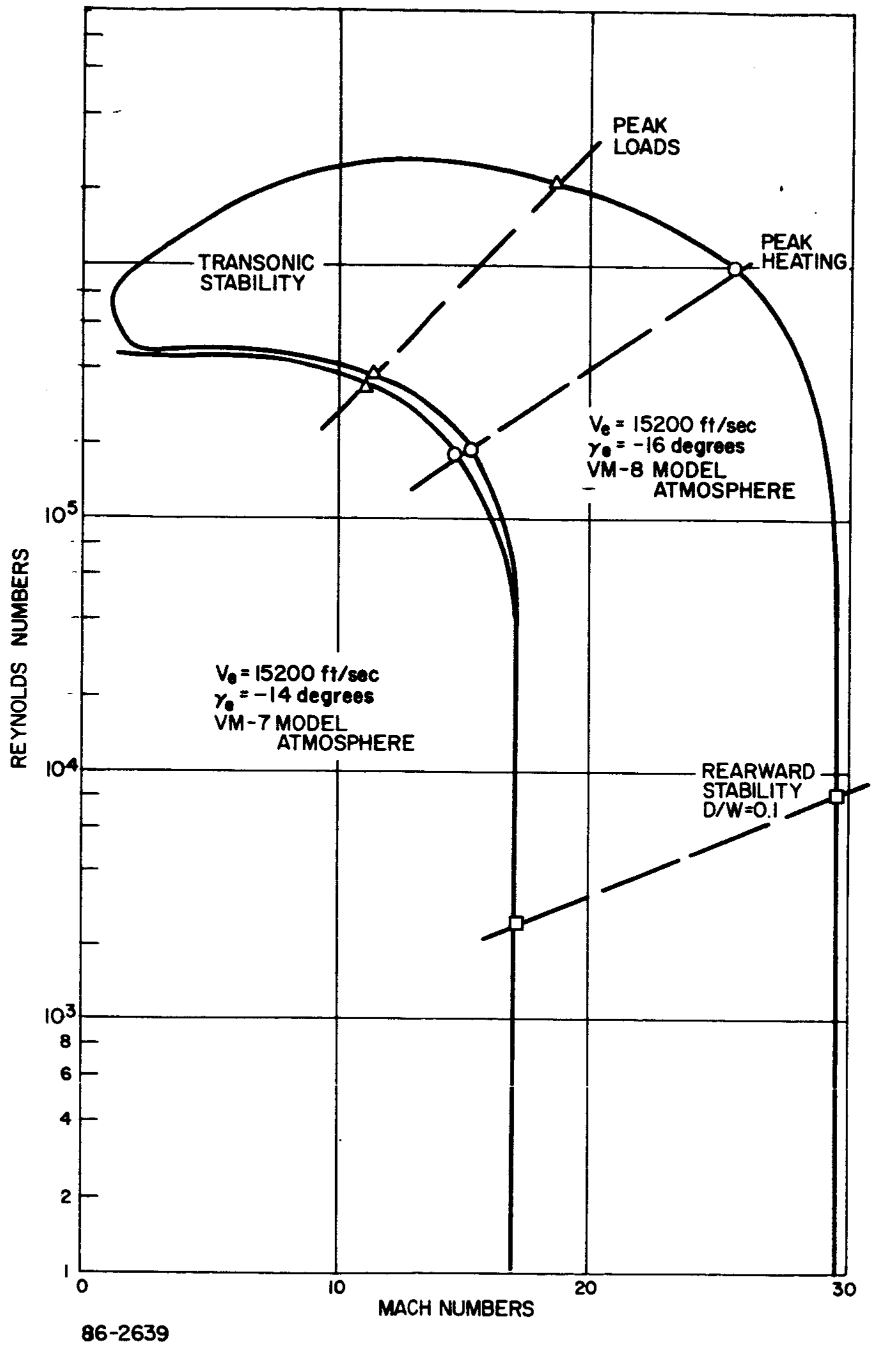

Figure 33 MARS ENTRY SIMULATION REQUIREMENTS

heat shield material and verify it during the ground test program, it is extremely difficult to predict the heat shield performance for a particular application without an extensive testing program. There are no ground-test facilities available now or projected in the near future capable of simultaneously duplicating or simulating the anticipated flight environment parameters. Such simulation, of course, would be necessary to assure the conformance of the preflight prediction with actual flight data for a material which was not flown before. The necessity of flight testing (assuming the existence of an extensive ground test program) depends on the degree of the conformance required of the design, which in turn depends on the safety margins allowed. It is not possible to design a heat shield with any degree of confidence without an extensive material characterization program including more than just "simulated" quasi-steady state entry heating arc-jet tests. The possibility of transient trajectory simulation in the arcs greatly enhances the predictability. The thermal protection system must survive the decontamination and sterilization environments, mechanical environments, possible exposure to vacuum, low temperatures anticipated in space, and then perform its thermal function in the entry environment.

The purpose of the heat-shield material test program is to determine the thermal, optical, and mechanical properties, and ablation characteristics of existing materials for design use (determination of heat shield thickness required) rather than development of new materials. The program should consist of preliminary screening tests and subsequent comprehensive development tests. No more than four materials should be used for the screening tests and no more than two materials should be considered for the development tests: one for the reference design and one for backup. The Purple Blend - Mod 5 and Cork Silicone are the most likely candidates as of now. Purple Blend was used as the reference in the conceptual design studies. The scope of the screening tests in terms of individual objectives, test conditions and their range, number of tests and samples, test procedures and techniques is outlined in Table XX. It indicates the number of tests at various points in the desired range for various conditions of the specimen prior to test. The number of tests presented is for the purpose of comparison with the development test-program requirements. The table describes the type of test (including the candidate facility, where pertinent) to be performed to obtain the necessary screening data. Two sets of candidate materials and samples would be exposed to the qualification sterilization cycle first to determine the effect of this environment, then one of the set of the samples would be exposed to the space vacuum simulation and tests would be repeated. After completion of the screening tests, the selected material(s) would be evaluated in a more comprehensive characterization program as described in Table XXI. This program involves the same and additional

TABLE XX

HEAT SHIELD MATERIALS SCREENING TEST

(PRECONDITIONED) DECONTAMINATED, STERILIZED AND EXPOSED TO SIMULATED SPACEFLIGHT

Element	Mission Phase of Concern	Design Analysis Problem Areas or Requirements	Test Objectives	Test Description	Test Conditions Desired
Ablator	Entry	Selection of efficient lightweight material and preliminary design for the expected thermal environment (atmosphere heat flux and duration, enthalpy and pressure)	1. Provide basic characterization of materials for design calculations of temp., mass loss, required thickness, leading to selection of material(s) for min. weight fraction (performance prediction).		1. Number of materials not to exceed 4. 2. Environmental test parameters or their derivatives to approach the design operating conditions. 3. No. of tests will depend on reliability requirements.
			a) Determine thermal properties	Measurement of thermal conductivity	True virgin materials and three fully charred samples Temp. range -50°F to surface temperature expected
				Measurement of heat capacity	Same as above but 2 samples only
			b) Determine optical properties	Measurement of thermal emittance	Same as heat capacity
				Measurement of transmittance/ reflectance	Same as above
			c) Determine other chemical and physical properties	Measurement of density	Same as conductivity
				Measurement of porosity	None for screening
				Measurement of permeability	None for screening
				Measurement of internal rate constants	3 temperature rates
			d) Determine ablation characteristics and flow effects	Measurement of laminar ablation parameters	Five samples H_m/RT_o:50-200; q_c as required
				Measurement of turbulent ablation parameters	
			2. Verify theoretical ablation model usage of degradation parameters, surface and internal reactions, blowing and atmosphere	Measurement of ablation rates, weight loss, density changes and temperature distribution under simulated entry conditions for a thermocouple instrumented sample transient test.	13 samples H_m/RT_o:50-200; $T_{structure}$ as required by design (Approx. 500°F at the bond line) Atmospheres: air and 2 other compositions.
			3. Provide preliminary design information on mechanical behavior of materials to assure integrity and compatibility with the structure.		
			a) Determine tensile properties	Experimental determination of stress-strain curves and measurement of the thermal strain	Five samples of each test Temperature range - 150 to approximately 500°F.
			b) Determine compressive properties	Experimental determination of stress-strain curves and measurement of the thermal strain	Five samples of each test Temperature range - 150 to approximately 500°F.
			c) Determine Poisson's Ratio	Experimental determination of stress-strain curves and measurement of the thermal strain	Five samples of each test Temperature range - 150 to approximately 500°F.
			d) Determine Thermal Expansion	Experimental determination of stress-strain curves and measurement of the thermal strain	Five samples of each test Temperature range - 150 to approximately 500°F
	Decontamination/ Sterilization Spaceflight	Changes in material decomposition and behavior during these phases of mission and the ensuing difficulties in cost control, material selection, evaluation, design and test	1. Select material requiring minimum preconditioning treatment needed to minimize changes due to the decontamination/and sterilizing cycles and vacuum exposure.	Measurement of selected thermal properties and ablative characteristics.	a) same as for entry but material decontaminated and sterilized only b) Same but also exposed to simulated space condition.
			2. Adjust composition to minimize degradation and provide maximum stability	Measurement of mechanical properties	a) Same as (a) above b) Same as (b) above
				Determination of chemical composition by infrared spectrophotometric and gas chromatography studies.	a) Material decontaminated and sterilized, process simulated b) As decontaminated, sterilized c) As exposed to decontamination, sterilization and space conditions
Bond	All Phases	Bond strength at elevated temperatures	Provide thermal properties for design.	No thermal screening required. Manufacturer's data to be used in preliminary design. (See also Structures Testing).	

TABLE XXI

HEAT SHIELD ABLATOR DEVELOPMENT TEST
(Sterilized and preconditioned)*

Element	Mission Phase of Concern	Design Analysis Problem Area or Requirements	Test Objectives	Test Description	Test Conditions Desired
Ablator	Entry	1. Determination of H/S weight fraction and prediction of response of the H/S to expected environments.	1. Provide property & characteristics parameters for design use & performance prediction.		1. No. of materials not to exceed 2. 2. Environmental test parameters of their derivatives to approach the design operating conditions. 3. No. of tests will depend on reliability requirements.
		2. Preparation of H/S Material specifications	a) Determine thermal properties	Measurement of thermal conductivity Measurement of heat capacity	Six virgin mat'ls and six fully charred samples. Temperature range -50° to surface temperature expected. Same as above but 4 samples only
			b) Determine optical properties	Measurement of thermal emittance Measurement of transmittance/reflectance	Same as heat capacity Same as above
			c) Determine other chemical & physical properties	Measurement of density Measurement of porosity Measurement of permeability Measurement of internal rate constants	Same as conductivity To be determined after screening tests Same as above Three temperature rates
			d) Determine ablation characteristics and flow effects	Measurement of laminar ablation parameters. Measurement of turbulent ablation parameters. subsonic	10 samples H_m/RT_o 50 -200; q_c and p as required. Six samples H_m/RT_o 50-200; q_c and p as required
			2. Verify theoretical ablation model usage of degradation-parameters, surface & internal reactions, blowing and atmosphere.	Measurement of ablation rates, weight loss, density changes and temperature distributions under simulated entry conditions for a thermocouple instrumented sample transient test.	25 samples H_m/RT_o 50-200; q_c and p as required T(structure-as required by design (approx. 500°F at the bond line) Atmosphere: air and 2 other compositions.
		3. Compatibility with the structure.	3. Provide design information on mechanical behavior of materials to assure integrity & compatibility with the structure. a) Determine tensile properties b) Determine compressive properties c) Determine Poisson's Ratio d) Determine thermal expansion	Experimental determination of stress-strain curves and measurement of thermal strain	Five samples for each test Temperature range-150 to approximately 500°F.
	Decontamination/ Sterilization/ Spaceflight	Effect of Heat shield exposure to decontamination, sterilization and space vacuum on its performance	Provide design information for the material performance evaluation in "as exposed" condition for thermo-structural & thermal control performance prediction.	See tests for entry phase, and screening program.	
	Post Separation	Impingement of ΔV rocket plume on heat shield.	Determine plume heating and its effect on heat shield performance.	Exposure to rocket plume	Actual motor in Vacuum
	Misc. Environments	Assurance of performance and satisfaction of specifications.	As required by Government specifications		
	Manufacturing	Assurance of reproducibility of materials, homogenity and integrity during exposure to various elements.	1. Raw materials a) Identify and control contamination. b) Determine batch to batch chemical variation. c) Control moisture.	See description in Section	
			2. Develop process for scale-up from laboratory techniques and select fabrication process.	Depends on the screening test results and selection of reference materials.	
			3. Develop nondestructive test method. 4. Verify heat shield process (including humidity effects)		
Bond	All phases	Same as for the ablator except no requirement for ablative performance test. See Structural Test.			
Thermal Control Coating/ H/S/Bond	All phases	No critical thermal protection problem areas.	1. Determine thermostructural compatibility. 2. Determine thermal control/heat shield material compatibility	See Structure Test See Thermal Control Test.	
Structure Composite					
Joints, Interfaces, Protuberances	Entry	1. Prediction of H/S performance in areas where potential aggravation problems exist. (See also Aerothermodynamic tests - difficulty in environment prediction.) 2. Selection of local substitute materials or design configurations to assure performance.	1. Determine empirically the effect of aggravation on material response 2. Predict Performance.	Measurement in a joint test with aerothermo changes in the environment. Measure the erosion (ablation) rates in the vicinity of the aggravation, together with temperature response.	Depends on design configuration

*Unless otherwise noted

tests as included in the screening tests and will completely characterize the remaining candidate material(s) to allow final choice of a material.

5.2.1.3 Structures

The structural development test plan represents the minimum testing required to obtain design information and verify performance to ensure that an efficient structural design is evolved.

The scope of the tests depends to a great extent on the criticality of the structural weight fraction. If there is an ample allowance in the capsule system for structural weight, and if conservative design practices may be used with large margins of safety in areas of uncertainty, the number of the tests can be minimized. If, however, weight restrictions require that more or less unconventional or untried methods be used for analysis, with small margins of safety, more extensive testing will be required to verify theoretical analyses and performance predictions.

The development plan is divided into two categories: tests for design information and tests for performance predictions. The division depends to a degree on whether a component can be treated separately or has a major interaction with a nonstructural element.

The major design requirements for development tests occur in the entry - shell structure. The reference design consists of a honeycomb sandwich conical shell stiffened by a ring at the forward and aft end with another integral ring serving as a hard point for attachment of the payload.

There are many possible modes of failure for the sandwich shell and honeycomb core in which specific test data is lacking - for example; the general instability of conical shells is based on test data obtained for homogeneous isotropic cylinders. The edge restraints in the tests also do not simulate the actual elastic restraints that occur in the reference design. In addition, core strength requirements for the design were determined using data obtained from tests on flat plates and columns.

In other areas, such as the internal structure, numerous assumptions have to be made in order to reduce the size of the analysis effort. In this relatively complex structure, in some cases, it will be more economical in time and cost to test rather than analyze in detail a subcomponent.

The analysis of the structure for dynamic launch environments generally uses a combined analytical and experimental approach. A mathematical dynamic model of the structural system is developed and then modified by the results of vibration tests. The improved mathematical model is then used to predict the response of the structure to other dynamic environments.

The tests described therefore range from obtaining data which is not presently available for a certain class of structures to more or less conventional tests which directly support the design effort. A description of the recommended tests is given in Table XXII.

5.2.1.4 Thermal Control

The thermal control system function is to maintain the temperature levels of the various components of the flight capsule within prescribed limits.

A secondary objective is to provide pre-entry temperature levels for the entry shell to minimize their weight while maintaining their thermostructural compatibility. Finally, the temperature control system should minimize flight-spacecraft, temperature excursions after separation as well as minimizing spacecraft power requirements before separation.

The thermal control is basically a passive system augmented by heating elements placed at required locations. It is incorporated by applying coatings and utilizing the existing structural members for heat-flow management and heat leakage control; local insulation may also be required. The thermal control development problems and technical requirements for either the entry shell or canister subsystems are similar (low emissivity coatings are required for both); however, the canister subsystem is simpler since the coating would be applied to a metallic substrate. For the entry vehicle shell the substrate is organic and presents outgassing, potential low temperature (below transition phases), and decontamination/sterilization problems. Thus, even though discussed for the entry vehicle shell only, the discussion is also applicable to the sterilization canister. The thermal control system consists of the coatings, insulation materials, and heaters. The radiative heat interchange between the internal surfaces is controlled by proper surface conditioning, and convective heat transfer is usually negligible although it may depend on the prevailing g-level and the degree of internal pressurization.

Since the flight capsule is primarily in the shade of the spacecraft, a low emissivity ($\epsilon = 0.05$ to 0.1) coating is essential. The operating temperature limits of the components appear to be quite compatible with the lower temperature heat shield limit (approximately -100°F).

TABLE XXII

STRUCTURAL DEVELOPMENT TESTS

Element	Mission Phase of Concern	Design Analysis Problem Area or Requirements	Test Objectives	Test Description	Test Conditions Desired	Typical Test Facilities & Equipment
Entry Shell Structure	Entry	Conical Shell-End Ring Stability	Verify the theoretical analysis of the shell-end ring stability	Measurement of stability as a function of relative stiffness of shell and ring, pressure distribution.	1. Force free boundary conditions at large diameter. 2. 1/4-scale or less 3. Stiffness simulation of full-scale structure not required 4. Differential pressure less than 5 lb/in.^{2}	1. Subsonic wind tunnel
	Entry	Honeycomb Sandwich Conical Entry Shell stability	Verify theoretical analysis and obtain empirical design data for failure modes including general instability, intracell buckling, face-sheet wrinkling, core crushing, and core shear.	Measurement of the stability of honeycomb sandwich shell as a function of face-sheet thickness, core depth, core material, and cell size.	1. Hydrostatic pressure plus axial tension 2. 1/4-scale or less 3. Stiffness simulation not feasible due to gage limitation 4. Differential pressure less than 5 psi.	1. Pressure differential developed by partial vacuum in interior of shell 2. External forces applied by hydraulic jacks through load cells
		Entry Shell Structure Dynamics	Verify method of predicting frequency and mode shapes of entry shell structure	Measurement mode shapes and frequencies of conical shell structure as a function of shell stiffness, ring stiffness, and honeycomb core depth	1. Simulated boundary conditions associated with actual flight conditions 2. Frequency from 0.5 to 1000 cps	1. Electromagnetic shaker 2. Air jet shaker
	Sterilization and Spaceflight	Compatibility of ablation and substructure	Verify predicted strains, stresses deflections and margins of safety	Full-scale ablator and structure subjected to sterilization process and cold soak environment	1. Simulated restraints and supports of adjacent structure	1. Oven 2. Space chamber
	Entry	Thermal stresses due to entry temperature gradients	Verify predicted strains, stresses, deflections and margins of safety	Full-scale entry shell with temperature gradients simulated by quartz lamp radiant heaters	1. Critical temperature gradient combined with aerodynamic loading	
	Manufacturing	Selection of manufacturing process to minimize imperfections which will reduce strength of entry shell				
Joints, Fittings, Attachments and Bonds	Complete Mission	Selection of efficient structural details	1. Determine margin of safety for design concepts under combined and sequential loading 2. Provide design data such as stiffness characteristics for static and dynamic analysis	Specific tests will be designed to simulate critical loading for each particular component	Static, oscillatory and shock-loading as determined by prior analysis.	
Ablator	Sterilization	Effect of sterilization cycle on mechanical properties of ablator	Provide design data for analysis of ablator and structural compatibility	Measurement of mechanical properties after exposure to sterilization cycle: a) Stress-strain curve b) Thermal strain c) Dimensional stability	1. Simulated sterilization cycle	
	Spaceflight and Entry	Effect of spaceflight vacuum and thermal cycling on mechanical properties	Provide design data for analysis of ablator and structure compatibility and integrity during spaceflight and entry	Measurement of mechanical properties after exposure to spaceflight vacuum and thermal cycle.	1. Prolonged exposure to simulated spaceflight vacuum environment 2. Thermal cycle as predicted by analysis 3. Measurement made both in vacuum and ambient pressure	
Suspended Structure	1. Ground handling 2. Launch 3. Entry 4. Parachute Deployment	Stiffness and vibration characteristics required for use in static and dynamic analysis	Provide design information	1. Measurement of static influence coefficients 2. Measurement of natural frequencies of components	1. Static-force deflection measurement at critical locations determined by analysis 2. Sinusoidal frequency sweeps	
	1. Ground handling 2. Launch 3. Parachute Deployment 4. Entry	Performance of Complete suspended structure	Verify performance prediction of suspended structure	1. Simulated external forces, moments and inertial reactions applied to structure at critical locations determined by prior analysis 2. Simulated vibration input at critical locations	1. Critical static forces to be determined 2. Parachute deployment 18,000 pounds 3. Vibration 20 g's 2 to 50 cps 1.5 g's 50 to 300 cps	

Of importance are their optical and adhesion characteristics when applied to the substrate (the composite of coating and heat shield) and exposed to the environments. This in turn will require effort in the application methods development (bonding and surface preparation) to assure adhesion and proper coating thickness selection, and determination of the properties of the composite that are required to assure the performance. The effect of ETO decontamination and dry-heat sterilization cycles and the effect of low temperature and vacuum during cruise and orbit near Mars on the coating composite performance will have to be determined.

Prediction of the heat-flow and temperature distributions in the entry vehicle shell and payload modules is quite feasible; however, testing is required because of the uncertainties of actual contact resistances present in the many joints and interfaces and because of the many interacting radiative paths.

Consideration of thermo-structural compatibility per se (during spaceflight) may require model testing (depending on safety margins allowable). A half-scale model could be used. However, full-scale structural models may be available for other purposes.

The critical areas of the development are associated with the behavior of the composite of coating and heat shield, and the determination of heat-flow patterns through the structural members and joints to the payload for all environments anticipated. The degree of the severity of the problems depends on the allowable emissivity and temperature variation and structural safety margin, while skillful control may contribute to a decrease in thermal protection weight.

Facilities for testing present no critical problems even for full-scale tests. The tradeoff between full-scale and half-scale testing will reduce itself to a time and cost consideration, provided the half-scale model is sufficient for design purposes.

A summary of the recommended development tests is given in Table XXIII.

5.2.2. Sterilization Canister Development and Ground Tests

The sterilization canister acts as a sterilization barrier to prevent recontamination of the entry vehicle and as a passive thermal barrier to moderate heat loss. The thermal barrier function can be accomplished by the canister structure itself if the exterior finish has an emissivity of 0.05 to 0.1. Attainment of this emissivity is not a major problem, however, maintenance of the finish through the ground handling and mission environments may

TABLE XXIII

TEST SYNTHESIS SUMMARY - THERMAL CONTROL

Item No.	Primary Operating Function of the Element(s)	Critical Area	Description of Elements, Subassembly, etc.	Phase of Mission of Concern	Design Information	Performance Prediction	Concepts & Methods Test
1	Passive temperature control	Yes (performance data)	Thermal Control Coating/Heat Shield Composite	Cruise, planetary orbit and post separation	X	X	X
2	Thermo-structural	Yes (for survival of environment and use of properly conditioned material properties)	Thermal Control Coating/Heat Shield Composite	Decontamination and Sterilization	X	X	
3	Component Insulation	No (but "in place" property information needed)	Thermal Insulation Materials	Cruise, planetary orbit, post separation, entry, parachute descent	X		
4	Insulation	Same as Item 2	Thermal Insulation Materials	Decontamination and Sterilization	X		
5	Active Temperature Control	Yes (integration & performance)	Electric Heaters	Cruise and planetary orbit		X	X
6*	Active Temperature Control	Same as Item 2	Electric Heaters	Decontamination and Sterilization			
7	Local heat flow control and structural	Yes (performance data)	Separation mechanisms, heater interface, structural joints, payload components/support structure interfaces, etc.	Cruise, planetary orbit, post separation, entry, parachute descent	X	X	X
8*	Thermo-structural	Same as Item 2	Separation mechanisms, heater interface, structural joints, payload components/support structure interfaces, etc.	Decontamination and Sterilization	-	-	-
9	Overall heat flow management and thermal structural	Yes (overall performance verification)	Entry vehicle including suspended capsule	Planetary orbit, post separation entry, parachute descent	-	X	
10*	Thermo-structural	Same as Item 2	Entry vehicle including suspended capsule	Decontamination & Sterilization	-	-	

*It is assumed that in the sterilization program the effect of decontamination and sterilization on components will be determined.

present a problem. Advantage will be taken of other testing programs in this field and no extensive development testing appears necessary. As a sterilization barrier, the canister is required to maintain the mission probability to less than 10^{-4} of transferring viable microorganisms from Earth to Mars. Prior to orbit injection, the canister lid is separated. The maintenance of sterility and the lid separation will require development tests which are summarized as follow:

5.2.2.1 Pressure Control and Sealing Integrity

Pressure control and sealing integrity are important primarily from the standpoint of the maintenance of sterility. The necessary test program will develop the techniques to determine the relationship between leak rates and hole sizes in the welds and seals, the capability of the microorganisms to move upstream through a leak, and the method of detecting both the location of a minute leak and the penetration of it by organisms.

5.2.2.2 Recontamination

Tests are required to assure that the capsule is not recontaminated by handling and environmental conditions after sterilization. The conditions of concern are the ground handling shocks, launch-pad mating loads, ascent flight, and thermal gradients during the cruise phase. Under these conditions, the possibility exists that seals could momentarily open or that microscopic structural openings at joints and fittings could allow recontamination. Tests of full size canister assemblies must be performed under simulated environmental conditions to detect possible weak points in the design. A test is also required of the canister lid separation to determine its effect on sterility.

5.2.2.3 Canister Lid Separation

The design for separating the canister lid from the base consists of an encased mild detonating fuse (MDF). When the MDF is detonated, the explosive residue is retained within the encasing material which expands and shears the canister skin against an outer ring and then forces the lid to separate from the canister base.

Extensive development testing is required to size the MDF charge, to choose the encasing material and to generally determine sufficient information on the detail design to have confidence in its actuation after experiencing the severe mission environments.

Large scale testing is required to prove the anticipated separation characteristics, such as, tip off rates and gross impulse, and in conjunction with the recontamination problem, to assure delivery of a sterilized entry vehicle to Mars.

5.2.3 Separation Subsystem Development and Ground Tests

There are six separation subsystems in the flight capsule including the sterilization canister lid separation subsystem which was previously summarized. The remaining systems are summarized in this section.

5.2.3.1 Flight Spacecraft - Entry Vehicle Separation

The entry vehicle is separated from the flight spacecraft by release of a V-type clamp ring and by impulse from 10 compression springs. Element tests are required to check the explosive release mechanism performance (explosive nuts with bolt ejection) after exposure to the mission environments. System tests are then required to check the explosive release mechanism performance and, in addition, to provide confidence that the separating vehicle will not hang-up nor incur excessive tip-off rates. These tests require pendulum-type test equipment to duplicate separation characteristics under zero gravity conditions. The primary system test problems will result from the size of the equipment.

5.2.3.2 Entry Shell - Suspended Capsule Separation

The entry shell is separated from the suspended capsule by release of a V-type clamp ring. Unlike the release of the entry vehicle, springs are not required, the separating force being furnished by the drag of the parachute.

The explosive release mechanism is the same as for the entry vehicle release and the element tests of one set of these mechanisms shall suffice for the other. The system tests, though, require release of the shell under simulated worst-case parachute-loading conditions. To obtain these loading conditions, drop tests and full-scale flight tests will be required.

5.2.3.3 Parachute Ejection

The parachute system deployment begins by mortar ejection of the pilot chute into the air stream. This, in turn, pulls out the main parachute canister cover and, subsequently, the main parachute bag. As the bag is pulled from the entry vehicle the main parachute deploys; and the bag and pilot parachute are discarded. In case the pilot parachute fails to be ejected by the mortar, a back-up gas generator is ignited and the main parachute is ejected by an expanding bag.

Tests are required to size the explosive charges and to demonstrate actuation of both prime and back-up systems. To duplicate parachute environmental conditions at the time of operation, a flight test will be performed as discussed in paragraph 5. 3.

5. 2. 3. 4 Nosecap Separation

The nose cap must be jettisoned if the entry shell fails to separate. This is accomplished by actuation of four explosive thruster bolts. Tests are required to size the explosives and assure that no structural damage will occur.

5. 2. 3. 5 Penetrometer Separation

The penetrometers are retained against a spring force by three-legged straps. Two of the legs are held by explosive pin pullers; the release of either one will release the penetrometer. Development tests will be required to assure proper operation of the subsystem.

5. 2. 4 Parachute Development and Ground Tests

The two major items to be investigated via ground testing are 1) the flow field behind the blunt cone throughout the Mach number range of interest, and 2) the performance characteristics of the parachute itself including aerodynamic coefficients, inflation, stability, and shock-load attenuation.

Other ground testing, including initiation devices and/or circuitry and deployment mechanisms is standard and will not be discussed herein. Note that all of the test components must be put through the sterilization criterion before commencement of testing.

Flow field characteristics behind the blunt cone are required and can be accomplished in the wind tunnel. Results from Mach 0. 1 to 1. 2 are required across the entire traverse of the tunnel so that, q/q_{stag} and p/p_{stag} can be measured at varying distances behind the forebody stagnation point. The results of these tests will indicate whether or not inflation of the parachute is choked due to the blunt-body flow-field effects.

The performance characteristics of the parachute, both at deployment and during its subsonic descent, can be established via wind-tunnel testing. The parameters to be established are (a) drag coefficient, (b) stability (aero coefficients), (c) opening shock-load attenuation, (d) inflation, (e) canopy porosity effects and (f) blunt-body wake effects. Wind-tunnel instrumentation to evaluate the above parameters is standard in nature and will not be discussed here. Note that the results of the test conducted will be limited by scaling uncertainties.

5.2.5 Propulsion Development and Ground Tests

The separated vehicle requires a ΔV capability of 1400 ft/sec with a single firing cycle. In addition, only subsystems that would have their state of the art established by September 1966 should be considered for use in the flight capsule design. The other requirements were: sterilizability, reliability, space storageability, total impulse accuracy and 101,600 lb-sec total impulse.

The requirement that the rocket motor must meet its operational performance after being subjected to sterilization and long-term space storage imposes a condition to which space motors under development had not been previously subjected. Sufficient testing has been accomplished, however, to indicate that new technology is not required.

5.2.5.1 Propellant Development

Sterilizable propellant development has been underway for over 2 years by Thiokol Chemical Corporation. The development effort has been with TP-H-3105 propellant, the propellant being used in the reference propulsion system. In all the work done to date, test results indicate the TP-H-3105 propellant is able to meet the sterilization requirements without degradation in motor performance.

The details (rather than the basic nature) of the sterilization requirements and procedures are changing continuously and probably will continue to do so over the next 2 years. Therefore, it is the considered opinion of those concerned with this area of development that TP-H-3105 is a satisfactory propellant and that no extensive development program is required to obtain a sterilizable propellant. Development efforts similar to those underway will continue primarily to evaluate the limits of the propellant under various environments rather than to determine basic design information.

The propellant development portion of this rocket motor development will follow the approach used for an existing propellant, but being tailored to a specific motor design. In addition to the sterilization environment, the motor will be exposed to an environment of 10^{-6} mm Hg for up to 1 year necessitating some propellant space aging tests. Some work has been done with similar propellants and the results have indicated that no critical problems will be encountered, but, because the time period for this application is longer than those previously planned, more testing over a longer period will be conducted.

5.2.5.2 Motor Development

The motor development program required would follow the same approach as is used to develop similar rocket motors for space applications. Because of the sterilization requirement, additional tests would be required to verify that there are no degrading effects due to the sterilization procedures and environments. The development program would also determine and evaluate special manufacturing and assembly techniques because of the sterilization requirements.

The one area where there is little preliminary data on the effects of sterilization environments is ignitors. The ignitors use the same propellant as the motor so that no difficulty is anticpated with the ignitor propellant. The safing and arming device and squibs have not been exposed to heat-sterilization environments and are considered an unknown. Some work has been done to determine the squib designs that are compatible with the sterilization environment with favorable results. No work to date has been done to determine the RFI limits of sterilizable squibs. It is felt that state of the art development is not involved.

5.2.6 Attitude Control Subsystem Development and Ground Tests

The attitude control system consists of three major subsystems: 1) the inertial reference subsystem, 2) cold-gas reaction subsystem, and 3) hot-gas reaction subsystem. The design selected for each uses currently available hardware designed for missile and space applications. No unusual problems are expected in the development and ground testing to meet the mission requirements. The major factors that will warrant special attention are the requirement for sterilization, and the long term exposure to the low temperature and vacuum environments.

5.2.6.1 Inertial Reference Subsystem (IRS)

Some of the components of the IRS, such as gyros and digital computers, have been used successfully on long life satellite and interplanetary missions. Testing of gyros at sterilization temperatures has been conducted by some manufacturers, and although further testing is required to completely demonstrate successful operation after exposure to this environment, it does not represent a major development problem. During the development hardware program, testing of the IRS will include normal performance and environmental testing. Particular attention will be given to testing performance before and after exposure to sterilization cycles. Dynamic performance of the IRS platform will be demonstrated by use of a three-axis servo-driven flight table to simulate the expected entry angular rate time history.

5.2.6.2 Cold-Gas Reaction Subsystem

The use of cold-gas reaction control for interplanetary and satellite missions has demonstrated its high degree of development and reliability. In this mission, operating time is only 1-1/2 hours, although exposure to space environments is much longer. Consequently, the problems of achieving very long operating life with systems having moving parts are greatly mitigated. This advantage is partly overcome by the sterilization requirement which may require special design techniques to ensure that regulators and solenoid valves maintain their dimensional stability after being subjected to elevated temperatures. The design of pressure vessels and line complexes is straightforward and no problems are anticipated. System assembly and performance tests will be conducted under clean-room conditions in accordance with best-industry practice.

5.2.6.3 Hot-Gas Reaction Subsystem

The hot-gas system also uses components and technology developed for missile and aircraft applications. The solenoid valve selected is a fully flight qualified configuration used on Minuteman and is particularly attractive for space applications. The major portion of the development program for the hot-gas system is necessary to ensure compatibility with sterilization and long term space environments. It is current practice to expose solid propellant rockets to temperatures of 200°F for auto-ignition tests, and since sterilizable propellants have been developed for use in the main propulsion systems of interplanetary spacecraft (e.g., Thiokol TP-H-3105), no unusual difficulty should be expected in achieving the required performance. In addition to the normal performance and environmental tests, the one shot nature of the gas generator will require extensive testing according to a predetermined test matrix to demonstrate performance after exposure to a variety of combined environments. Systems tests of the generator and solenoid valve will be required to demonstrate compatibility of the system as a whole.

5.3 FLIGHT TESTS

The scope of the flight-test development program evaluation in Part II of the study was contractually restricted to the vehicle subsystems, to the exclusion of the payload subsystems. System qualification tests were also excluded. Of the vehicle subsystems considered (structure and heat shield, sterilization canister, separation subsystems, attitude control, propulsion and parachute) the only three found to require flight tests were the parachute, separation subsystems, and the heat shield. This conclusion was reached by first considering ground testing techniques as the more desirable approach. Where these techniques proved inadequate, flight testing was examined. It was also determined that flight tests would augment rather than replace ground testing in these three cases. Of the three candidates for flight testing, only one subsystem, the parachute, requires technological development. Consequently, early pre-Voyager flight testing is recommended for this system.

The recommended flight-test program is summarized in Table XXIV. The parachute flight-test program is divided into two parts: pre-Voyager tests and Voyager program tests. The pre-Voyager tests refer to the technological development program executed prior to the Voyager program. The Voyager program tests refer to the development testing accomplished as part of the Voyager hardware program (Phase D). The pre-Voyager parachute flight-test program consists of 32 one-tenth scale tests using a Dart test vehicle launched by a Nike/Nike as well as two full scale tests, rocket boosted in a climb from a high altitude balloon. The 32 one-tenth scale tests are divided into three blocks of tests. The first block will consist of a total of 12 tests of 3 types of parachutes (ring-sail, extended skirt, and annular), each at 4 deployment conditions. These tests will utilize suspended payload weight force simulation,* which will be defined subsequently. It is anticipated that one of the candidates will be eliminated on the basis of the results of the first block of tests. The second block will consist of a total of eight tests of the two remaining candidates, each at four deployment conditions. These tests will utilize suspended payload mass simulation* which will be defined subsequently. As a result of these tests, the reference configuration will be selected. The third block will consist of 12 tests of the selected configuration at various deployment conditions for 2 generic canopy geometries, for two generic suspension geometries and for both suspended payload weight force and mass simulation. Some of the deployment conditions will extend beyond the Mars operational envelope to higher Mach numbers and lower dynamic pressures in a search for critical performance limits. The two pre-Voyager full scale parachute tests are recommended to verify the scaling validity of the subscale tests and to check possible blunt-body wake effects on the parachute performance. One flight will check scaling effects and will simulate both suspended payload weight force and mass by jettisoning extra ballast during the parachute descent. The other flight will primarily check possible blunt-body wake effects by delaying separation of the entry vehicle shell until 20 seconds after parachute deployment. This will avoid possible transient effects associated with the operational separation which occurs immediately after parachute deployment.

The Voyager parachute test program consists of ten one-tenth scale tests using the Nike/Nike/Dart and ten full scale tests with the Little Joe II launch vehicle. The separation subsystems test are incorporated in the full scale parachute tests. The Little Joe II booster is used instead of a balloon launched test vehicle for the full scale tests because of the difficulty of providing proper test conditions for both the parachute and separation systems with a balloon-launched vehicle. The Nike/Nike/Dart subscale tests are similar to the pre-Voyager subscale tests except for the parachute test article which will be a refined

*These simulations differ due to the difference between Mars and Earth gravity.

TABLE XXIV

FLIGHT TEST PROGRAM SUMMARY

Test	Test Technique	Number of Tests
Parachute Pre-Voyager Tests		
1/10 Scale	Nike/Nike	32
Full Scale	Rocket Climb from Balloon Launch	2
Parachute - Voyager Program Test		
1/10 Scale	Nike/Nike	10
Full Scale	Little Joe II	10
Separation	Included with Little Joe II Parachute Test	
Heat Sink	Atlas SLV-3	1
Heat Shield	Atlas SLV-3	2
	Total	57

design based on the experimental results of the pre-Voyager test program and better adapted to the specific requirements of the actual Voyager capsule design. The subscale Voyager program consists of ten flights at six deployment conditions for both suspended payload weight force and mass simulation. Four of the deployment conditions will be at the extremities of the operational deployment envelope for both mass and weight simulation. Two flights with only mass simulation will be made at dynamic pressures slightly higher than the operational envelope. These two flights are dynamic structural tests and hence require only payload mass simulation since the weight simulation will produce smaller loadings on the parachute. The full-scale Voyager parachute tests which are combined with the separation subsystems tests are required for design verification of the parachute which has evolved from the pre-Voyager and Voyager subscale tests. The number of flights are determined by the number of deployment and simulation conditions which should be checked. The program consists of ten flights at seven deployment conditions for both mass and weight simulation. Two flights with only mass simulation will be made at dynamic pressures slightly higher than operational values. Additional details of the full-scale test conditions are discussed on page 139 of Volume III, Book 3.

The heat-shield flight-test program consists of one heat-sink test and two heat-shield performance tests. The purpose of the heat-sink test, which utilizes a beryllium heat sink instead of the operational ablative heat shield, is to measure the entry heating environment unencumbered by processes of ablation. Two heat-shield performance flights are scheduled to obtain repetitive measurements.

5.3.1 Parachute Flight Tests

The technological development status of the parachute was judged inadequate because, 1) the tenuous atmosphere of Mars requires parachute deployment at very low dynamic pressures (4 lb/ft^2 for which very limited experience in the Earth's atmosphere exists, and for which present analytical techniques are not applicable, and 2) many facets of the mission and system design are significantly dependent on the parachute performance capability. The latter requires accurate determination of the parachute capability before the mission and system definition phase of the Voyager procurement begins. Flight testing to augment ground tests is considered mandatory because of limitations in ground testing techniques. These limitations are due to scale factors and infinite mass effects. One-tenth scale (scaling based on area) is generally considered a reliable limit. This means that the scale model should be at least 25.5 feet in diameter for the reference parachute diameter of 81 feet. Existing wind tunnels cannot accommodate this diameter at the correct flow condition ($M = 1.2$) and dynamic pressure (4 lb/ft^2). Sled tests, whirl towers and the like cannot simultaneously simulate $M = 1.2$ and $q = 4$ lb/ft^2 because the sea level atmosphere is too dense. So called infinite mass effects, refer to the effects of fixed tie-down of the shroud lines in ground testing (i.e., wind tunnel). Under actual conditions the shroud lines are attached to a finite mass (the payload) and there is a mutual interaction between the dynamics of the payload and the dynamics of the parachute. As a consequence, fixed tie down conditions may yield invalid results, particularly in canopy inflation, opening shock loads and parachute/payload stability.

Subscale tests were selected for most of the pre-Voyager parachute program in the interests of economy. The two full scale tests were scheduled to check possible scaling effects and large blunt-body wake influence on parachute performance. Various surface-launched and balloon-launched test vehicles were considered for the subscale program in both one-tenth and one-quarter scale. One-quarter scale was included to weigh the penalties of improved scale versus its advantages. The evaluation reduced to three logical candidates: 1) a surface launched Nike/Nike/Dart vehicle in one-tenth scale, 2) a surface launched Honest John/Nike/Cree in one-quarter scale, and 3) a balloon launched, newly designed test vehicle (in one-quarter scale), propelled in a climb by an Iroquois rocket motor. The three candidates were compared on the basis of cost, test condition dispersion, launching ease, flexibility in adjustment of test condition, and probability of test success as illustrated in Table XXV. The Nike/Nike/Dart

TABLE XXV

COMPARISON OF SUBSCALE PARACHUTE TEST VEHICLES

	Nike/Nike/Dart	Honest John/Nike/Cree	Balloon Released Vehicle
Cost (Relative)	1	1.5	3.3
Dispersion: Δq (psf) at M_{NOM}	6	12	1
Dispersion: ΔM at q_{NOM}	0.2	0.3	0.1
Launching Ease	A	A	C
Flexibility in Adjustment of Test Condition	B	B	A
Probability of Test Success	A	A	B

proved superior as indicated by the ratings in the table. The comparative ratings are explained in greater detail in Volume III Book 3, page 96.

The Nike/Nike/Dart is a two-stage, surface launched vehicle which is aerodynamically and spin stabilized by canted fins on each stage. It consists of a Nike solid rocket motor for each stage and a non-propelled Dart payload vehicle, 9 inches in diameter and weighing 200 pounds. The Nike/Nike/Dart configuration is illustrated in Figure 34 and an inboard profile of the Dart vehicle is shown in Figure 35.

The flight sequence of the one-tenth scale tests is illustrated in Figure 36. The test parachute is deployed during the ascent coast at altitudes between 100,000 and 170,000 feet and velocities between $M = 0.7$ and 1.5. This represents a considerable extension of the Mars operational deployment envelope of $M = 0.7$ to 1.2 and $q = 4$ to $5\ lb/ft^2$. The envelope was extended in order to determine limit parachute performance in Mach number and minimum dynamic pressure and to allow for possible changes in future capsule designs and atmospheric models. After parachute deployment, ballast is ejected to simulate mass changes due to entry-vehicle shell separation in the operational flight. The vehicle is recovered for post-flight examination of the parachute and camera records. Telemetry and ground tracking provide additional data. Both mass and weight-force simulation flights are made. In one, the Mars parachute area/suspended-payload mass ratio is duplicated; and in the other, the Mars parachute area/suspended-payload weight ratio is duplicated. These ratios are different in Earth-atmosphere testing because of the difference in the gravitational fields of the two planets. The ratio variation is provided by changing parachute size, not payload mass.

Only two candidates were considered for the pre-Voyager full scale parachute tests: a surface launched Little Joe II booster and a balloon launched vehicle, propelled in a climb by a solid rocket. The Little Joe II was the only logical surface-launched candidate due to the large diameter (15 feet) of the full scale test vehicle. Even the Little Joe II required a hammerhead ascent shroud because the payload diameter was larger than the booster diameter. The balloon-launched vehicle was chosen on the basis of cost. The balloon/vehicle configuration consists of a high altitude, zero-pressure balloon, recovery parachute, balloon adapter, and test vehicle suspended in that order as illustrated in Figure 37. The recovery parachute canopy is attached to the base of the balloon and its shroud lines support the balloon adapter which in turn supports the test vehicle. The parachute is used to recover the balloon adapter after test vehicle release. The zero pressure balloon is fabricated of bonded Mylar film gores, reinforced with Dacron scrim bonded to the Mylar. The balloon volume is 6.5 million cubic feet, helium filled and will lift the total payload of 3000 pounds to the release altitude of 110,000 feet. The balloon adapter is a triangular truss structure which contains balloon and test vehicle remote control and

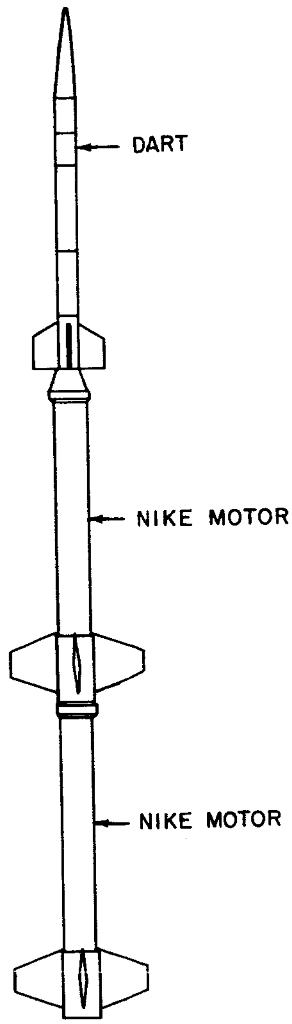

861569

Figure 34 NIKE/NIKE/DART -- 1/10 - SCALE PARACHUTE FLIGHT TEST CONFIGURATION

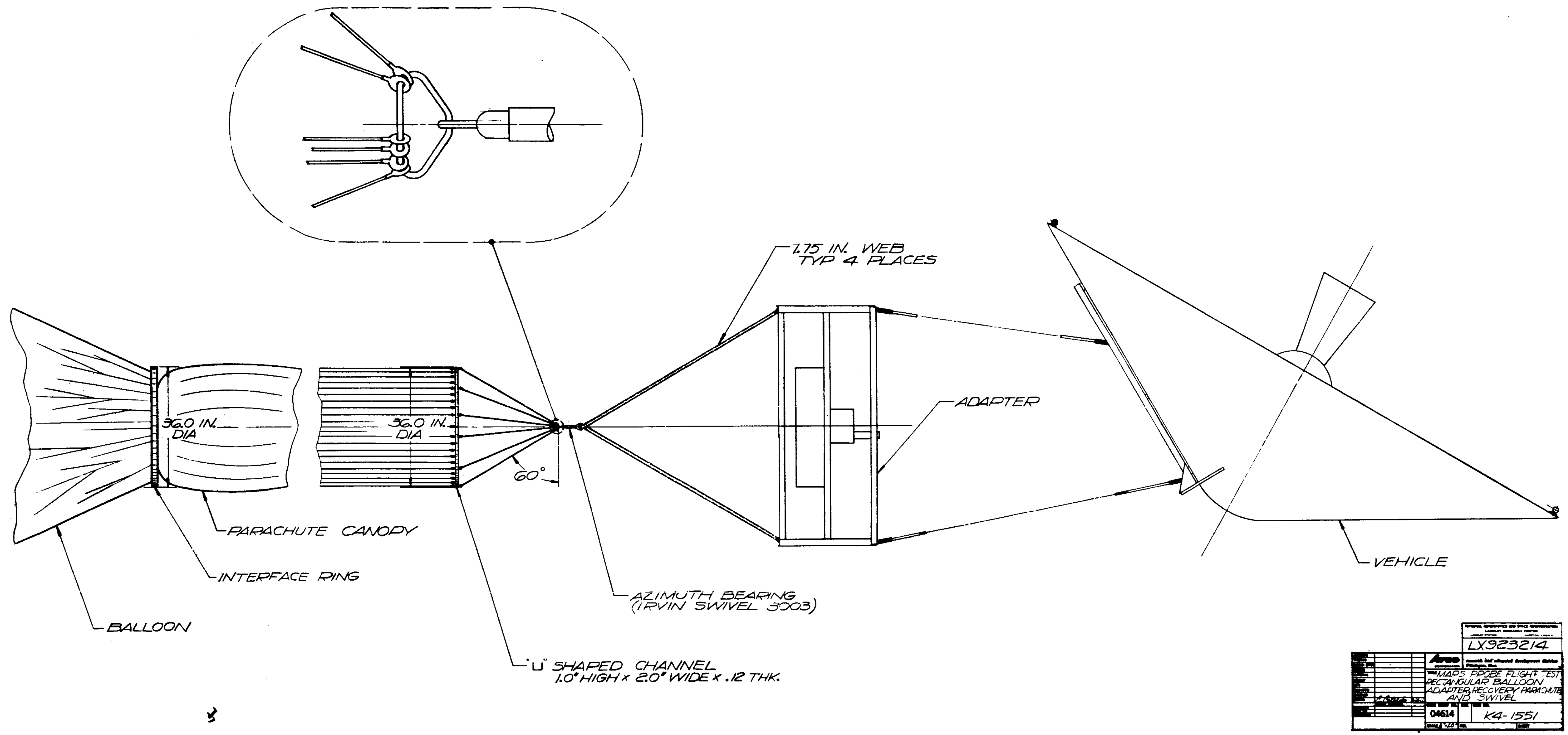

Figure 37 BALLOON ADAPTER CONFIGURATION—FULL-SCALE PRE-VOYAGER PARACHUTE FLIGHT TESTS--ROCKET CLIMB FROM BALLOON RELEASE

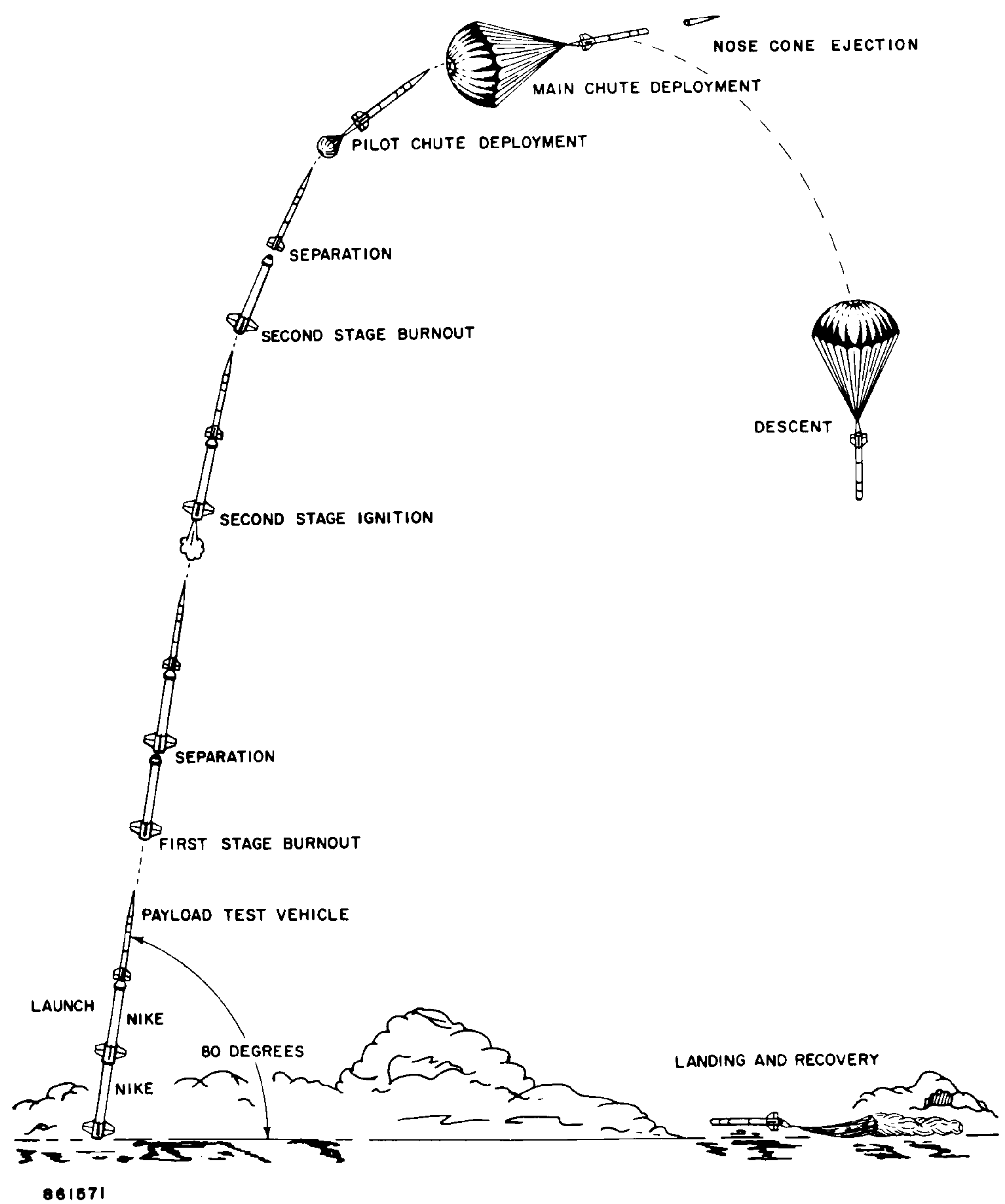

Figure 36 NIKE/NIKE/DART -- 1/10-SCALE PARACHUTE TEST -- PRE-VOYAGER AND VOYAGER FLIGHT SEQUENCE

external support equipment. This equipment consists of command receiver, altimeter transmitter, gas valve control, ballast and ejection control, azimuth control, camera, battery, and vehicle separation mechanism. This equipment provides ground control of balloon ascent rate, vehicle prelaunch checkout, release camera coverage, vehicle launch azimuth, vehicle power sources, vehicle release, and adapter recovery. The adapter is supported from the recovery parachute by a bearing which permits rotation of the adapter and vehicle to the launch azimuth with torquing provided by cold-gas reaction jets.

The test vehicle is illustrated in the inboard profile of Figure 38. The configuration consists of three major subassemblies: 1) the blunt cone external shell, 2) internal structure which is the payload suspended from the test parachute, and 3) an Alcor rocket which accelerates the vehicle in a climb after release from the balloon. The test parachute canister and supporting subsystems such as telemetry, instrumentation, power, etc. (and Alcor rocket) are mounted on the internal structure.

The flight sequence for the pre-Voyager full-scale parachute test is illustrated in Figure 39. The test vehicle is spin stabilized at its release attitude (60 degrees climb) by spin rockets immediately after release. The Alcor solid rocket motor is then fired to accelerate the vehicle from the release altitude of 110,000 feet, to the deployment altitude of 140,000 at a velocity of $M = 1.2$. The parachute is deployed during ascent coast, followed by external shell jettisoning after the parachute and suspended payload descent for about 30 seconds, the expended Alcor rocket case and attached ballast are jettisoned to reduce the suspended payload weight to a value equal to the Mars weight force. Both the payload mass simulation and payload weight simulation can be accomplished in the same flight in this case, because the weight allowance in the weight simulation mode is large enough to accommodate necessary equipment such as telemetry, instrumentation and power. This weight allowance was inadequate in the one-tenth scale tests previously discussed. In one of the full scale tests, separation of the external shell will not occur at the peak parachute opening shock load as in the operational flight but will be delayed about 20 seconds. This will allow more reliable measurement of possible blunt body wake effects on parachute performance than that possible because of the transient character of the operational mode.

In the pre-Voyager parachute test program just described, the purpose of the program will be to evaluate various types of parachutes and attachment configurations to establish the limit of parachute performance in Mach number and minimum dynamic pressure, and to provide experimental data to support preliminary design of parachutes for the low dynamic pressure environment. In the Voyager parachute test program, the purpose of the program is development testing for design confirmation of a specific

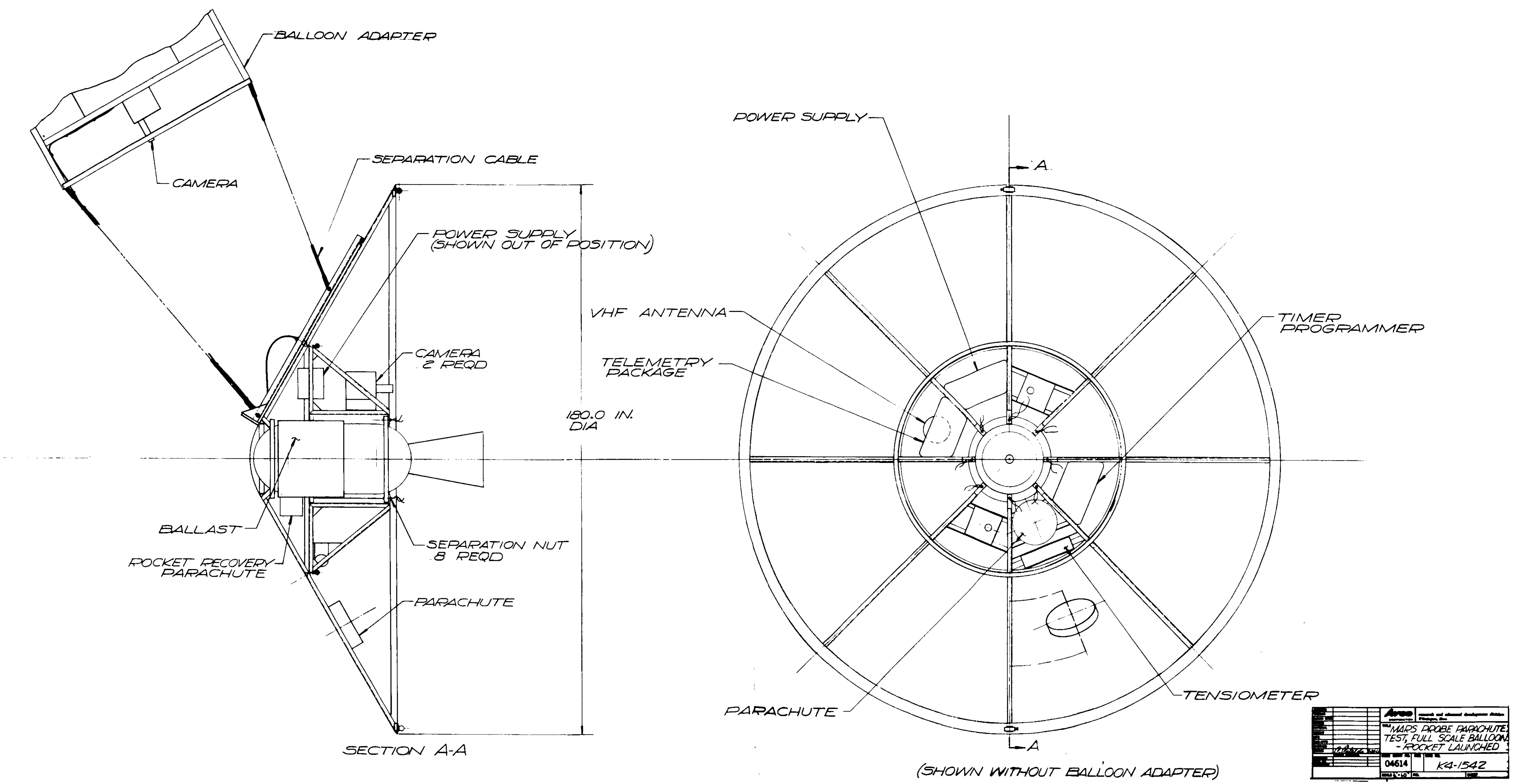

Figure 38 INBOARD PROFILE OF FULL-SCALE PRE-VOYAGER PARACHUTE FLIGHT TEST VEHICLE--ROCKET CLIMB FROM BALLOON RELEASE

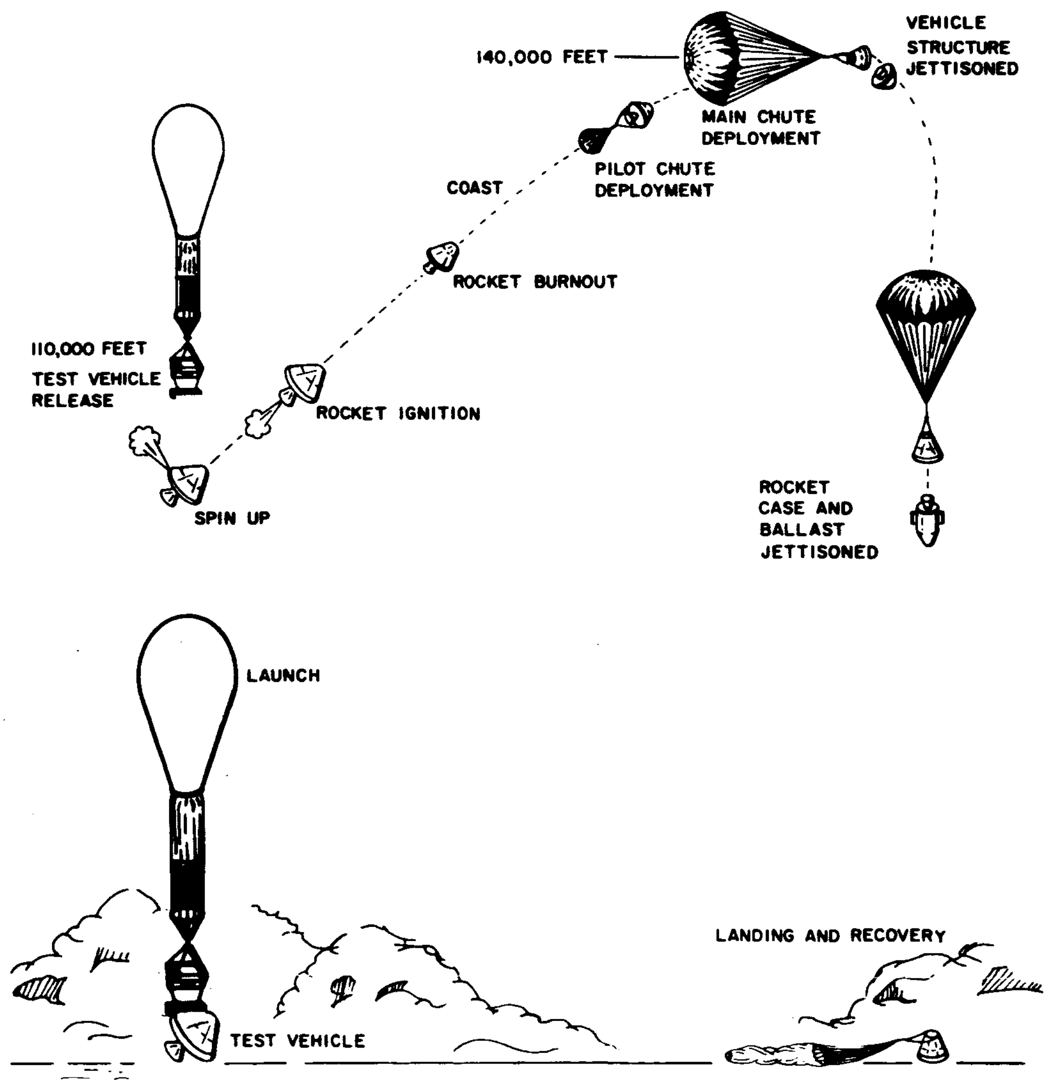

Figure 39 FULL-SCALE PRE-VOYAGER PARACHUTE TEST -- ROCKET CLIMB FROM BALLOON RELEASE -- FLIGHT SEQUENCE

parachute optimized for a specific mission, vehicle interface, and deployment envelope. The recommended program incorporates ten one-tenth scale tests using the same Nike/Nike/Dart vehicle as before, and ten full-scale tests using a Little Joe II launch vehicle. The Little Joe II has been chosen instead of the balloon-launched approach because the separation systems tests have been included with the parachute tests. This complicates the balloon-launch technique as will be described subsequently.

5.3.2 Parachute/Separation Subsystems Flight Tests

Development flight testing of the separation subsystems was judged necessary because of the large number of separation functions, the complexity of some of the separations, and limitations in ground-test physical simulation. The separation of the sterilization canister lid, the capsule from the spacecraft, and the entry vehicle shell from the suspended payload are complex separations involving large structures with mechanical interfaces of large dimensions. The entry vehicle shell separation, in particular, occurs in a dynamic environment with aerodynamic loads on the shell, large parachute-opening shock loads on the suspended payload, and with the vehicle possibly spinning and oscillating in angle of attack. Adequate simulation of this environment in ground tests in not feasible. Despite the lack of simulation, ground tests are still recommended because of their vastly superior instrumentation and opportunity for visual observation. It should also be noted that ground test simulation can be very good for vacuum flight separations, such as the canister lid, when tested with ballistic pendulum techniques. Incorporation of the separation tests with the parachute flight tests was a logical choice, since all but two of the separations (canister lid and capsule/spacecraft) occur as part of parachute deployment or during parachute descent. These separations are pilot parachute, main parachute, entry vehicle shell, and penetrometers.

The candidate vehicles for the Voyager program tests of the full scale parachute/separation systems were the same as the pre-Voyager full scale parachute candidates: Little Joe II and a balloon launched rocket climb vehicle. In this test, however, the balloon approach required a programmed climb trajectory, which eliminated vehicle spin, and required an active, autopilot controlled system for thrust-vector control. The programmed climb trajectory was necessary to provide (in one flight) conditions suitable for both the vacuum flight separations and the parachute deployment. A spin stabilized climb was not feasible because of the limit on maximum climb angle due to the presence of the large diameter balloon above the vehicle. The increased complexity of the vehicle, which requires its own development flight tests, led to the choice of the flight proven Little Joe II.

The Little Joe II is a versatile launch vehicle designed to accomodate clusters of Algol solid rocket motors of various quantities up to seven. An autopilot, controllable aerodynamic fins, and reaction gas jets provide flight path and attitude control. It was designed primarily to carry large dimension heavy payloads on suborbital flights. For the parachute/separation test, the required configuration is 2 and 1 Algol rocket staging, four Recruits for retropropulsion, 198-inch hammerhead shroud, controllable fins, and the pitch-roll gyro replaced with rate gyro integration to accommodate the large attitude maneuvers required for the vacuum flight separations.

The flight sequence of the Little Joe II test is illustrated in Figure 40. After the two stage Algol rocket burnout the ascent shroud is jettisoned but the test vehicle remains attached to the launch vehicle. The vacuum flight separations, canister lid and capsule/spacecraft, take place near apogee at 170, 000 feet at low speed. The Little Joe II provides attitude orientations at these separations which will minimize the chance of collision and fires its retropropulsion rockets after the capsule/spacecraft separation. The parachute is deployed during descent at the desired deployment conditions and the entry vehicle shell is jettisoned just after the peak-opening shock load. The remaining separation (the penetrometers) occurs during parachute descent.

As explained in more detail on page 140, paragraph three of Volume III, Book 3, the trajectory apogee must be restricted to a maximum of 170, 000 feet in order to achieve the desired parachute deployment conditions during descent. Testing the vacuum flight separation subsystems at 170, 000 feet will not yield an exact simulation since this attitude is within the sensible atmosphere. The apogee velocities are very low, however, providing very-low dynamic pressures ($q = 0.1$ lb/ft^2). It is felt that the loading is not large enough to invalidate the test. The only alternative is to provide independent flight tests of the vacuum flight separation subsystems.

The test vehicle configuration for the parachute/separation test consists of boiler mockups of the entry vehicle and sterilization canister in which the mass characteristics and external configuration of all subassemblies closely match operational values. This is necessary in order to properly simulate separation dynamics and mechanical clearance between adjoining structures during separation. An inboard profile of the test vehicle is shown in Figure 41. The separation mechanisms and parachute system will be design prototypes. Ejectable ballast is provided to simulate mass change due to expenditure of the deorbit rocket propellant. This ballast is jettisoned after capsule/spacecraft separation and before parachute deployment. Additional ballast is jettisoned during the parachute descent to switch from payload mass simulation to payload weight simulation. Supporting equipment such as telemetry, instrumentation and power supply are mounted on the suspended payload. A number of cameras are installed to record the various separations and parachute performance.

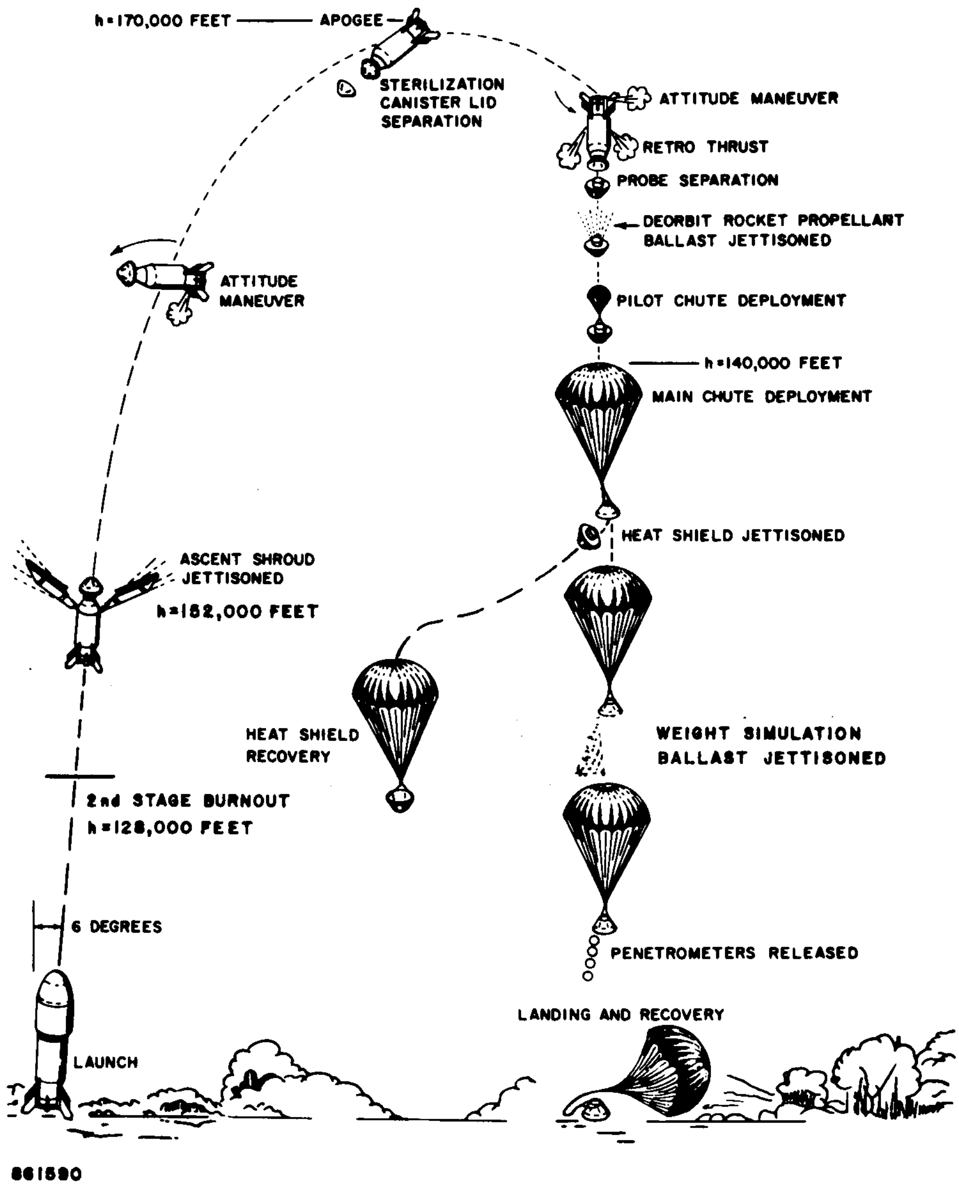

Figure 40 FULL-SCALE PARACHUTE/SEPARATION TEST -- LITTLE JOE II LAUNCH -- FLIGHT SEQUENCE

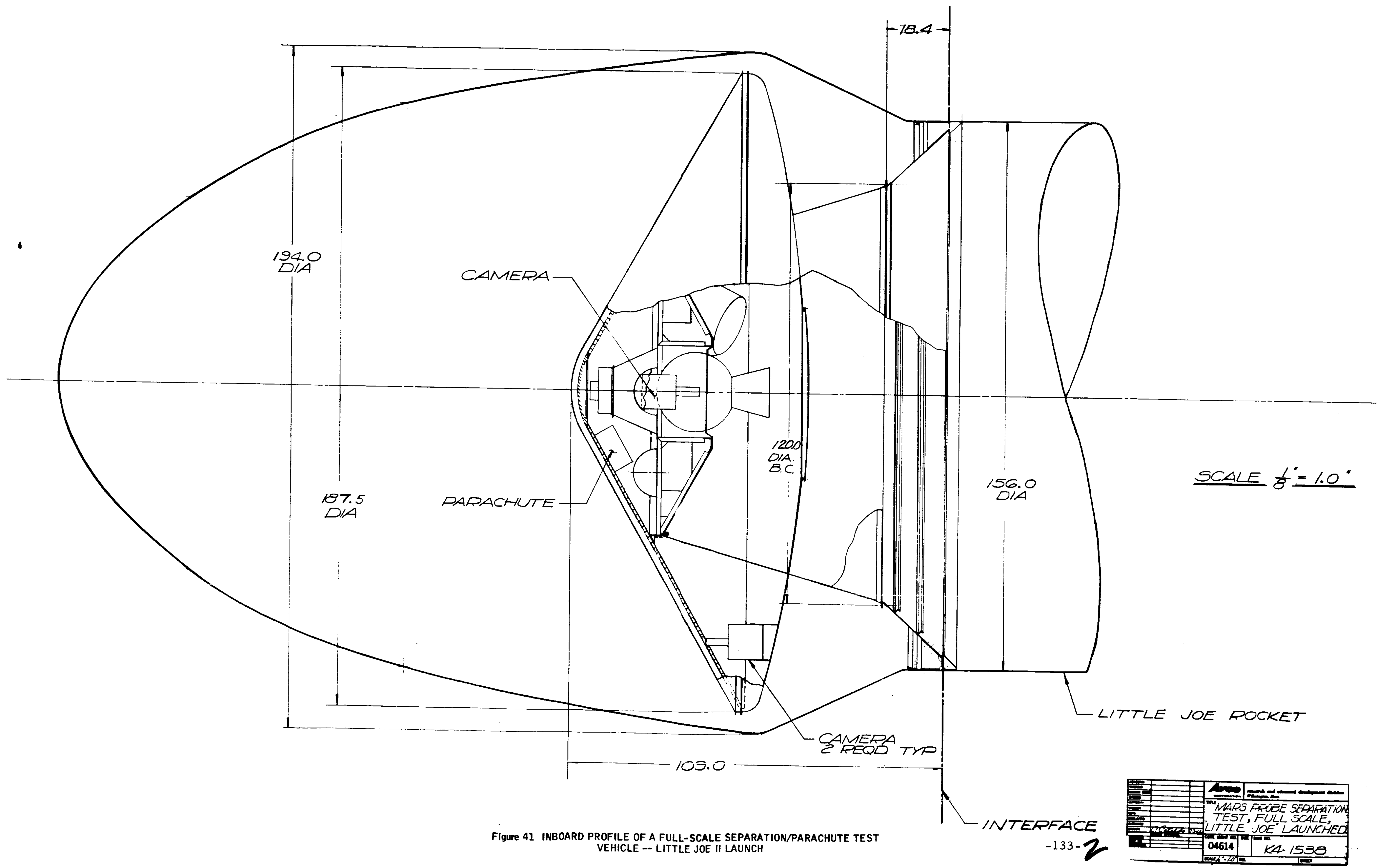

Figure 41 INBOARD PROFILE OF A FULL-SCALE SEPARATION/PARACHUTE TEST VEHICLE -- LITTLE JOE II LAUNCH

133-1

Some of these cameras are mounted on the sterilization canister afberbody, which remains attached to the Little Joe II, and must be hardened to survive the booster impact. The others are mounted on the suspended payload and are recovered after parachute descent.

5.3.3 Heat-Shield Performance Flight Tests

Reentry flight tests of the Mars heat shield in the Earth's atmosphere were considered necessary for the following reasons:

a) Simultaneous match of stagnation pressure, heat flux, and enthalpy in existing ground-test facilities is not possible.

b) The transient character of the heating environment is difficult to match in ground test facilities.

c) The large weight fraction of the heat shield (15 to 20 percent of entry weight) limits design safety margins necessary for unpredictables such as ground-test scale effects and Mars atmospheric variations.

d) The candidate heat-shield materials have never been flight tested.

e) Past experience has revealed differences between ground-test and flight-test results.

The flight envelope parameters affecting the heat-shield performance (temperature response and mass-loss characteristics) are the entry velocity (V_e), entry angle (γ_e), ballistic coefficient (m/C_DA), and angle of attack (α_e). Their influence, however, is exerted through the following derivative environmental parameters: aerodynamic heating (Q), heating rate (q), enthalpy (m/RT_o), pressure (p), shear (τ), duration of the heat pulse, as well as the atmospheric composition. Design and flight experience, plus consideration of the postulated ablation mechanism for the candidate ablators, indicate that the ablation process is best simulated by providing simultaneous duplication of the heating rates, enthalpy, and pressure within reasonable limits. The simultaneous duplication is provided by the selection of the proper combination of the flight envelope parameters: V_e, γ_e, α_e, and m/C_DA. Fortunately, direct simulation of the heating pulse is not necessary because the combined dynamics and heat-pulse simulation would be impossible to attain for this particular case. The flight test should be tailored to provide a heat pulse that is only typical of the anticipated heating, with due recognition of thermal protection requirements, booster limitations and instrumentation requirements. Since entry out of orbit results in low stagnation enthalpies, the entry velocity for the Earth test should be restricted to values near those for Mars to ensure accurate wall enthalpy interactions (other than those introduced by atmospheric composition). A tradeoff between simulation of the total integrated heating and heating rates is possible by variation of the flight envelope, but in any case, a transient history similar to Mars entry is obtained. Typical Mars-entry heating pulses for various stations are illustrated in Figure 42 and for the maximum diameter station in Figure 43. Figure 43 indicates a discontinuous variation in the heating which is associated with the rapid variation in the stagnation-point location. In order to simulate this characteristic pulse, the dynamics would have to be simulated. The simulation of the exact heat pulse is not critical for each body station. It is required instead that the heating on the flight test vehicle at a particular body station be related to some point on the Mars entry vehicle, the vehicle scale being compatible with this requirement.

The simulation possible with an Earth entry is demonstrated in Figure 44. Earth entry conditions consisting of a 15, 000 ft/sec. entry velocity and zero entry angle were required to match the Mars entry (V_e = 15, 200 ft/ sec., γ_e = -14 degrees and atmosphere model = VM-7). Heating rates are presented as a function of stagnation enthalpy, and local pressures are indicated at discrete points. Two points on the body (stagnation point and sonic point) are compared with the corresponding points for the Mars entry. Although there is no one-to-one correspondence of vehicle stations between Earth and Mars entry test vehicles, there is an overlap providing points on the Earth test vehicle which match a region on the Mars entry vehicle. In such a region, a simultaneous, transient simulation of the heating rates at appropriate enthalpy levels is possible with small differences in the pressures. A comparison of the Mars and Earth entry heat pulses (see Figure 45) shows that simultaneous simulation of the total integrated heating and complete timewise heating-rate distribution is not feasible. It is concluded that an Earth entry test, although not executed in the same atmospheric composition as Mars, would provide an excellent test of thermal protection system performance. The atmosphere composition effect on performance would have to be demonstrated in the ground tests.

The degree of simulation of the Mars entry in ground-test facilities was investigated as well by superimposing their operating characteristics on the Mars entry environmental envelope previously shown in Figure 44. The resulting comparison is presented in Figure 46. This figure demonstrates the difficulty of obtaining low heating rates at the critical (for design) low-enthalpy levels, although the range of enthalpies is covered. Furthermore, the pressure simulation is off by an order of magnitude which may be important in evaluation of the ablation phenomena. Another well-known problem (not illustrated in Figure 46), is the difficulty of simulating timewise variations of the critical parameters in ground facilities. In addition to the proper simulation of the environment, it is important to conduct

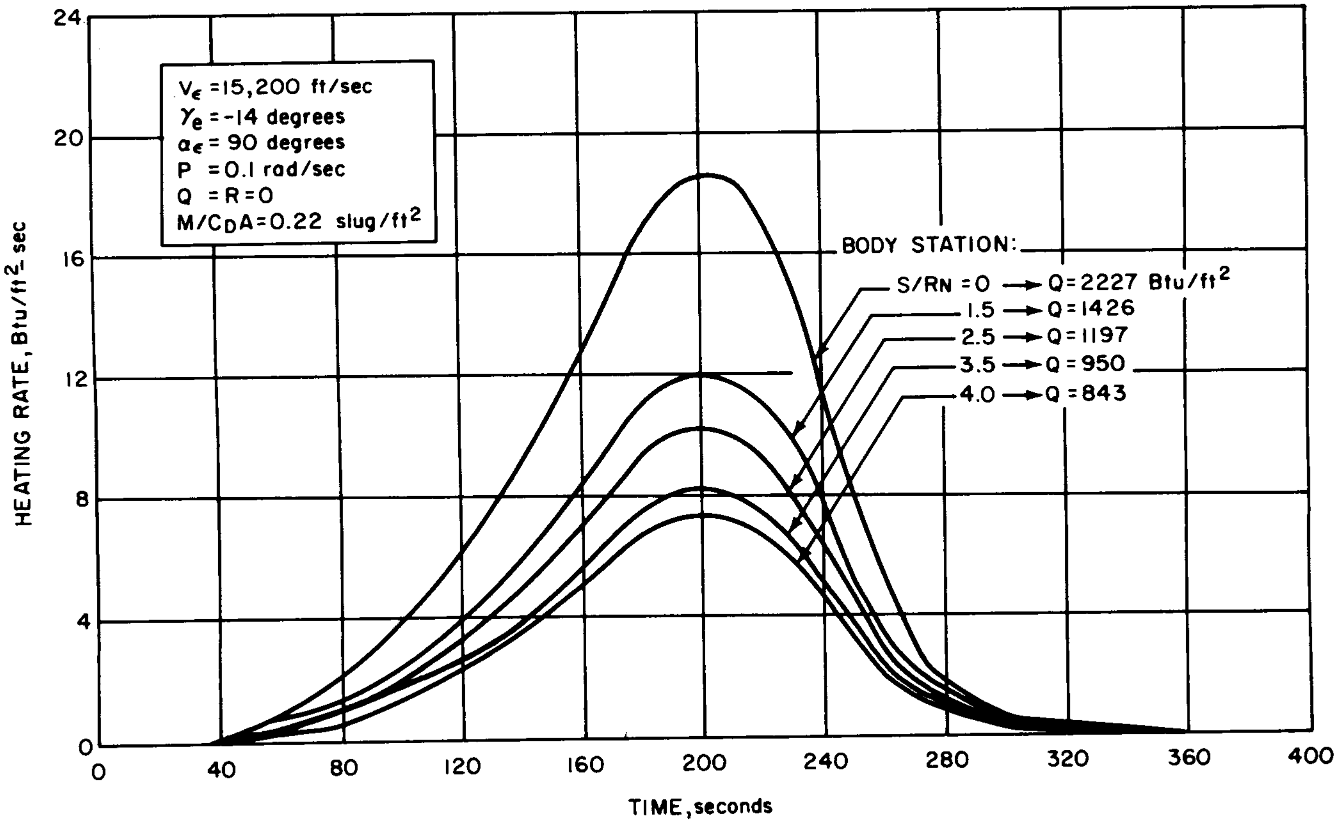

861595

Figure 42 MARS BLUNT CONE HEATING PULSE -- VARIOUS BODY STATIONS

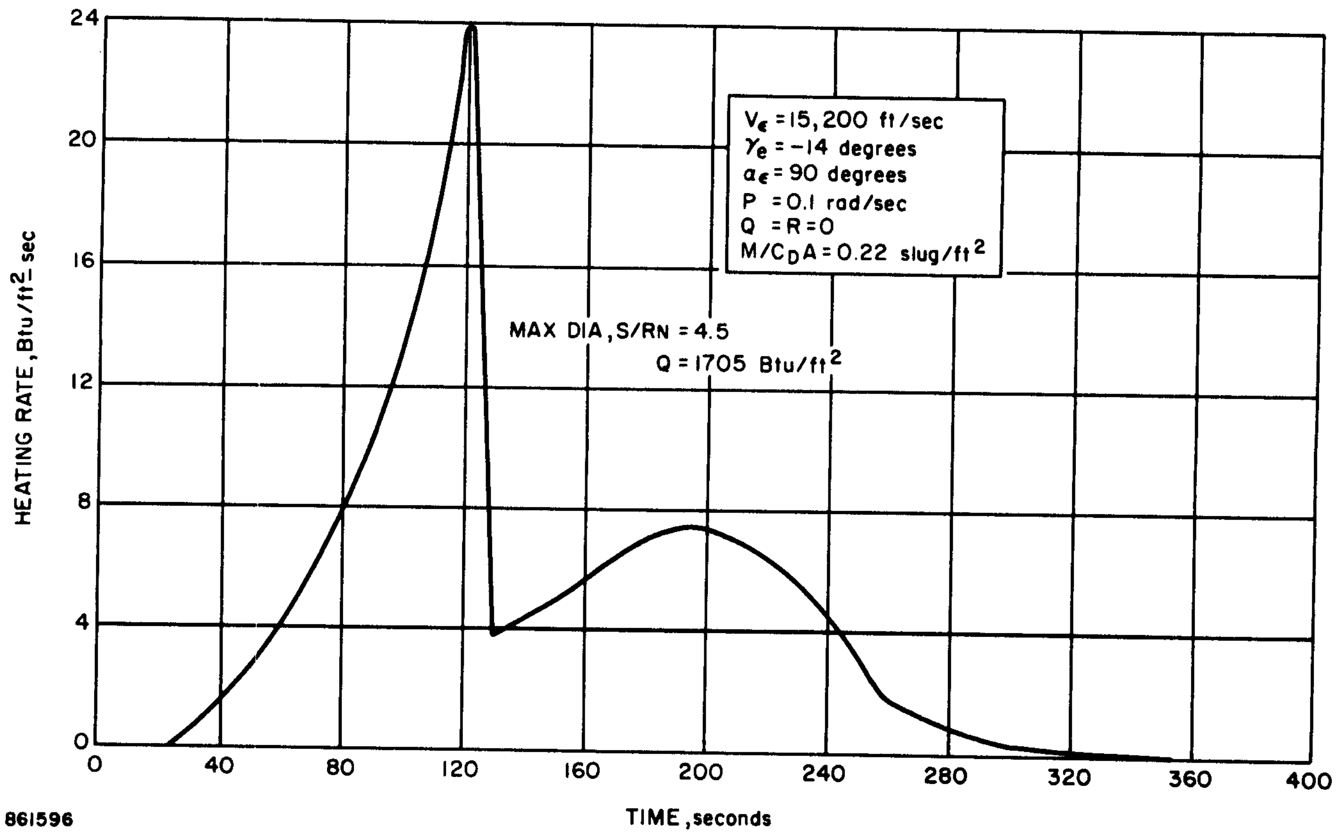

861596

Figure 43 MARS BLUNT CONE HEATING PULSE AT MAXIMUM DIAMETER

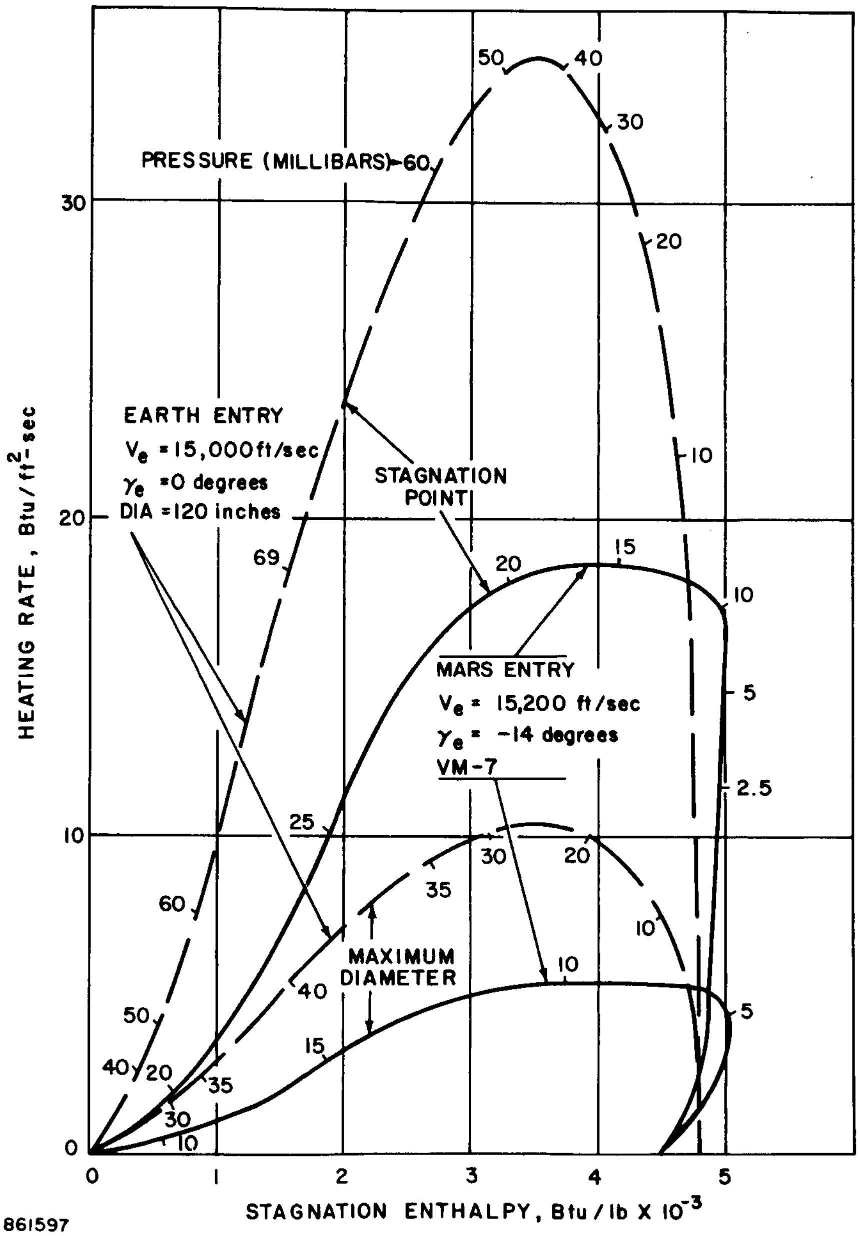

Figure 44 COMPARISON OF MARS HEATING ENVIRONMENT WITH SUBSCALE FLIGHT TEST SIMULATION

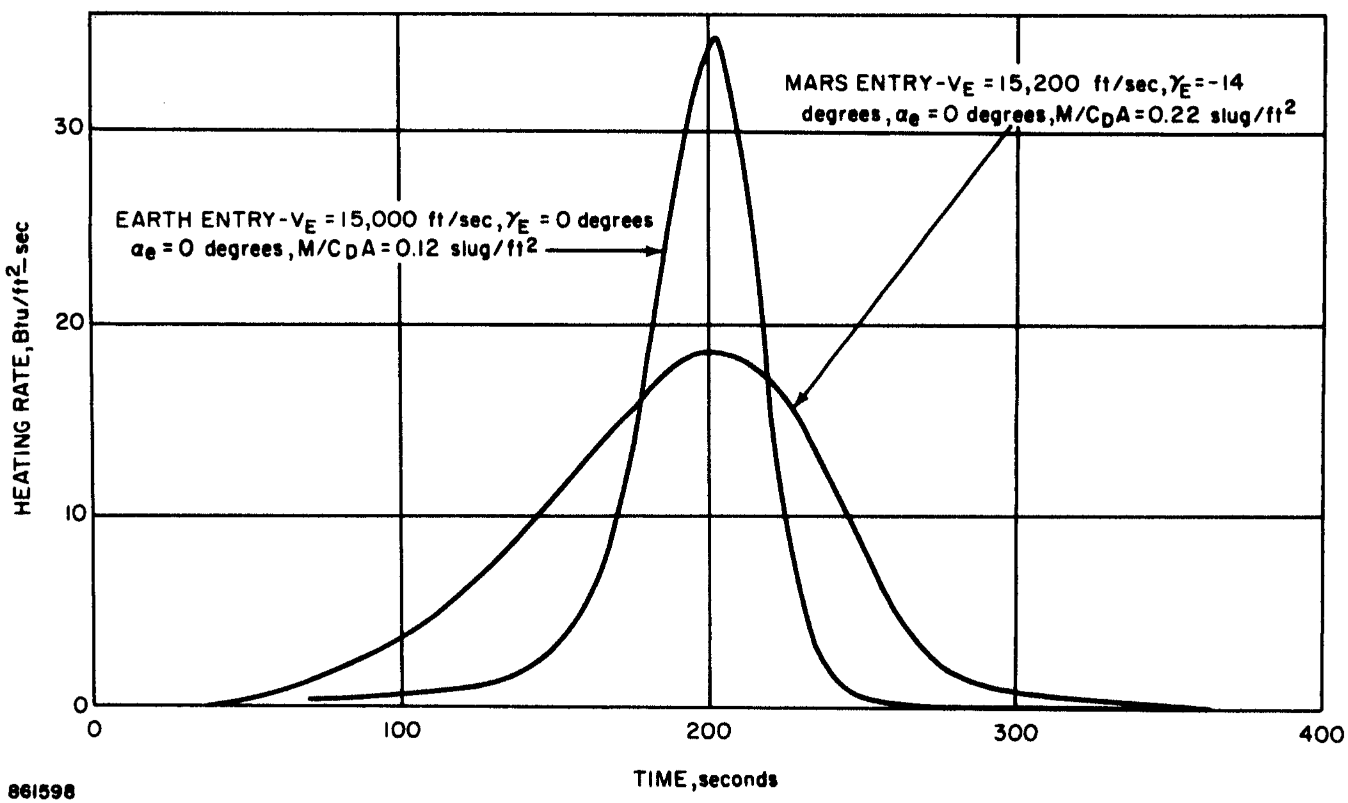

861598

Figure 45 COMPARISION OF MARS AND EARTH ENTRY BLUNT CONE HEATING PULSE

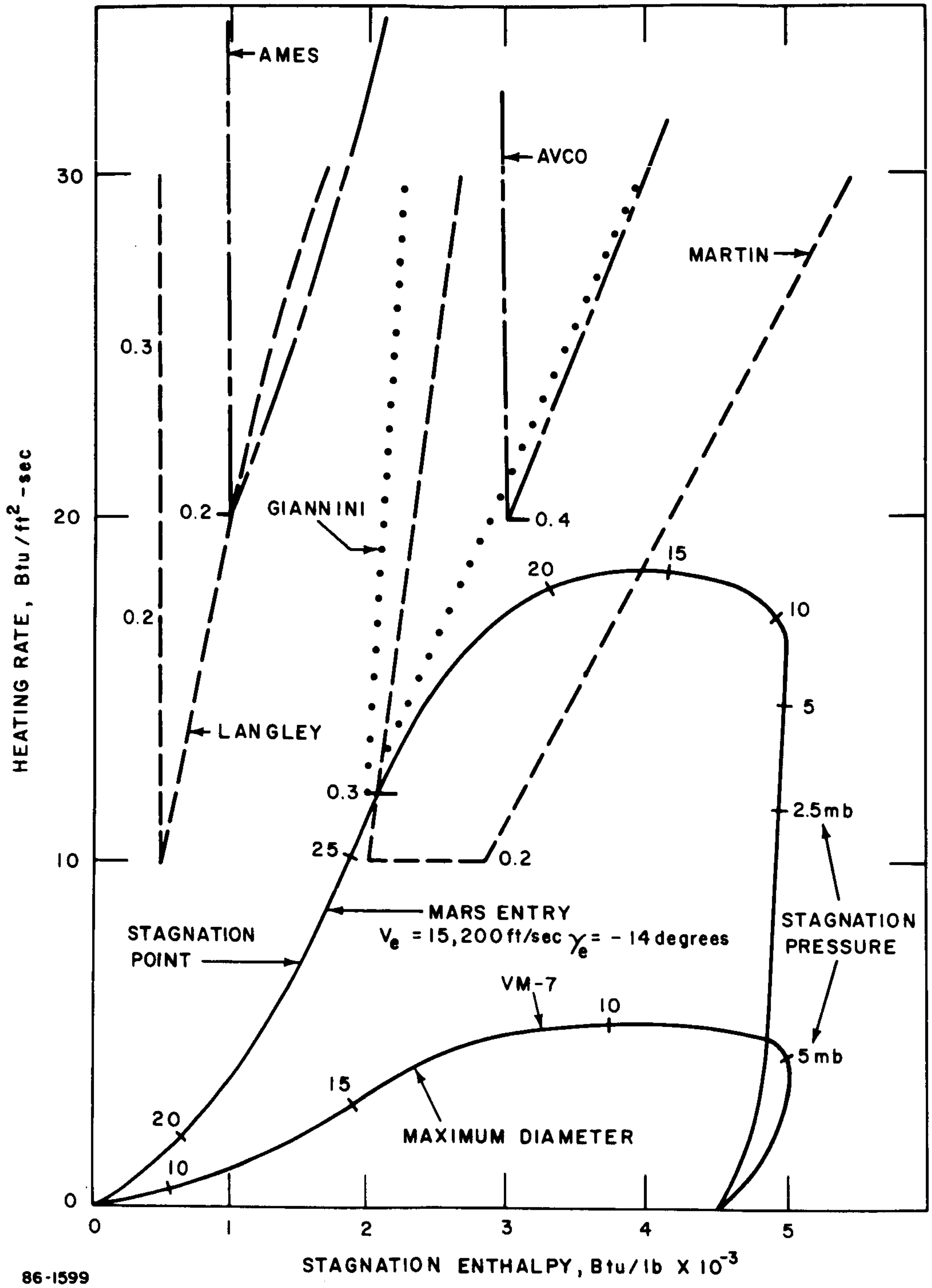

Figure 46 COMPARISON OF MARS HEATING ENVIRONMENT WITH GROUND TEST SIMULATION

tests on materials produced to the specification required of the final product, and on a scale approaching the prototype hardware. It is possible in principle to satisfy the material specification but not the scale requirement in ground testing. Thus, it is concluded that although design information may be acquired in the ground testing, the verification of the performance in these facilities will not provide the degree of confidence in the design that is required.

Selection of minimum scaling for the flight-test vehicle is very desirable from the viewpoint of minimum launch vehicle capabilities and the associated savings in cost. Unfortunately, significant reduction of the vehicle scale increases the heating flux to the point where adjustment of the other simulation parameters can no longer provide adequate simulation of the Mars heating environment. The studies indicated that the minimum suitable scaling is approximately 100 to 120 inches in diameter. Figure 44 which was previously discussed, shows that a 120-inch diameter vehicle can provide a point on the test vehicle which adequately simulates the Mars stagnation point heating. Further reduction of the test vehicle scale will drive the heating flux at any point on the body beyond the Mars stagnation point heating and eliminate the possibility of simulating the Mars heating environment.

The inspection of Mars entry conditions also reveals that an Earth entry test is feasible utilizing a heat-sink thermal protective system. This concept will allow calibration of ablator flights and provide definition of the environment unencumbered by ablation products and mass changes. Beryllium must be used for the heat sink to achieve desired entry weights. The large diameter of the test vehicle eliminated launch vehicles, such as the Scout, and reduced the logical candidates to the Atlas class. The Atlas SLV-3 (OAO) was selected because it met all requirements, would be available as an active booster in the ten year OAO program, and its ascent program for the OAO closely matched the reentry test requirements. The SLV-3 (OAO) configuration for this test will consist of a Surveyor ascent shroud with the cylindrical section removed, the OAO fixed adapter, a conical adapter to support the payload, and a cluster of solid rockets for booster retropropulsion. Retropropulsion is required because test vehicle separation from the Atlas occurs at the beginning of reentry at 400, 000 feet.

The flight sequence for the subscale heat-shield test is illustrated in Figure 47. The zero-degree reentry angle is an unusual requirement but is easily implemented by terminating the powered ascent trajectory at the reentry conditions, without the usual long range ballistic flight between burnout and reentry. The ascent trajectory is similar to that required for the low altitude orbit of the OAO satellite. The desired ascent trajectory is implemented by a pitch-rate program during sustainer engine burn. The ascent shroud is jettisoned at 300, 000 feet or higher during sustainer engine burn. The pitch rate program provides an asymptotic approach to the

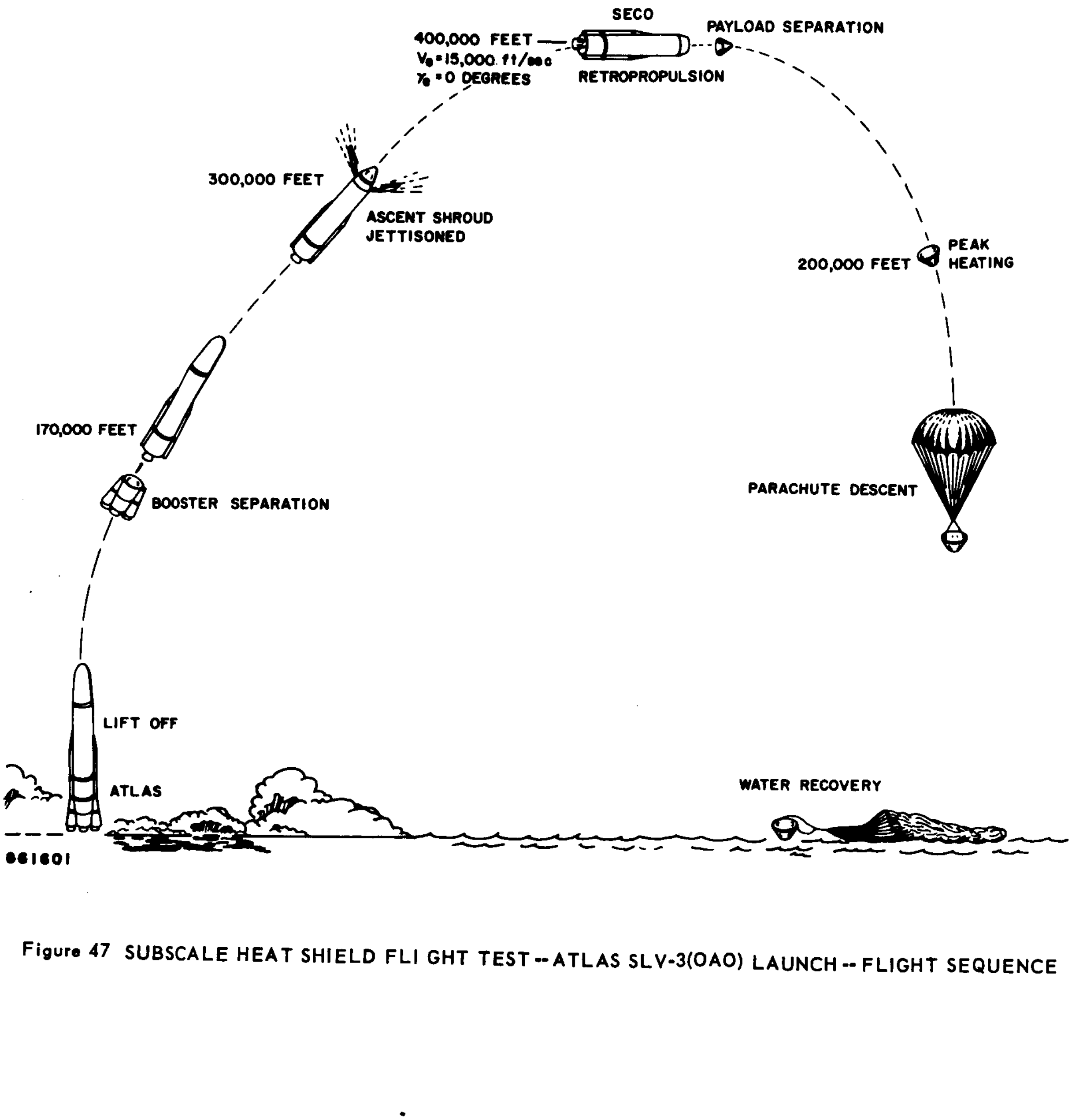

Figure 47 SUBSCALE HEAT SHIELD FLIGHT TEST -- ATLAS SLV-3(OAO) LAUNCH -- FLIGHT SEQUENCE

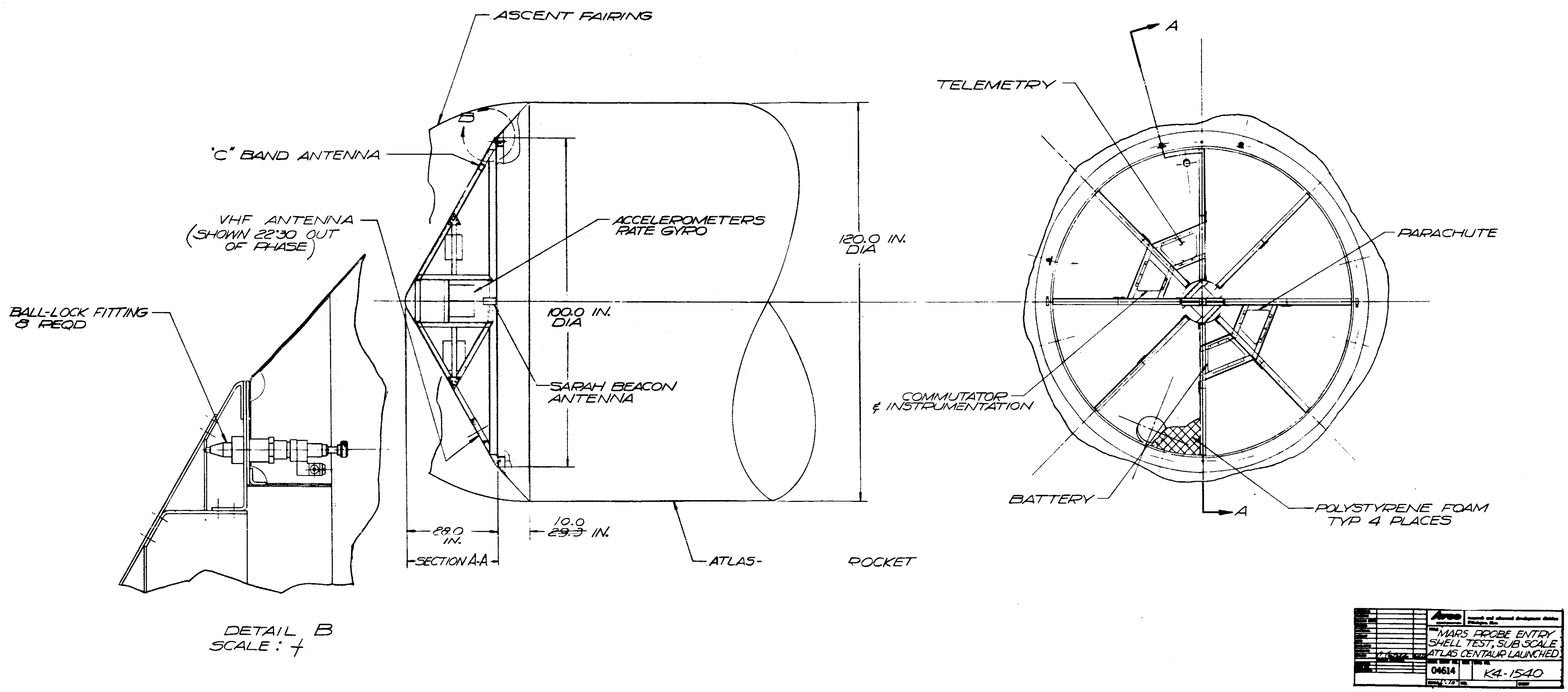

Figure 48 INBOARD PROFILE OF SUBSCALE HEAT SHIELD TEST VEHICLE — ATLAS SLV-3 (OAO) LAUNCH

11) Sterilization control, to furnish the required assurance that the design is basically sterilizable, and that each flight article satisfies the sterilization requirement.

The sterilization investigations conducted as part of the study have addressed themselves primarily to the definition of a plan for an integrated sterilization control and management program. (See Figure 49.) The results of these studies are described in Volume IV. The remaining sterilization efforts supported the design studies and are discussed in other volumes.

The approach in these investigations has been the following. An analysis and review has been performed of the causes of contamination during manufacturing/handling/assembly activities, the effectiveness of artificial decontamination (heating and ETO cleaning) and natural decontamination (die-off), the effectiveness of and the problems associated with the various methods of burden assay, and the problems associated with heat sterilization and the subsequent maintenance of sterility. Techniques, including a computer program, have been developed for performing burden estimates, and have been used to examine the implications of the aforementioned factors on the pre-sterilization burden. The results of these analyses have been used to select biological-burden control and sterilization plans for the two capsule designs considered in this study. These implementation plans spell out the activities which have to be undertaken, and the time, manpower and facilities that are needed to comply with the sterilization requirement.

Some of the highlights of this material are summarized in the following paragraphs.

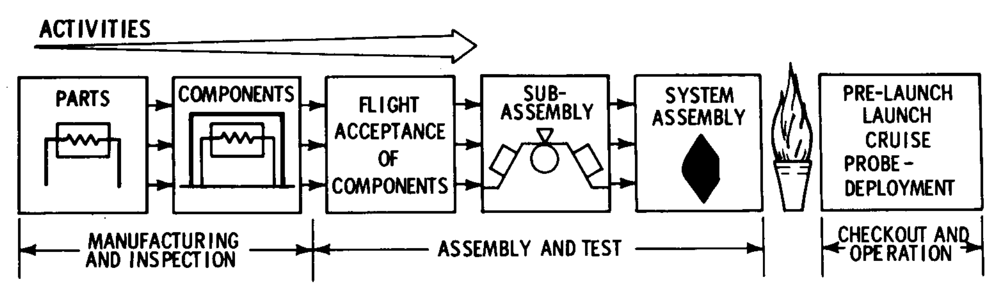

- CAUSES OF CONTAMINATION
- DECONTAMINATION FACTORS
- SYSTEM PHYSICAL CHARACTERISTICS
- METHODS OF BIOLOGICAL BURDEN ANALYSIS
- BURDEN CONTROL AND CERTIFICATION METHODS
- PROOFS OF STERILIZATION
- REPAIR
- STERILIZATION MAINTENANCE

Logistics • Economics • Safety • Sterility Risk • Performance Risk

760131P

Figure 49 CONSIDERATIONS IN SELECTION OF STERILIZATION PLAN

6.1 BASIC BURDEN FACTORS

The biological burden on a spacecraft prior to sterilization can be considered to consist of two parts, the initial internal burden of the constituent materials and parts, and the burden added or subtracted by the handling, assembly and decontamination processes.

The range of internal burdens of representative capsule parts and materials is given in Table XXVI. In general, they range from essentially 0 to 100,000 microorganisms, depending on the particular manufacturing process involved and the nature of the acceptance-test procedures employed. Thus, metallic structural components and heat shield elements, for instance, experience such high temperatures for prolonged periods of time during their manufacturing processes that they are internally sterile. Similarly, some high-reliability electronic components, such as transistors, are burned in and stabilized for long periods of time at temperatures higher than those encountered in the internal sterilization cycle and, as a result, are essentially sterile internally. On the other hand, some parts, such as transformers, are normally manufactured under conditions which result in very high biological loadings.

The contaminating and decontaminating factors associated with the handling, assembly/checkout flight-acceptance test and decontamination processes are shown in Table XXVII.

Experiments have shown that microbial fallout in existing aerospace assembly and test facilities is on the order of 30 to 50 organisms/in^2/day depending on the number of workers present and the degree of worker activity. The high values shown in Table XXVII for normal fallout are extremes that may be present in low-quality facilities, with poor environmental controls and with a great deal of particle generation by machining and grinding processes. Other tests in bio-clean facilities (high-efficiency filtered, vertical laminar-down-flow clean-rooms, per Federal Specification 209, Class 100) provide an improvement over normal fallout conditions of at least two orders of magnitude.

The burden attributable to handling depends on the number of individual hand contacts; in a bio-clean room, if proper clothes and gloves are worn, it will be nearly zero, but a conservative value two orders of magnitude below that for normal conditions is assumed in burden estimate calculations.

The burden on plastic surfaces may be magnified manyfold above that of normal fallout if they are electrostatically charged. Accurate values for this factor are not available, and estimates vary widely. Experiments

TABLE XXVI

PART AND MATERIAL INTERNAL BURDEN RANGES

Type	Estimated Internal Burden Range
Balsa wood	1-10/in.[3]
Battery cell	0
Capacitor	10-1000
Coaxial cable	0-100/ft.
Connector	100-10000
Crystal	0-10
Diode	0
Duplexer	0
Evacuation bellows	0
Explosive	1000/gm
Explosive trains	0-200/ft.
Fiberglass	0
Foam	1/ml
G-M tube	0
Inductor	1000-10, 000
Magnetic core	0
Magnetron	0-10
Metal	0
Nylon, Dacron	0
Optical system	10-100
PbS detector	0
Photomultube	0
Relay	100-1000
Resistor	0-10
Silicone int'd circuit	0-10
Silicone oil	1/ml
Silicone rubber	0
Teflon insulation	0
Thermal control	0
Transformer	10, 000-100, 000
Transistor	0
TWT	0

TABLE XXVII

BIOLOGICAL BURDEN CONTAMINATION AND DECONTAMINATION FACTORS

Contamination Factors	Consensus Value
Fallout on surfaces	
Normal facilities	32 - 128 org/in.^{2}/day
Bio-clean facilities	0.32 - 1.28 org/in.^{2}/day
Handling	
Normal facilities	1900 org/in.^{2} of contacted surface
Bio-clean facilities	19 org/in.^{2} of contacted surface
Electrostatic factor	1 - 10
Decontamination Factors	**Consensus Value**
ETO effectiveness	4D (10^{-4})
Flight acceptance heat test effect	12D (10^{-12})
Die-off	
Normal facilities	30 - 99 percent
Bio-clean facilities	30 - 99 percent

under artificially severe conditions have reported results as high as 13, but 5 appears to be a conservative value under realistic conditions.

The effectiveness of ETO as a surface decontamination process has been substantiated by experiment. However, ETO cleaning will not reach and decontaminate occluded capsule surfaces nor the interiors of sealed components. The decision of whether or not to seal a component against ETO penetration involves a tradeoff between the relative burden contributions and effects on system reliability.

Flight acceptance tests are conducted on each item of hardware that is to go into a flight version of the flight capsule in order to eliminate potentially defective components and to confirm that the unit is flightworthy. These tests involve exposure to environments at least as severe as those which are to be encountered in the mission, and are generally conducted in the order in which the environments are actually experienced in the flight. For a planetary landing capsule, these tests should include heat-cycle tests and ETO-exposure tests at the beginning of the flight-acceptance cycle.

Exposure to sterilization temperature conditions should be first in the flight-acceptance sequence, and the heat cycle should be equal to or higher than the terminal sterilization cycle. This will obviously result in sterile or near-sterile component interiors, and if the components are sealed, the interiors will remain in the sterile or near-sterile condition throughout the remainder of assembly. To minimize reliability and performance degradation, the flight-acceptance and the terminal-sterilization heat cycles (specifically, the temperature and duration of each) should be optimized simultaneously. This optimization is as important to sterility maintenance as it is to performance, as it will also reduce post-sterilization repair requirements and, consequently, recontamination risk. Flight acceptance tests should also be performed for susceptibility to ETO exposure; these tests could be conducted after the flight acceptance tests for the heating environment, if it is desired to eliminate early those elements failing the heat testing, thereby reducing the number of elements requiring subsequent testing.

Biological organisms on or in aerospace components (i.e., under non-nutritive conditions) tend to die off gradually from natural causes. The extent of die-off depends on the time and the rate, and the latter depends somewhat on the nature of the surface as well as the temperature and humidity of the environment, i.e., the season and geographical location. The die-off rate is typically in the order of 1 percent a day, which is equivalent to about 30 percent a month and 99 percent over the period of a year.

6.2 BURDEN ESTIMATES

The physical characteristics which are of significance to presterilization burden loadings are summarized in Table XXVIII for the two capsules designed in this study for the entry-from-orbit (EFO) and entry-from-approach-trajectory (EFAT) cases, with their different requirements and constraints. Also included in this table, for comparison, is a small capsule in the 100-pound class (the Ames Atmospheric Probe concept).

With the large number of parts and the wide variety of contamination and decontamination factors, it is convenient to perform a burden analysis by means of a simple computer program of the type shown schematically in Figure 50. Five types of inputs are used to define the system and assembly/sterilization program, as indicated in Table XXIX. The program is designed to cycle completely for each assembly process, during which new parts may be added, or two or more assemblies may be put together without the addition of new parts. The number of parts are specified by the system, and the number of handling operations are determined by the assembly process.

A biological burden analysis for the EFAT case was performed early in the study (before the aforementioned computer program was available) and the results are summarized in Table XXX. In this analysis it was assumed that all operations, with the exception of the assembly of the suspended capsule, would be conducted under conventional aerospace environmental conditions. The suspended capsule was considered to be assembled in a Class 100 vertical downward-laminar-flow clean-room, with a biological fallout reduction effectiveness of 90 percent. Viable organisms on exposed surfaces are destroyed upon application of ETO just prior to terminal sterilization, leaving only the burden internal to parts and occluded within components and on mated surfaces to be killed during the terminal heating process.

A review of these results indicates that the bulk of the total burden accumulation is caused by fallout on the parachute. If the parachute is decontaminated by ETO before it is packaged within a container, its contribution to burden can be reduced significantly, resulting in a total Probe/Lander loading of 27×10^6. The reduction in burden attributable to utilizing a clean-room during payload assembly was estimated to be only 10×10^6, indicating that if it had not been used, the total count would still be manageable although it would exceed the required limit by about 5 percent.

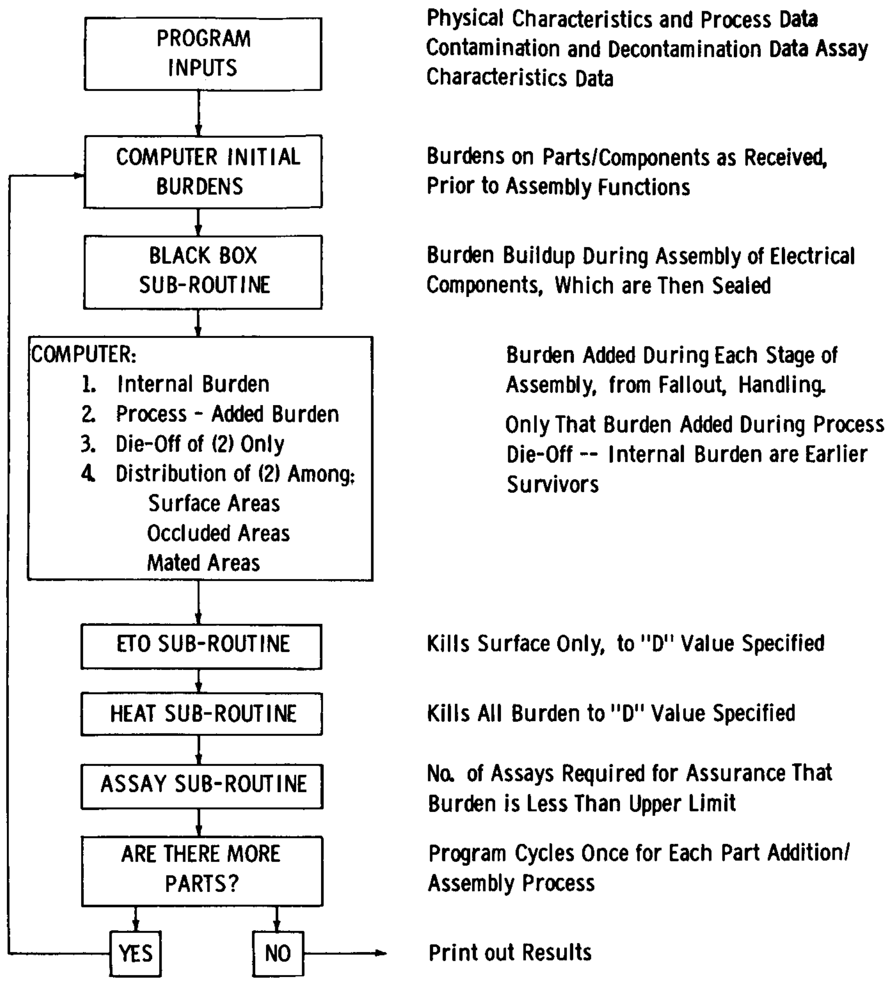

760135P

Figure 50 COMPUTER PROGRAM SCHEMATIC DIAGRAM

TABLE XXVIII

PHYSICAL CHARACTERISTICS OF CAPSULES

	Probe (Entry From Orbit)	Probe/Lander (Entry From Approach Trajectory)	100-Pound Class (Ames) Capsule
Weight	3,000 pounds	2,500 pounds	107 pounds
Diameter	15 feet	15 feet	30.5 inches
Components	140	165	. 60
Electronic parts	15,000	33,000	1,500
Magnetic cores	8 x 105	30×10^5	6×10^3
Volume: (In.^{3})			
Heat shield	20,000	16,500	84
Impact attenuator	15,000 (4 Penetrometers)	168,000	---
Propellant	12,000	1,260	20
Plastic (sterilization container, foam padding)	18,000	22,000	1,500
Surface area: (In.^{2})			
Occluded	479,000	505,000	24,000
Component interiors	420,000	430,000	20,000
Electronic	110,000	112,000	19,000
Other	310,000	318,000	1,000
Mated	59,000	75,000	4,000
Exposed	260,000	325,000	15,000
Parachute	2,660,000	2,440,000	---

TABLE XXIX

COMPUTER PROGRAM INPUTS

(1) Part/Component Inputs	(2) Electronic Part Input/Part	(3) Constants for Given Run	(4) Assay Requirements	(5) General Inputs
Level Control point Part number Facility code Percent plastic Initial surface area Initial occluded area Initial volume Assembly mated area No. personal contacts Area contacted ETO "D" value Heat "D" value Assay technique	Level Control point Part number Facility code Part area No. parts Internal burden Percent plastic	Subroutines: Black box Assay Die-off ETO use Heat application Die-Off rate Heat subroutine: Growth rate Death rate ETO subroutine: Growth rate Death rate Initial burden levels Metal, surface Metal, occluded Plastic, surface Plastic, occluded Plastic, internal Electrostatic factor Personnel contamination rate Fallout rate Duration exposed factor Master facility code	No. of assay types Upper burden limit Confidence level code Assay accuracy for subassemblies Confidence level required	Table of assay types and accuracies Table of "t" Distribution values for different confidence levels

TABLE XXX

INITIAL BURDEN ESTIMATE PROBE/LANDER, EFAT
(number of viable organisms x 10^{-3})

	Surface Burden	Internal Burden	Occluded Burden
Entry Vehicle	8225	7426	94723
Entry shell	6161	771	5185
Suspended capsule	1036	6655	89538
External payload	147	2042	86273
Science	1	1571	289
Propulsion A. C.	16	459	193
Parachute	3	0	5823
Other	----	12	18
Impact attenuation	76	1617	246
Flotation	----	69	286
Landed payload	168	2927	2738
Science	34	301	390
Communication	2	2250	414
Sequencing and data handling	1	89	1381
Other	----	289	848

Although this analysis was preliminary in nature and prepared for the capsule designed for the probe/lander case, it indicated several trends which are generally valid and which influence the development of the sterilization plans for both capsules. They are:

1. The total burden can be maintained within the required limits.

2. The parachute, under normal conditions, is a major burden contributor and deserves special handling; if it is pre-cleaned, decontaminated by a surface agent, and sealed in a container prior to assembly, the capsule loading is reduced significantly.

3. The principal source of remaining organisms which must be destroyed during terminal processing is on occluded surfaces encapsulated while mating components during system assembly, rather than within basic parts. The packaging design should, therefore, allow cleaning by ETO.

4. Assembly operations conducted in clean rooms reduce the system burden substantially, but may not be necessary, because there are more effective burden-limiting techniques.

As part of an effective sterilization-control plan, the burden must be defined at every step of the assembly/test process. Such an analysis has been performed for the probe case using the aforementioned computer program, based on the internal contamination values for piece parts and materials indicated in Table XXVI, and on the premise that all manufacturing, assembly and test operations are carried out in conventional facilities with an average continuous fallout rate of 32 organisms per square inch per day. The burden accumulation on the surfaces of plastic parts is assumed to be five times this value due to the electrostatic effects, and it was assumed that 90 percent of the population dies off due to natural causes during the time taken for the manufacturing cycle.

Under these conditions, the burden on and within the equipment at various stages of the process is shown in Figure 51. At the completion of the manufacture of components, it is 778 million organisms. At this stage, major items, such as the parachute assembly, are subjected to ETO cleaning before encapsulation within their containers. Also, all components are subjected

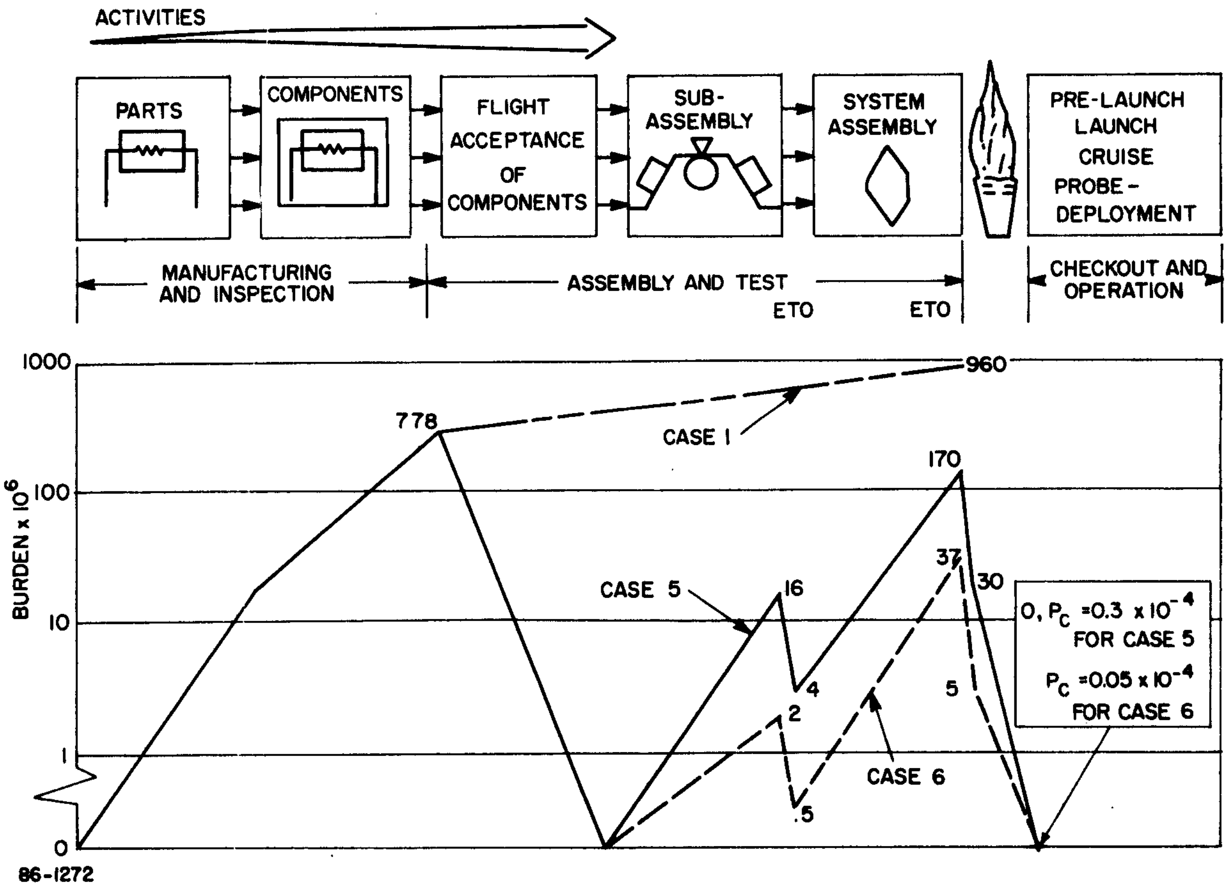

Figure 51 BURDEN AS A FUNCTION OF ACTIVITIES

to a thermal soak at least as severe as the thermal-sterilization soak which is part of the flight-acceptance process. Similarly, all parts are subjected to an ETO-exposure flight-acceptance test. As indicated previously, whether electronic components are left unsealed and subsequently cleaned with ETO inside and out, or whether they are sealed and cleaned on the external surface only, has to be resolved in each individual instance; generally, the flight acceptance sequence is sufficient to reduce all internal burdens of electronic components to an acceptable level.

The next step consists of the assembly of the three major electronic subsystems (modules). This assembly and check-out process takes place under conventional environmental conditions and results in a load of 16 million organisms. Prior to sealing, the modules are exposed to ETO, thereby reducing the burden to about 4 million organisms, assuming a burden reduction of 4D for this process, which is conservative. If the flight-acceptance-test process is delayed until after the subassemblies are complete, the heat exposure of the test would reduce the burden essentially to zero even without the ETO cleaning process indicated in the preceding paragraph. The decision as to whether to perform the flight acceptance test before or after completing the subassemblies has to be made on the basis of an evaluation of the risk of success against schedule, logistics, and cost, and depends heavily on the detail design as well.

The final and major viable organism buildup occurs during the assembly of the modules and structures to form a complete capsule and during its encapsulation in the sterilization container. This burden, 170 million organisms, is reduced to 30 million organisms by flushing the system with ethylene oxide. The remaining organisms are, for the most part, on the surfaces of modules which are mated during the final assembly process and cannot be reached by the ETO. (Quite clearly, this burden would be lower if the design is changed to reduce these mated surfaces. However, it is quite low and well within the prescribed kill tolerance of the terminal heat sterilization cycle.) The probability of an organism surviving after application of the specified 12D terminal heating process is then 0.3×10^{-4}, which is less than the specified value of 1×10^{-4}.

If all operations, from the inception of component assembly to final assembly, were conducted in clean rooms, the biological loading would obviously be much lower. This condition is represented by the dashed line of Figure 51. Operating under such conditions would also tend to result in higher system reliability, but the cost of such an operation would be much higher. Inasmuch as this approach is not necessary to the control of burden, it has not been selected in the reference plan.

6.3 BURDEN SENSITIVITY

A brief analysis has been performed to determine the sensitivity of the burden to some of the contamination/decontamination parameters, as well as to variations in the sterilization plan. The results for the variations in the contamination factors are shown in Table XXXI. The two most important factors are fallout, where an increase from 32 to 128 organisms per square inch per day increases the burden by 60 percent, and natural die-off, where an increase from 30 to 99 percent die off reduces the burden 80 percent. On the other hand, the system can increase in complexity (in terms of number of piece parts) by a factor of 10 with only a 40 percent increase in the burden, which is of the same order as an increase in the electrostatic factor from one (no electrostatic effect) to 10. In Section 3.0 of this volume many possible variations are discussed, and a series of nomograms are presented which summarize the results of the analysis. A typical one is shown in Figure 52; tolerable limits are shown for the contamination factors of concern which yield an acceptable presterilization burden; and for the sake of comparison, the conservative values used in the preceding section are shown as well.

TABLE XXXI

BURDEN SENSITIVITY TO CONTAMINATING FACTOR VARIATIONS

Parameter	Variation range	Percent Variation of Total Burden
1. Internal burden	± Order of magnitude	38.5
2. Fallout	32 to 128 org/in.^{2}/day	59.5
3. Electrostatic factor	1 to 10	33.3
4. Die-off	30 to 99 percent	80

Conditions: Each parameter varied holding others constant
no FA heat test, ETO or Clean-Room

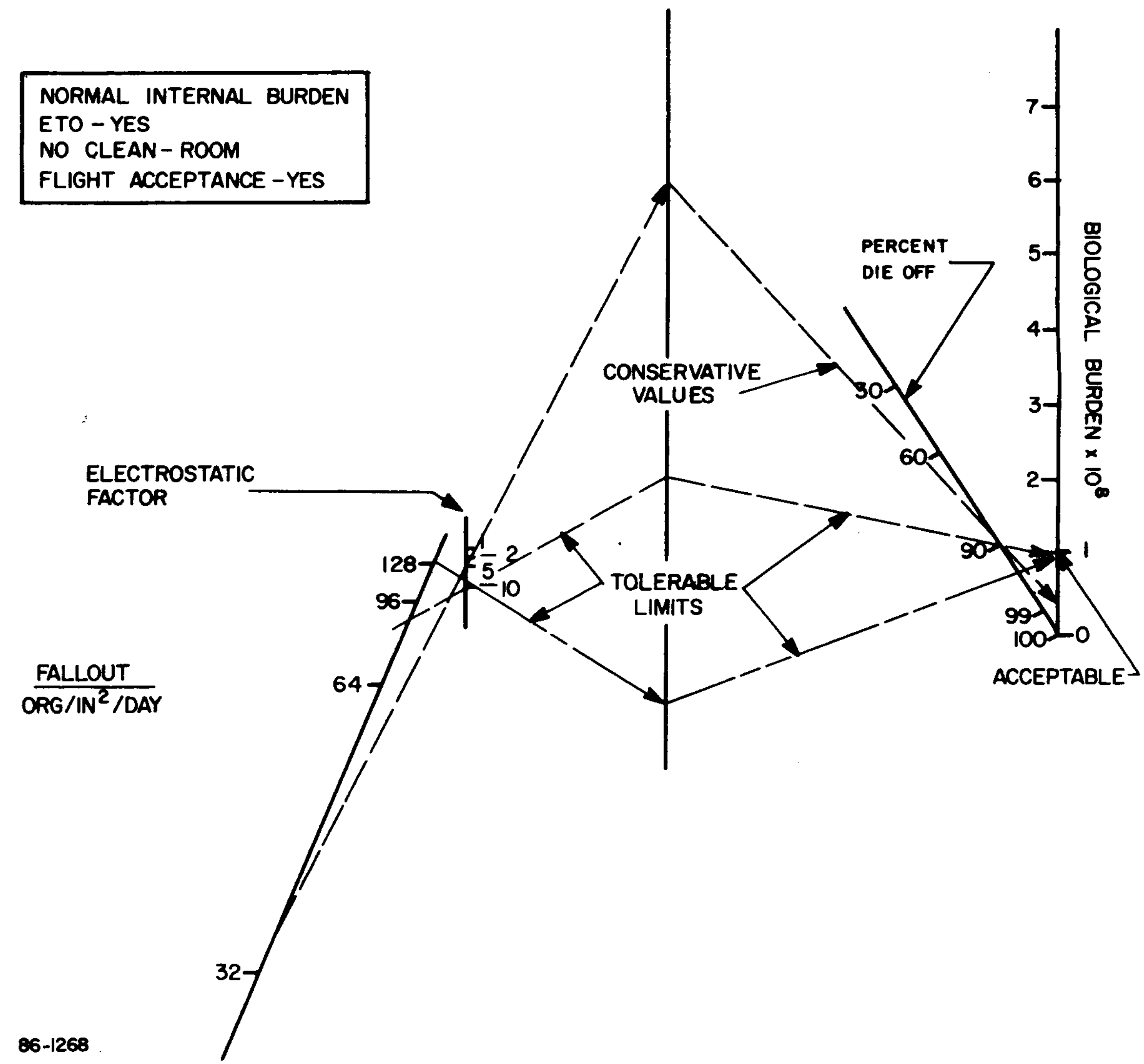

Figure 52 CONTAMINATION SENSITIVITY NOMOGRAM

A number of alternative sterilization plans have been analyzed in addition to the reference plan, one of these being indicated by the dashed lines in Figure 51. It may be of interest, that in the extreme case of no controls and no flight acceptance heat soaks, the total presterilization loading would be 960 million for the design and conditions discussed in the preceding section, rather than 30 million.

6.4 ASSAY REQUIREMENTS

Once the permissible burden on each part of the flight capsule at each stage of the assembly/test process has been established, it is essential to verify during the program that these burdens are not exceeded. The basic tool for this verification is the biological assay, which consists essentially of two parts: the recovery of the sample and the determination of the number of viable organisms in the sample.

Recovery of organisms from the interior of a part can be done in a number of ways, each suited for certain applications, but all destructive in nature. Methods would include disassembly, fracturing, sawing, crushing, grinding, and others. For exterior surfaces, a number of non-destructive sample-collection methods are available. These include swabbing, impression techniques, agitation, rinse methods, immersion and ultrasonic release.

After a sample has been collected, the basic technique for determining the number of vital organisms is culturing in various media. A direct count is generally impractical for the applications of interest here.

With these recovery techniques it is never possible to recover all the viable organisms, and with culture techniques not all the viable organisms will reproduce in a given medium. These factors limit the accuracy of assay techniques. The currently accepted recovery rates are shown in Table XXXII, and conservative accuracies based on these recovery rates are shown in Table XXXIII.

The number of assays required to furnish a given degree of assurance that the burden on a given part is not greater than a given control (specified) value depends on the control value, the assayed value, the desired degree of assurance, and the accuracy of the assays. An estimate of this number can be made by conventional statistical techniques (e.g., using the Student's "t" distribution). The aforementioned computer program contains a subroutine which performs the required simple calculation. Some typical results are shown in Figure 53 for a control burden limit of 10^8, a desired degree of assurance of 0.9999, and for several assay accuracies, bracketing the range indicated in Table XXXIII.

With the better accuracies, two or three assays are required to establish that the burden is no more than 10 times that assayed, and about 8 are required to demonistrate that is no more than twice that assayed. With the poorer accuracies, many more assayed are required or; conversely, with a reasonable number of assayed (say 10) one can only establish that the burden is no more than 2.5 to 10 times that assayed.

TABLE XXXII

REPORTED ASSAY RECOVERIES

Surface Burden	Precision	Recoveries (percent)	Reference
Swabs	Poor	52 to 90	Angelotti, '58(1)
Rinse or spray rinse	Fair	80	Buchbiner, '47(2) Angelotti, '58(1)
Agitation	Fair	80	Wilmot Castle Co.*
Immersion with ultrasonics	Excellent	90 to 99	Wilmot Castle Co.*
Rodac	Good	41	Angelotti, '64(3)
Internal burden			
Size reduction techniques	Very poor	1	Reed, '65(4)
Filtration (for assay of liquids)	Excellent	99 to 100	Wilmot Castle Co.(5)

*Based on unpublished data

[1] Angelotti, R. and M. J. Foter, A Direct Surface Agar Plate Laboratory Method for Quantitatively Detecting Bacterial Contamination on Nonporous Surfaces, Food Research, 23, pp. 170-174 (1958).

[2] Buchbiner, L., T. C. Buck, Jr., P. M. Phelps, R. V. Stone, W. D. Tiedeman, Investigation of the Swab Rinse Technique for Examining Eating and Drinking Utensils, American Journal of Public Health, 37, pp. 373-378 (1947).

[3] Angelotti, R., J. L. Wilson, W. Litsky, W. G. Walter, Comparative Evaluation of the Cotton Swab and Rodac Methods for the Recovery of Bacilus Subtiles Spore Contamination from Stainless Steel Surfaces, Health and Laboratory Science, 1, pp. 289-296 (1964).

[4] Reed, L. L., Microbiological Analysis Techniques for Spacecraft Sterilization, J. P. L. Program Summary No. 37-32, IV, pp. 35-44 (30 April 1965).

[5] Ernst, R. and A. Kretz, Compatibility of Sterilization and Contamination Control with Application to Spacecraft Assembly, Contamination Control, 3, No. 11, p. 10 (1964).

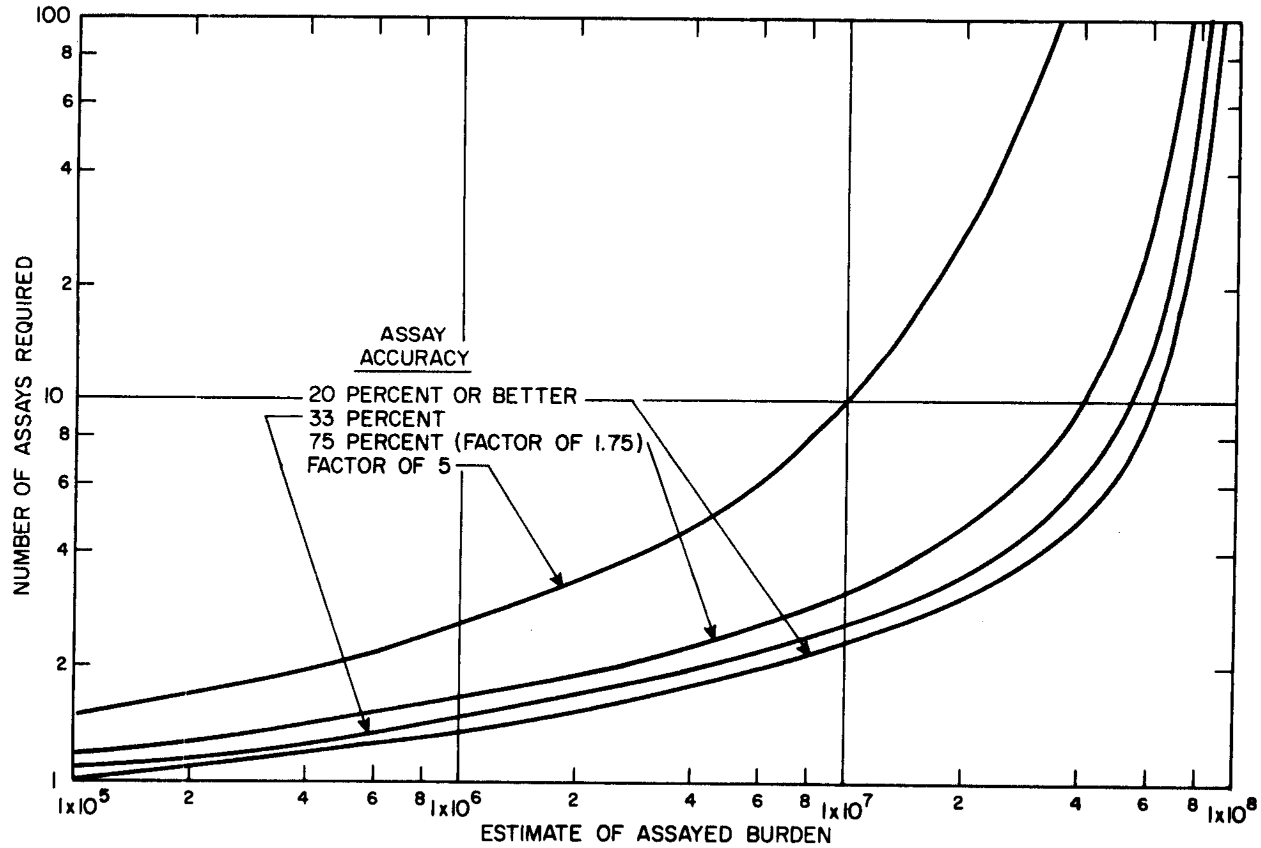

86-5692

Figure 53 NUMBER OF ASSAYS REQUIRED TO DEMONSTRATE THAT THE ASSAYED BURDEN IS BELOW 10^8 ORGANISMS WITH A CONFIDENCE OF 99.99 PERCENT

TABLE XXXIII

OVERALL ASSAY ACCURACIES

	(percent)
Swab	60
Rinse	20
Agitation	20
Immersion	15
Rodac	75
Filtration	10
Internal	factor of 5
Black boxes	33*
Subassembly, general	75(factor of 1.75)**

* Mixture of Swab, immersion and internal (fracturing, drilling, etc.)
** Mixture of Rodac, some swab

Assays of the interior and exterior of the parts and subassemblies must be performed initially to verify the estimated burden, and the burden values must then be monitored continuously to preclude the possibility of deterioration of the processes used. In addition, measurements are also required of the basic contamination/decontamination factors (fallout, die off, etc.) in the assembly process, again to verify the estimated values initially and then to monitor them in order to catch any deterioration of the process.

6.5 TERMINAL STERILIZATION

In the final step in the assembly process, the flight capsule with its biological burden controlled to less than 10^8, is inserted into the sterilization canister. (The permissible value of 10^8 includes the burden on the interior surface of the canister, which may therefore have to be decontaminated by cleaning with ETO). This assembly is then subjected to dry heat applied externally by a forced-convection oven (see Figure 54). If heat is applied only externally, the rise time for a system of this size is about 60 hours. This long period of time is undesirable because it may degrade the system reliability somewhat without any appreciable

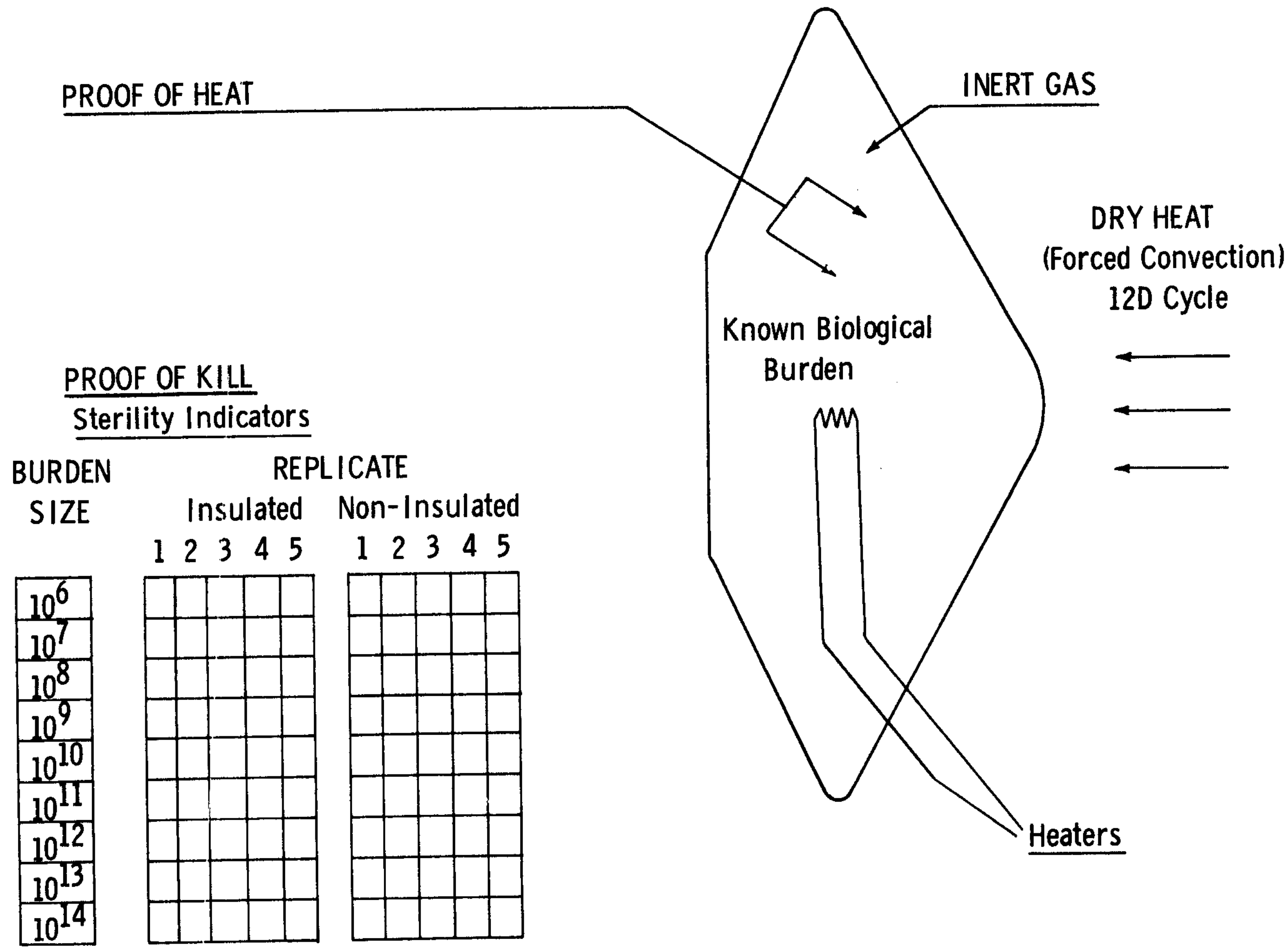

Figure 54 TERMINAL STERIALIZATION CONFIGURATION

improvement in the sterilization process. External-temperature overshoot provides little improvement in this situation, in that the relaxation in the temperature cycle experienced by components in the interior of the capsule is bought at the expense of a more severe cycle for components on the exterior of the capsule and on the sterilization canister. Forced convection of inert gases in the interior of the capsule can speed up the heating-up process considerably, but at the expense of complicating the system by the introduction of active mechanical devices (the blowers) which add to the weight of the system and must themselves be sterilizable and highly reliable. Internal heaters, however, can decrease the heat-up time by an order of magnitude with little additional weight and complexity, and are therefore recommended at this time.

In principle, the capsule can be sterilized in the form of several major subassemblies, which furnish relatively better exposure of the interior parts to externally applied heat, and these subassemblies can then be assembled into the complete capsule/canister assembly under sterile conditions (i.e., within the oven, using tunnel suits). At present this concept appears less attractive than the aforementioned one, because of lack of engineering experience in this type of facility. For reasons of post-sterilization repair and insertion of heat-sensitive components, it may be necessary to develop this capability, but even so, it will probably be best to utilize it sparingly and to perform the basic assembly process under unsterile (although possibly bio-clean) conditions.

After the dwell at maximum temperature, the cool-down also takes about 60 hours to reach ambient conditions for the most highly insulated elements, although the external capsule surface reaches ambient conditions in only a few hours. Although this period of time could be shortened by external-temperature under-shoot and/or internal convection of cold gases, these steps are probably not worth while.

Thermocouples are installed within the capsule to verify heat application. In order to get a true picture of the temperatures throughout the interior with a reasonable number of thermocouples, they must be located at all critical points. The selection of these points requires a very detailed knowledge of the heat paths and other thermal-control characteristics of the capsule. This information can be generated in the very extensive thermal-control test program which will have to be conducted on the capsule.

The kill effectiveness of the cycle may be verified by means of sterility indicators in the form of known organism populations which are exposed to the heat cycle in the same oven as the capsule. These indicators can be designed to have the same insulation characteristics as remote capsule interiors. Non-insulated indicators furnish an indication of the basic kill-effectivity of the cycle. By using indicators with a range of population sizes, one can obtain a quantitative measure of the probability of capsule sterility.

6.6 POST-STERILIZATION MAINTENANCE

Subsequent to terminal sterilization and prior to launch, the capsule experiences extensive testing and integration with other systems. (See Figure 55). Sterility during these phases can be verified only indirectly, by measuring any leakage of a pressurized inert gas stored within the system; traces of helium can be detected and helium may be the proper gas to use. However, this does not guarantee sterility if a large leak develops, because evidence indicates that organisms can flow "up stream" if the hole is large enough. Other protection can be provided by storing the capsule/container system in a handling container filled with ETO.

Repairs, or at least adjustments, may be required for a complex system during the time from terminal sterilization to launch. This requires either technique (design features, equipments, facilities and procedures) for such repairs under sterile conditions or the capability on the part of the capsule of tolerating additional sterilization heat cycles, which represents a severe penalty for some components. A combination of these approaches, with a limited repair capability and a limited capacity for additional heat cycles may be the best choice.

Little is known about the possible recontamination risk that may be encountered by the capsule during and after canister-lid opening prior to orbit injection; this area therefore requires some additional investigation.

The risk can be minimized by use of the appropriate design techniques, possibly at the expense of complexities in the system. A similar problem area is the meteoroid bumper, if one is used on the outside of the sterilization canister; by making such a bumper of metal, which is internally sterile, rather than fiberglass, the possibility of contaminating the capsule as a result of puncture of the bumper is greatly reduced.

6.7 RECOMMENDED ADDITIONAL STUDIES

A great deal of work remains to be done in virtually all areas of the spacecraft sterilization problem. The following are a few items which suggest themselves as a result of the investigations carried out under this study.

In the areas of basic contamination factors, the most significant outstanding question appears to be that of electrostatic effects on the surface accumulation and retention of biological burdens, which appears to have a fairly significant effect on the total burden. Additionally, it may be worth while to investigate the possibility of reducing the internal burden of some of the relatively "dirty" parts, such as transformers and the material used in parachutes. Lastly, the existing information on fallout in bio-clean facilities is based on studies of relatively small clean-rooms,

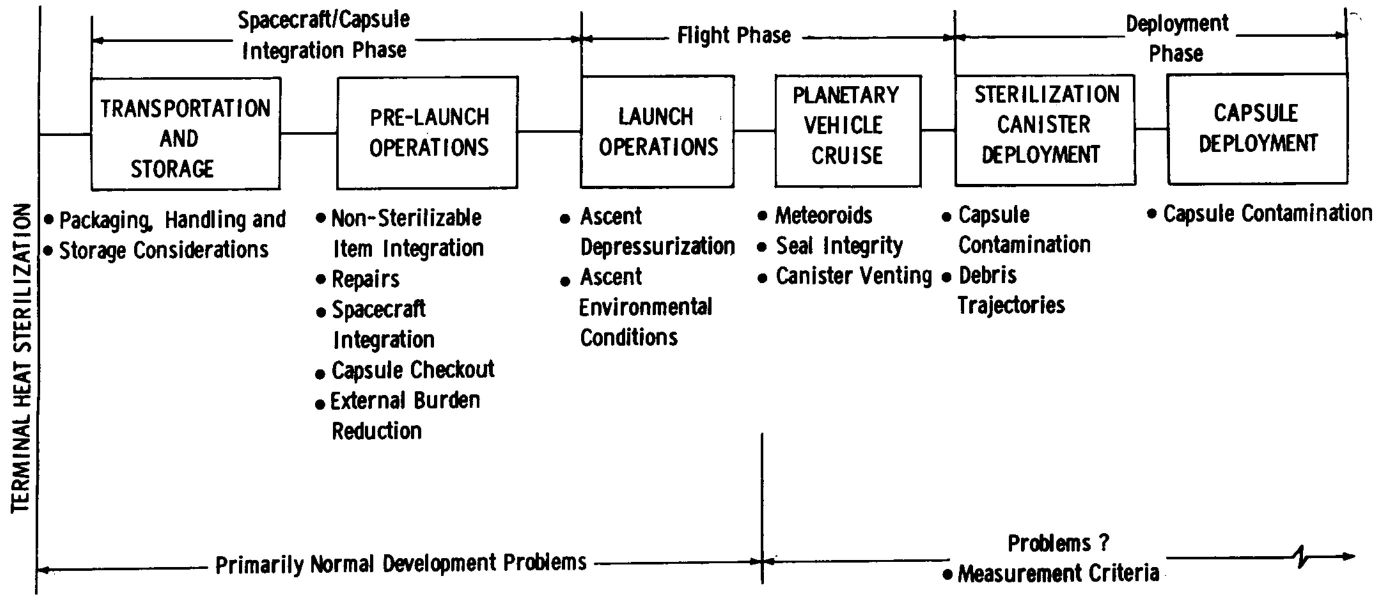

760125P

Figure 55 POST-STERILIZATION MAINTENANCE in the order of 20 x 20 feet, and it would be useful to establish by a survey of existing facilities and extrapolation of the results what the fallout might be in similar facilities scaled up considerably and used for the typical assembly and test operations of a spacecraft.

The accuracy of assays has a significant bearing on the number of assays required and is at present not too well established. Perhaps the present-day assay concepts are characteristically incapable of furnishing results with much better accuracies than the ones quoted herein. This should be investigated, and if it is determined that there are no inherent limiting factors, attempts should be made to improve the accuracy of these techniques.

As a result of the somewhat conflicting requirements of sterility and reliability, heat-cycle optimization is an area which should be investigated thoroughly. The two most promising areas are:

1. Joint optimization of the flight-acceptance and thermal-sterilization heat soaks.

2. Effective utilization of the heat-up and cool-down periods, particularly in the thermal-sterilization heat soak, which requires a definition of the die-off rates at temperatures below that of the basic soak cycle.

Post-sterilization repair represents a major problem. The tentative Voyager operational plan calls for field-sparing at the capsule level, in order to allow gross substitution if failures occur. With the enormous investment involved in such a program, with the severe launch-window constraints, and because of the degree of complexity of the system, sound logistic planning should allow for capsule repairs or at least adjustments. Repeating the sterilization cycle to repaired capsules (several times, if necessary) may degrade the reliability of the system severely. Therefore, efforts to incorporate design features and to provide a sterile facility in which repairs can be undertaken could well make the difference between mission success and failure.

Another major problem area is post-sterilization calibration of scientific instruments. In some instances, sterilizable calibration devices can be built into the capsule; in other areas it may be necessary to accept partial or indirect results of presterilization calibrations.

Perhaps the main problem area associated with post-sterilization recontamination is the possibility of impingement of contaminated particles from the separation system or the exhaust products of the attitude-control and propulsion systems of the flight spacecraft on the sterile capsule. The likelihood of this occurence can be established with ground-test programs, and if such a likelihood exists, design studies can be performed to minimize it. Additionally, it may be worth while to develop a means for establishing whether or not an impingement takes place before (by a meteoroid), during and after canister opening.

The type of burden-sensitivity analysis described herein forms a useful tool for guiding future work in many aspects of the sterilization problem, by highlighting areas where the greatest gains are potentially available as a result of additional work. Therefore, it would be useful to expand the present results by further studies of the effects of variations in the several contamination and decontamination factors, handling concepts, ETO decontamination effectiveness, fallout in the assembly area, etc. Also, it would be possible to establish the significance of mated areas, the implications of conducting the flight-acceptance heat soak later rather than earlier in the assembly sequence, etc. Lastly, it would be useful to extend these results to other design concepts and to capsules designed for basically different (i.e., more or less sophisticated) mission requirements and, consequently, with substantially different physical sizes and complexities; this would furnish an insight into the sensitivity of the basic conclusions reached herein to specific design features and the size/ complexity of the system.